SATELLITE BASED WATER BALANCE MODELING IN LAKE BURDUR BASIN, TURKEY

ASLIHAN KOL
February, 2016

SUPERVISORS:
Dr.Ing.T.H.M. Rientjes
Ir.G.N.Parodi

SATELLITE BASED WATER BALANCE MODELING IN LAKE BURDUR BASIN, TURKEY

ASLIHAN KOL
Enschede, The Netherlands, February 2016

Thesis submitted to the Faculty of Geo-Information Science and Earth Observation of the University of Twente in partial fulfilment of the requirements for the degree of Master of Science in Geo-information Science and Earth Observation.
Specialization: Water Resources and Environmental Management

SUPERVISORS:
Dr.Ing.T.H.M.Rientjes
Ir.G.N.Parodi

THESIS ASSESSMENT BOARD:
Dr.M.W.Lubczynski (Chair)
Prof.P.(Paolo)Regianni (External Examiner, University of Siegen)

ABSTRACT

Lake Burdur constitues one of the 14 internationally protected Ramsar areas of Turkey. The lake is located in south-west of the country with an area of 145.7 km^2. The Lake has experienced severe decline in water level of approximately 10m in recent decades. The Lake area has reduced by approximately thirty percent.

This thesis investigates the water balance of the Lake and identifies the causes for the decline in lake level between 2010 and 2014. Level of the Lake decreased 1.8 m from 843.3 m to 841.5 m between the time period. Water balance terms of the Lake and Lake level changes by availability of a bathymetric survey are calculated at monthly base. Simulated lake levels were compared with observed levels for five years.

Rainfall is one of the main components of the water balance of the lakes; and for water balance study it requires accurate and reliable estimates. Estimates of rainfall are required to simulate over-lake rainfall and for simulation of the rainfall-runoff relation from sub-catchment that drain into the lake. Low density and unevenly distributed stations in the study area constrain overall lake rainfall estimation in addition to estimation of streamflow from sub-catchments that drain to the lake. To overcome this problem of the low number of available stations for rainfall representation, satellite based rainfall assessment was used as an alternative method. To compare satellite based rainfall with gauged rainfall, bias factor and relative error are estimated and finally satellite based rainfall products were corrected with bias factor.

Potential evapotranspiration (PET) is a crucial process in water balance modeling because runoff models require PET estimations. In this study, satellite based product, Famine Early Warning Systems Network (FEWS NET) PET, was studied for daily PET estimation in order to use in runoff modeling. A-Pan monthly evaporation from the lake was obtained from General Directorate of State Hydraulic Works, Ankara and was used for lake balance modelling.

This study examined daily runoff for water balance modeling of the Lake. A semi-distributed Representative Elementary Watershed (REW) model was used to simulate sub-catchments streamflows that drain to the Lake. Runoff coefficients of the sub-catchments served to evaluate the model reliability, since observation time series of stream flow are insufficient for the basin. Calculated runoff coefficients are in the value range 0.16 to 0.26 that is expected in a semi-arid area.

Since there are many abstractions from the Lake, three different assumptions based on abstractions were applied to see the effects on Lake water level. Findings on lake levels simulations based on different abstractions rate conclude that abstractions effect directly the lake level. Finally the study is concluded based on three closure error assumptions.

ACKNOWLEDGEMENTS

First of all I am grateful to General Directorate of State Hydraulic Works (DSI) and Ministry of National Education of Turkey for granting me to study Master of Science degree. This opportunity has greatly impacted my life in GIS and Earth Observation for Water Resources and Environmental Management.

I would like to express my gratitude to my first supervisor Dr.Ing.T.H.M Rientjes for his supervision, guidance and critical comments throughout the thesis period. His critical comments and guidance gives me a chance to explore further. My sincere appreciation goes to my second supervisor Ir. G.N.Parodi for his encouragements and help for my research work.

My deepest gratitude goes to Dr.M.N.Koeva for her encouragements and her kind support throughout my entire study. I would like to thank also Ir. A.M. van Lieshout and Prof.Dr.Z.Su for their kindness and for help to start my education here. Very special thanks to Dr.Z.Vekerdy, Dr.Ir.S.Salama and Dr.Ir.R.van der Velde for their expertise and support during my study.

Graciously, I like to extend a large amount of thank for Dr. Bulent Selek (DSI), Dr. Murat Hatipoglu (DSI) and Dr. Hakan Aksu (DSI) for their guidance, valuable support and help especially during fieldwork and my entire study.

I am extremely fortunate to have friends from all around the world here. I will forever cherish the friendship we made with Soodabeh, Sasha, Anna, Jesse, Chang, Kingsley, Assayew and many more I could not possibly mention all, with whom I shared many meaningful conversations and wonderful time.

Lastly, my everlasting gratitude goes to my lovely family. They have supported me always and give me strength at difficult times during my stay here. Also, I will never forget my uncle Selahattin Erdogan and his family for helping and supporting me all the time. I will be indebted to them forever.

TABLE OF CONTENTS

1. INTRODUCTION ... 1
   1.1. Background ... 1
   1.2. Problem definition and importance of the study ... 2
   1.3. Thesis objectives and research questions ... 3
   1.4. Thesis Outline ... 4
2. STUDY AREA AND DATA PREPARATION ... 5
   2.1. Study area ... 5
      2.1.1. Topography ... 5
   2.2. Lake level history ... 6
   2.3. Acquired data ... 6
      2.3.1. Gauged streamflow data ... 6
      2.3.2. Rainfall data ... 6
      2.3.3. Meteorological data ... 6
3. METHODOLOGY ... 9
   3.1. Introduction ... 9
   3.2. Lake water budget ... 9
   3.3. Rainfall estimation ... 11
      3.3.1. Bias estimation ... 13
      3.3.2. Relative error estimation ... 15
      3.3.3. Methods ... 15
   3.4. Evapotranspiration estimation ... 17
      3.4.1. Introduction ... 17
      3.4.2. Potential evapotranspiration estimation ... 17
      3.4.3. Open water evaporation ... 18
   3.5. Hydrological modeling ... 19
      3.5.1. Introduction ... 19
      3.5.2. REW model ... 20
      3.5.3. Governing equations ... 21
      3.5.4. Runoff estimation ... 22
      3.5.5. Runoff estimation ... 25
4. RESULTS AND DISCUSSION ... 29
   4.1. Rainfall results ... 29
   4.2. Evapotranspiration Results ... 32
      4.2.1. PET results ... 32
   4.3. Runoff Results ... 34
      4.3.1. Catchment comparison ... 34
      4.3.2. Runoff coefficient estimation ... 34
      4.3.3. Results ... 35
   4.4. Lake water balance assesment ... 36
5. CONCLUSION AND RECOMMENDATIONS ... 39
   5.1. Conclusion ... 39
   5.2. Recommendations ... 40

LIST OF FIGURES

Figure 1 Distribution of Earth's Water *Source: Shiklomanov (1993)* 1
Figure 2 Lake Burdur water levels over decades 3
Figure 3 Study area 5
Figure 4 Mean monthly temperature for the year of 2013 7
Figure 5 Bathymetric map *Source: DSI* 8
Figure 6 Area-Volume graph of the Lake 8
Figure 7 Flow chart 10
Figure 8 Rainfall stations 11
Figure 9 Location of redesigned stations 13
Figure 10 Flow chart of rainfall estimation 16
Figure 11 Evaporation pans Source : *http://www.hko.gov.hk/wxinfo/aws/evap_pan.htm* 19
Figure 12 3-D spatial entity of a REW *Source:(Reggiani, 2012)* 21
Figure 13 Separated DEM of the Lake Burdur basin area 23
Figure 14 Extracted stream network of Lake Burdur basin area 23
Figure 15 Catchment delineation - REWs extraction 24
Figure 16 Streamflow network of the Lake Burdur basin 26
Figure 17 Comparison of simulated and gauged streamflow 27
Figure 18 Streamflow results after warming processes 27
Figure 19 Annual rainfall distribution over the catchment 29
Figure 20 Lake Burdur mean monthly rainfall between 2010-2014 30
Figure 21 Mean monthly rainfall depths over the year 30
Figure 22 Annual rainfall over the Lake 31
Figure 23 Mean annual PET 32
Figure 24 Mean monthly PET from 2010-2014 33
Figure 25 Comparison of the basins a)Estimated by Tardem b)Obtained from DSI 34
Figure 26 Lake level comparison with different amount of irrigation 36
Figure 27 Result of nearest point method for the month of January 49
Figure 28 Map list 50
Figure 29 Above: Average rainfall map of the month January Below: Total monthly rainfall map 50
Figure 30 Resampled total monthly rainfall map 51
Figure 31 Resampled map calculation result 51
Figure 32 Monthly rainfall over the Lake Burdur 52
Figure 33 Areal rainfall depths 52
Figure 34 FEWS NET PET map 53
Figure 35 Point Map overlayed FEWS NET PET map 53
Figure 36 FEWSNET map list 54
Figure 37 Daily PET rates in 2010 54

LIST OF TABLES

Table 1 Spatial features of the rainfall Stations....7
Table 2 Monthly wind speed and direction for Burdur and Tefenni stations 7
Table 3 TRMM and gauged rainfall depths for Senirkent station 14
Table 4 Result of bias factor 14
Table 5 Relative error estimates at the Senirkent station 15
Table 6 A-Pan data 18
Table 7 Mass balance equation 22
Table 8 Momentum balance equation 22
Table 9 Non-delineated area and neighbour catchments 25
Table 10 Catchment properties 25
Table 11 Monthly estimated rainfall depths 31
Table 12 Mean potential evapotranspiration 33
Table 13 Runoff coefficient estimation 35
Table 14 Annual streamflow (m^3/s) 35
Table 15 Lake level increases in mm by streamflow contribution.... 35
Table 16 Annual components of the lake water balance for the five hydrological years.... 36
Table 17 Results 37
Table 18 Lake level increases in mm by streamflow contribution.... 59

1. INTRODUCTION

1.1. Background

Water covers over the 70 percentage of the Earth's surface with only 2.5 percentage of water on the Earth available as fresh water (Figure 1). Fresh water is available largely as groundwater, ice, permafrost and lakes that cover only 1.2 percent of freshwater resources on the Earth, and fresh water lakes cover 20.9 percent of all the fresh water sources(Shiklomanov, 1993).

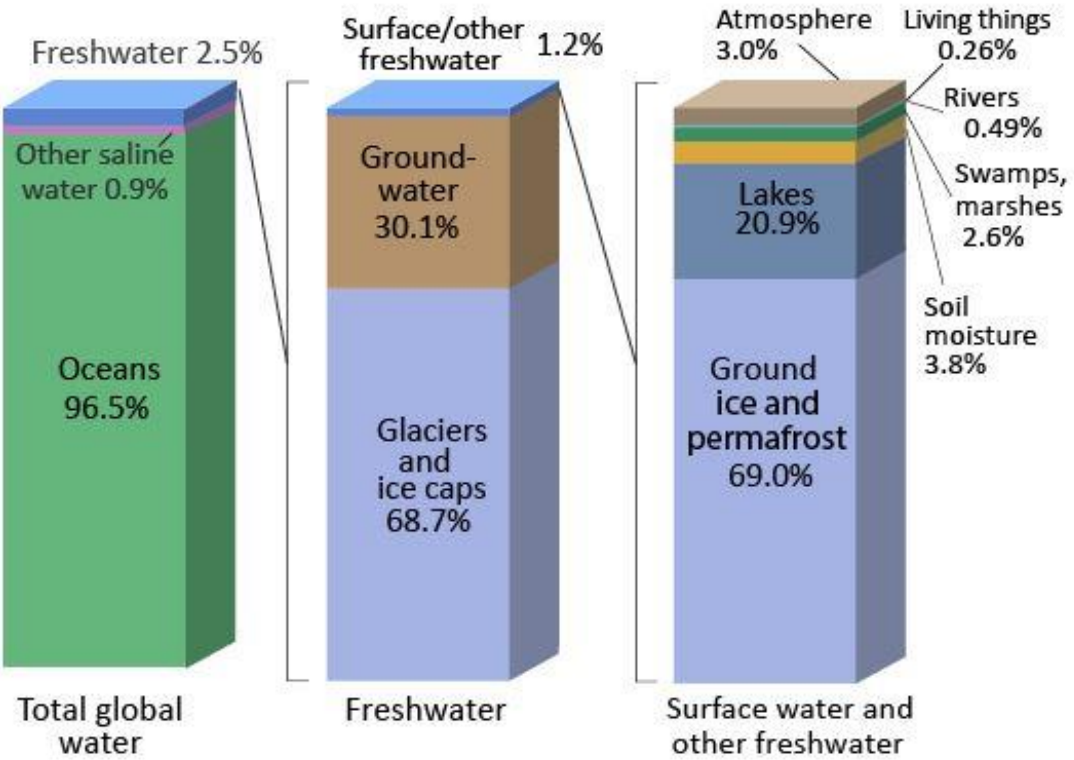

Figure 1 Distribution of Earth's Water *Source: Shiklomanov (1993)*

For many fresh water lakes on the globe, water levels decreases are reported. Causes for decreases are numerous including effect of climate change with lower rainfall and effect of land use change resulting in changes in the hydrological regime. With respect to climate change, for many countries across the globe droughts are reported to occur more frequent with increased periods of dryness, both adversely affecting lake water storage. Lake level decreases may also be as a results of anthropogenic influences such as dam construction, reservoir operation, river channelization (Wantzen et al., 2008). Construction of dam intercepts river flows for reservoir filling and thus directly affects lake water inflows and lake water levels. Increase in fresh water demands for irrigation or domestic water uses, or by reservoirs are important causes for lake water variations, and depend on catchment size and characteristics, the amount of precipitation, evaporation and discharge conditions(Hofmann et al., 2008). Particularly in semi-arid and arid areas since rainfall is relatively low compared to evaporation demands, water level decrease can be observed noticeably.

Changes of water level may differ in the time domain subject to processes and factors that effect lake water storage. Bishop (1990) stated that water level changes are observable due to storms at hourly time step while due to climate changes in the long term that lasts years and decades. Addition to time domain the change of water level varies also according to the size of the lake. For instance, changes of water level of small lakes are more pronounced than for large lakes because of water storage volumes decrease when lake size decreases.

Aspects of dam construction, climate change and human behavior also affected lake water inflow and lake water storage that also applies to Lake Burdur (Turkey) that is selected for the present study. The lake reduction in water storage and decreases in lake levels are reported since measurements of lake levels started in 1960s. Studies to assess and to quantify on possible causes of the lake level decreases are still unknown for Lake Burdur, although urgently needed given the significant lake level reduction over the past five decades.

1.2. Problem definition and importance of the study

The area of study for this thesis is Lake Burdur basin area, which is one of the deepest and largest lakes in Turkey. The Lake water level is reported to have reduced by 15 meter over the past 4 decades, with lowest lake levels recorded in recent years. In Figure 2, a diagram is shown with lake level behaviour from 1960 until 2015. The figure shows that although certain period's water level increases, overall, lake level has decreased consistently. For the historic period between 1965-1970 an increase of 5 m is indicated, whereas for more recent periods 1978-1982 and 2002-2005 small increase of 1-2 m are shown. Considering these increases, some 10 meter of water level has been lost from the lake. Although the lake level decrease is pronounced, clear reasons on the cause of the drop are not available. At respective organisations that are responsible for Lake water level monitoring and management, there is much speculation on the cause of the changes and lake level drop. Causes considered are effects of earthquakes, effects of dam construction, effects of climate change and effects of water use. For a number of causes, the vertical arrows are indicated to show the years of occurrence. However, a cause-effects pattern cannot be indicated with, for instance, a quick water level decrease as a result of a dam construction; as such effects of dam construction on lake level behaviour only are minimal. As a preliminary finding of result of this thesis study, it is suggested that lake level decreases must be associated with too high water abstractions. Lake inflows are smaller than lake losses and cause decrease in lake water storage. Therefore, this study will aim at lake water balance simulation and assessment.

Lake water balance modeling permits an assessment on the lake level depending on the various hydrologic components (Cooper, 2010). Many studies have addressed issues of decline of water levels by using the water balance assessment. According to the Swenson and Wahr (2009), Lake Victoria (East Africa) have the largest decline as the second largest freshwater on the Earth, and they evaluate the impact of climate and human management effects on the lake level by using a linear reservoir based hydrological model. Another example is Lake Ikeda in Japan, where the hydrologic budget was studied by a water budget model that specifically was developed to examine the lake water level variation for the lake (Ito et al., 2009). Lake level variation of Lake Tana Ethiopia was studied by MSc Research studies at ITC by Wale (2008) and Perera (2009). The study relied on availability of lake level-storage relations and hydrological models to simulate lake levels by solving the water balance of the lake.

For a better understanding of the causes of lake level fluctuations, a scientific literature review is crucial. It contributes to a better understanding on cause-effects relation and approaches to evaluate the lake water balance. However, lack of scientific literature related to the lake water storage in Lake Burdur is a major challenge. Although the decline of water level endangers the lake, existing scientific studies have focused on the geological structure of the basin area instead of hydrological models. In order to understand the decrease in water level, a representation of the real world characteristics of the lake through hydrological modeling is important.

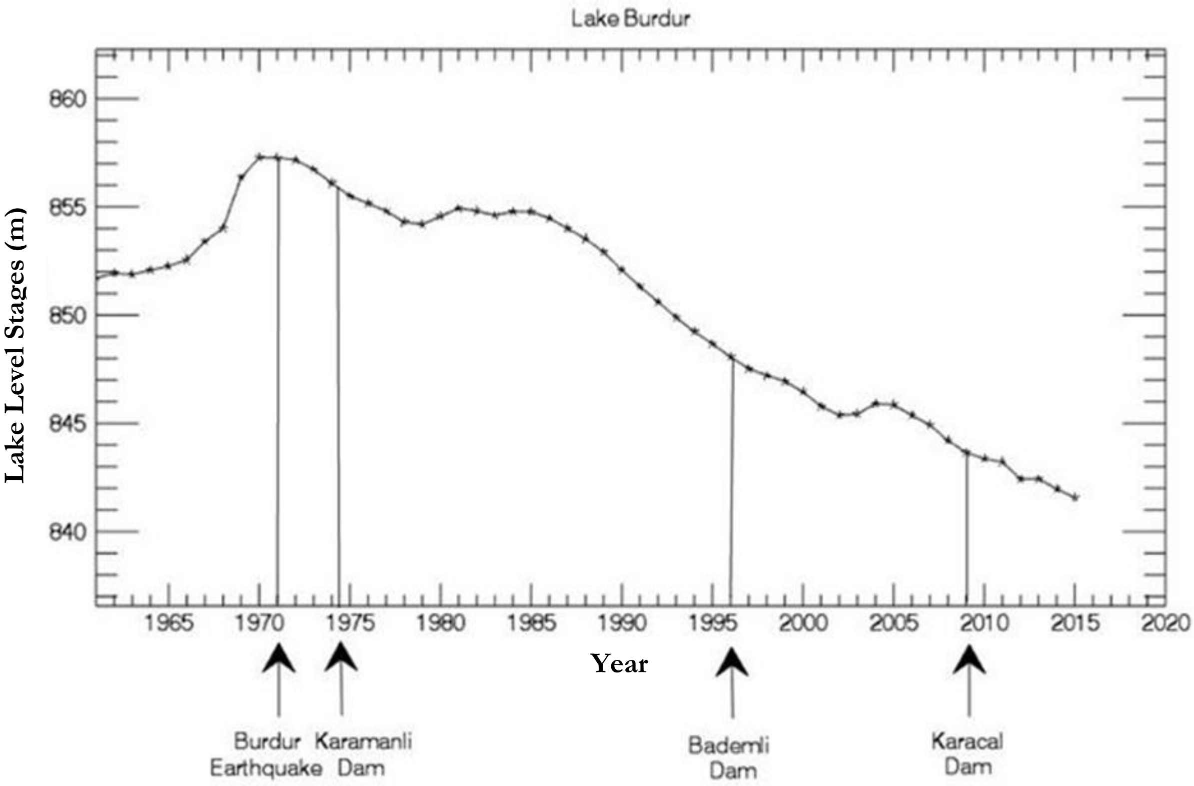

Figure 2 Lake Burdur water levels over decades

The use of gauged data for rainfall and for lake inflow from catchments is prerequisite to simulate changes of lake levels. In order to study fluctuations of the lake level, it is not only the availability of data that is important but data time series also should be consistent. Time series provide information and knowledge on the various water balance terms to solve hydrological problems. However, in this study area lack of gauged data to ensure a comprehensive representation of the Lake Burdur basin balance is a major obstacle. The numbers of ground stations that record meteorological (9 stations) and flow observations (2 stations) are available in the basin area; however, time series data may be unreliable, inaccurate and inconsistent. Moreover, most of the sub-catchments are ungauged since streamflow gauging stations are absent. As such, detailed observed data on lake inflow is missing and thus has major implications to the assessments on Lake Burdur water balance and its closure.

1.3. Thesis objectives and research questions

The main objective of this study is to simulate the water balance and lake level of Lake Burdur at monthly time step to identify and to assess the cause of the lake level reduction. For simulation of the water balance, rainfall and evaporation estimations over the lake are needed as well as simulation of streamflow from gauged and ungauged catchment by means of a hydrological model. For estimation of rainfall and evaporation, satellite products are used since measurement data from gauges are sparse and incomplete.

For simulation of the water balance and lake levels, the following specific objectives are defined:

- To identify the topology of the area to define the ungauged sub-catchments in the study area
- To correct bias of the satellite rainfall products that are selected
- To estimate potential evapotranspiration in the catchment by using satellite products
- To simulate streamflow from gauged and ungauged catchment using REW model
- To estimate streamflow from ungauged catchments through regionalization
- To calculate monthly base water balance for five years
- To identify abstraction effects on the water level decrease.

To address the objectives the following questions are formulated:

- How to correct satellite rainfall estimates by availability of only few rainfall stations?
- How to regionalize streamflow from ungauged catchments?
- Is there an effect of abstractions quantity on the lake water level decrease?
- Can the lake water balance be closed with certainty?
- What is the main cause of lake level decrease?

1.4. Thesis Outline

This thesis consists of 6 chapters. Chapter 1 gives a general introduction about the research with emphasis on lake water balance and objective of the study. Chapter 2 gives a brief explanation about the study area and data availability. Chapter 3 explains the methodology that also involves the detailed information about water balance components. Chapter 4 presents results and discussion on the water budget estimations.The final chapter 5 concludes on the findings of the study and recommendations.

2. STUDY AREA AND DATA PREPARATION

2.1. Study area

Turkey consists of twenty-five basins of which Lake Burdur is one of the largest. The area that drains to the Lake Burdur basin can be considered a closed basin and comprises 13 catchments all of different size. The basin area is located in the southwestern part of the country. Figure 3 shows the location of the study area. The Lake is located between the cities of Burdur to the south and Isparta to the north having coordinates 29°39' - 30°33' E longitude and 37°80' - 38°20' N latitude. Lake Burdur Basin covers an area of about 3263 km², with 145.7 km² lake surface area having average 835 meter above mean sea level (m.a.s.l). Out of 13 major catchments that drain to the lake, two are gauged although streamflow time series are incomplete with unknown reliability. Therefore, in essence all of the catchments must be considered ungauged.

The lake is fed by several rivers included River Bozcay, which flows from the south to the north as the main tributary. Two other important rivers are Suludere and Keciborlu, which flow from the eastern and the northern parts of the basin into the lake, respectively.

2.1.1. Topography

The basin has elevation ranging from 841 meters m.a.s.l to 2317 m.a.s.l (Figure 3). The surrounding mountains prevent warm and humid air that is coming from the Mediterranean Sea, and it hardens the climate. The annual mean temperature of the area ranges from 0°C to 26°C, and have the highest temperature in August whereas the lowest temperature is measured in December (General directorate of State Hydraulic Works, DSI, Turkey).

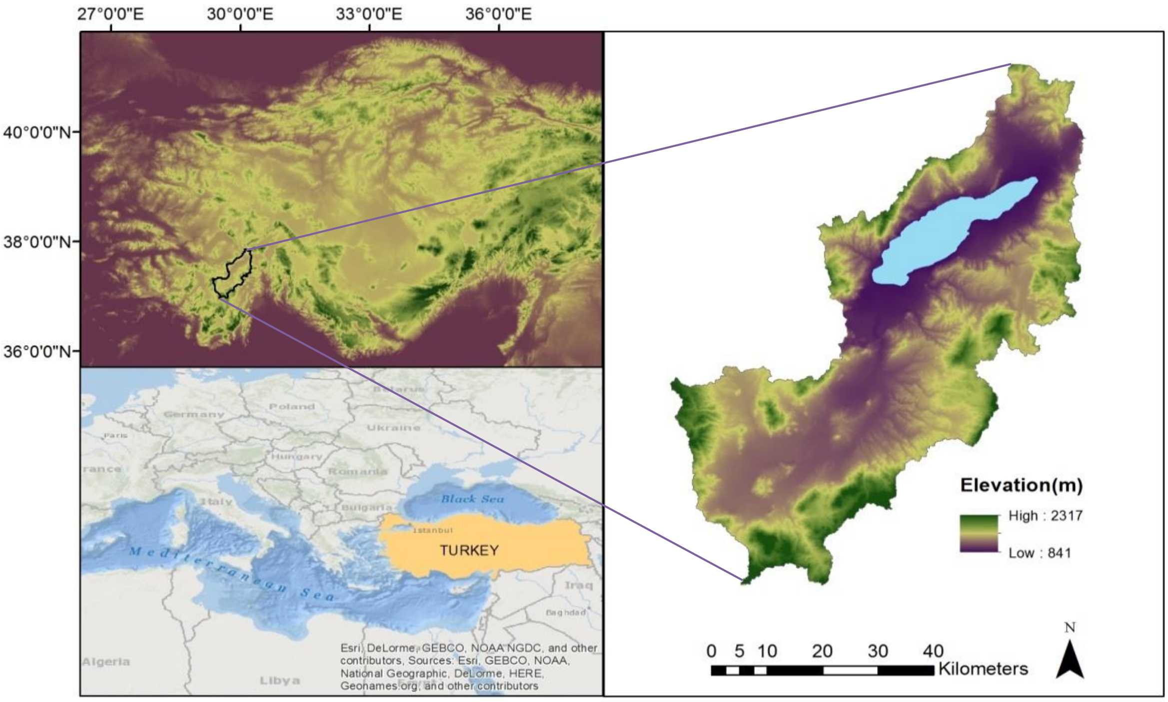

Figure 3 Study area

2.1.1.1. Land cover

Vegetation cover in Lake Burdur basin is dominated by forest, shrub, and meadow. There are many irrigated farmlands to the south, southeast and east of the Lake. Villages are located across the basin. The basin area contains a limited area of desert, which can be found among the basin.

2.1.1.2. Seismic properties

Lake Burdur basin area is a closed basin with Lake Burdur that represents a local depression. The area is known for its tectonic movement and is located in the first-degree, tectonically active seismic hazard zone (*http://www.deprem.gov.tr/*). The area has experienced a number of earthquakes in the last century with a major earthquake (i.e., Burdur earthquake) in 1971 causing large-scale damages.

2.2. Lake level history

The highest water level of the Lake was measured in 1975. For the period from 1975 to 2015, the lake level decreased consistently although some short periods with increase of the water level are shown in Figure 2. The level decreased approximately 10 meters from its highest elevation of 857 in 1970 to about 847meter in 2015 (Figure 2). Although some studies address causes of the lake level decrease, quantitative assessments or descriptive reasoning of the lake level decrease are still not available and missing to improve water management.

2.3. Acquired data

A field survey was executed from 6th of September to 26th of September in 2015. During the survey, the data was collected mainly from General Directorate of State Hydraulic Works (DSI) and from a private company named Hidromark, which are located in Ankara, Turkey. In order to visit the study area and to collect regional data, Isparta regional office of DSI is visited.

2.3.1. Gauged streamflow data

There are two streamflow stations, which are Bozcay and Suludere station. However, most of the years there is lack of daily available data set from these stations.

2.3.2. Rainfall data

Nine rainfall stations provide daily rainfall data in the study area. However, during the fieldwork only monthly rainfall data could be obtained. The station names, locations and data availability is shown in Table 1.

2.3.3. Meteorological data

Two meteorological stations are available in the study area, which are Atabey and Tefenni stations that are located in Burdur city. Temperatures and wind speed data are available from both stations, whereas relative humidity, pressure, vapour pressure and sunshine hour are available only from Tefenni Station.

2.3.3.1. Temperature

The station measures the lowest temperature in the study area during the winter that is between the months of November and December. The temperature is between 0-7°C during the period. The area has the highest temperature in summer period between the months June and August having the maximum temperature approximately 27°C. Figure 4 illustrates the area temperature pattern in the year of 2013, which shows the observed monthly mean temperature values for two stations.

Table 1 Spatial features of the rainfall Stations. Note: The coordinate system projection is Lat-LonWGS84

City	Station Code	Station Name	Easting(m)	Northing(m)	Altitude(m)	Data Availability
Burdur	17238	Burdur	30.2	37.7	957	2012-2014
Isparta	17240	Isparta	30.5	37.7	997	2010-2014
Isparta	17826	Senirkent	30.5	38.1	959	2010-2014
Afyon	17862	Dinar	30.1	38.0	864	2012-2014
Isparta	17864	Uluborlu	30.4	38.0	1025	2010-2014
Isparta	17882	Egirdir	30.8	37.8	920	2010-2014
Isparta	17885	Atabey	30.6	37.9	1000	2012-2014
Denizli	17890	Acipayam	29.3	37.4	941	2012-2014
Burdur	17892	Tefenni	29.7	37.3	1142	2012-2014

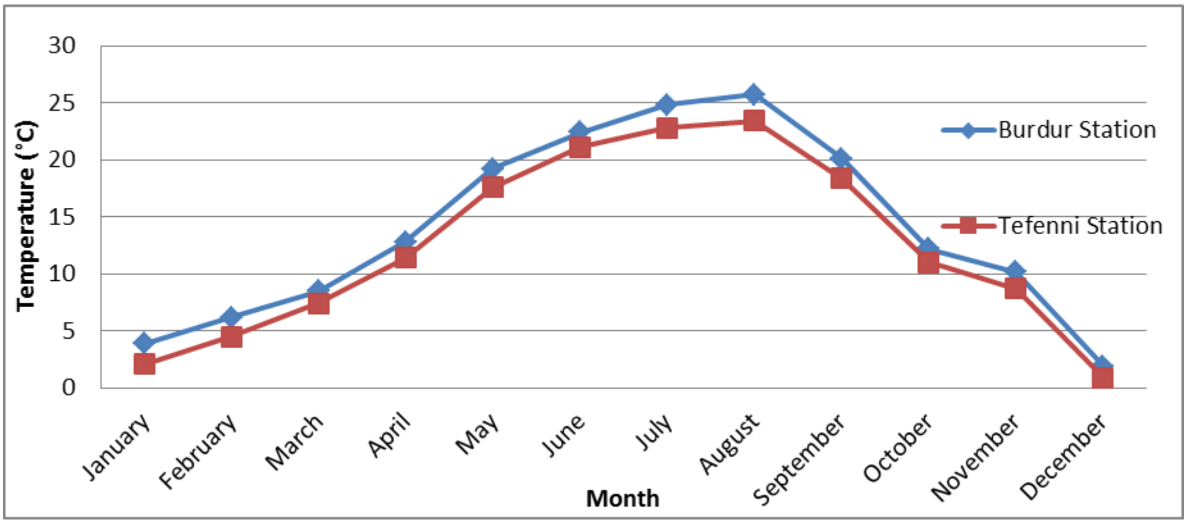

Figure 4 Mean monthly temperature for the year of 2013

2.3.3.2. Wind speed

Wind speed and direction measured in two stations that are Tefenni and Burdur. Table 2 shows wind speed and wind direction, observed at the 10 m height for the year of 2013. The units of wind speed are in m/sec.

Table 2 Monthly wind speed and direction for Burdur and Tefenni stations

Burdur Station	January	February	March	April	May	June	July	August	September	October	November	December
Wind Speed	19.1	16.2	23.6	22.4	15.1	16.6	11.6	10.1	11	15.6	16.5	14.5
Direction	SSW	S	SSW	SE	SSE	S	ENE	NE	S	S	S	NNE

Tefenni Station	January	February	March	April	May	June	July	August	September	October	November	December
Wind Speed	10.7	10.1	14.9	12.8	8.8	13.2	10.1	9.7	9.7	12.5	9.6	12
Direction	WSW	SW	WNW	SSW	W	WSW	ENE	NNW	ENE	S	WSW	NE

2.3.3.3. Relative Humidity,Pressure,Vapor Pressure and Sunshine hours

Daily relative humidity, pressure, vapor pressure and sunshine hour data are available from 2013 to February,2015.

2.3.3.4. Lake bathymetry

The bathymetry map of the lake was prepared in 1998 by a survey. Bathymetric map gives the depth estimation of the Lake. By using bathymetric map (Figure 5), the surface area of the Lake is known subject to the lake level. The map was obtained from DSI with estimated area and volume of the lake. The graph in Figure 6 was prepared to show the surface area and volume relations depend on the Lake level. It gives explanation about the area of the lake based on the lake levels.

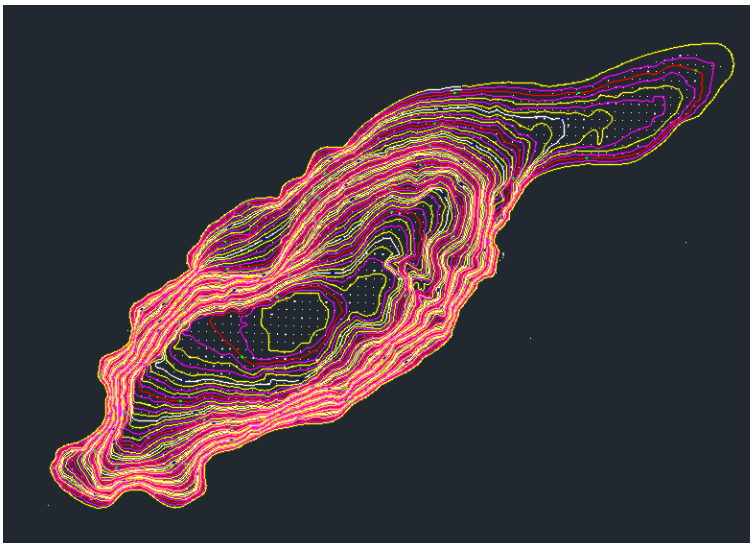

Figure 5 Bathymetric map *Source: DSI*

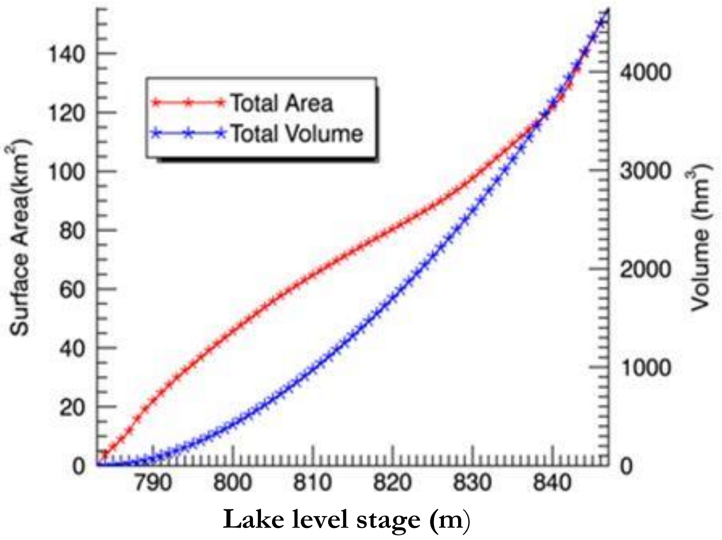

Figure 6 Area-Volume graph of the Lake

3. METHODOLOGY

3.1. Introduction

The overall methodology in this study relies on availability of observed lake level data to establish the relation between lake level decrease and reduction in lake water storage. Therefore, changes in simulated lake levels can be related directly to changes in the simulated water balance of the Lake. In this study, from 2010 to 2014 the period is chosen to estimate lake level decrease because of satellite and station data availability.

3.2. Lake water budget

A water budget of a lake reflects the relationship between input and output of water. This water budget involves both surface water and groundwater. Inflow to the lake comprises surface inflow, direct precipitation, and groundwater inflow. Outflow from the lake comprises direct evaporation, lake water usage, and possibly groundwater outflow. The simple water balance equation is formulated as follows:

$$\Delta S/\Delta T = \text{Inflow} - \text{Outflow}$$

General water balance equation of a lake can be written as :

$$\Delta S/\Delta T = (P + R_i + GW_{in}) - (E + R_o + GW_{out}) - A$$

Where ΔS is change in lake water storage, ΔT is a change in time, Ri is surface water inflow, P is over-lake areal rainfall, GWi is groundwater inflow, Ro is surface water outflow, E is lake evaporation, GWo is groundwater outflow and A is abstractions from the lake. Since the study area is a closed basin, there will not be any surface water outflow and groundwater outflow. Additionally, while the groundwater inflow estimation requires extensive study, in this study, net lake-groundwater exchange was ignored in the water balance equation. However, base flow component of a streamflow hydrograph results from groundwater inflow to the river channel. In this study, base flow is not considered as a groundwater instead treated in surface water inflow component. The balance may be re-expressed as:

$$\Delta S/\Delta T = P + R_i - E - A$$

For estimation of rainfall over the lake, as well as for estimation of rainfall for runoff modeling, satellite based rainfall estimates (SRE's) from TRMM 3B42 daily product were used. In the approach, SRE's were compared to observed time series data from gauges. Comparison is at monthly time step as described in section 3.3. Satellite data was also used to estimate potential evapotranspiration by the FEWSNET product, and for representing elevation by means of a Digital Elevation Model (DEM). Figure 7 indicates a simplified flow chart of the methodology.

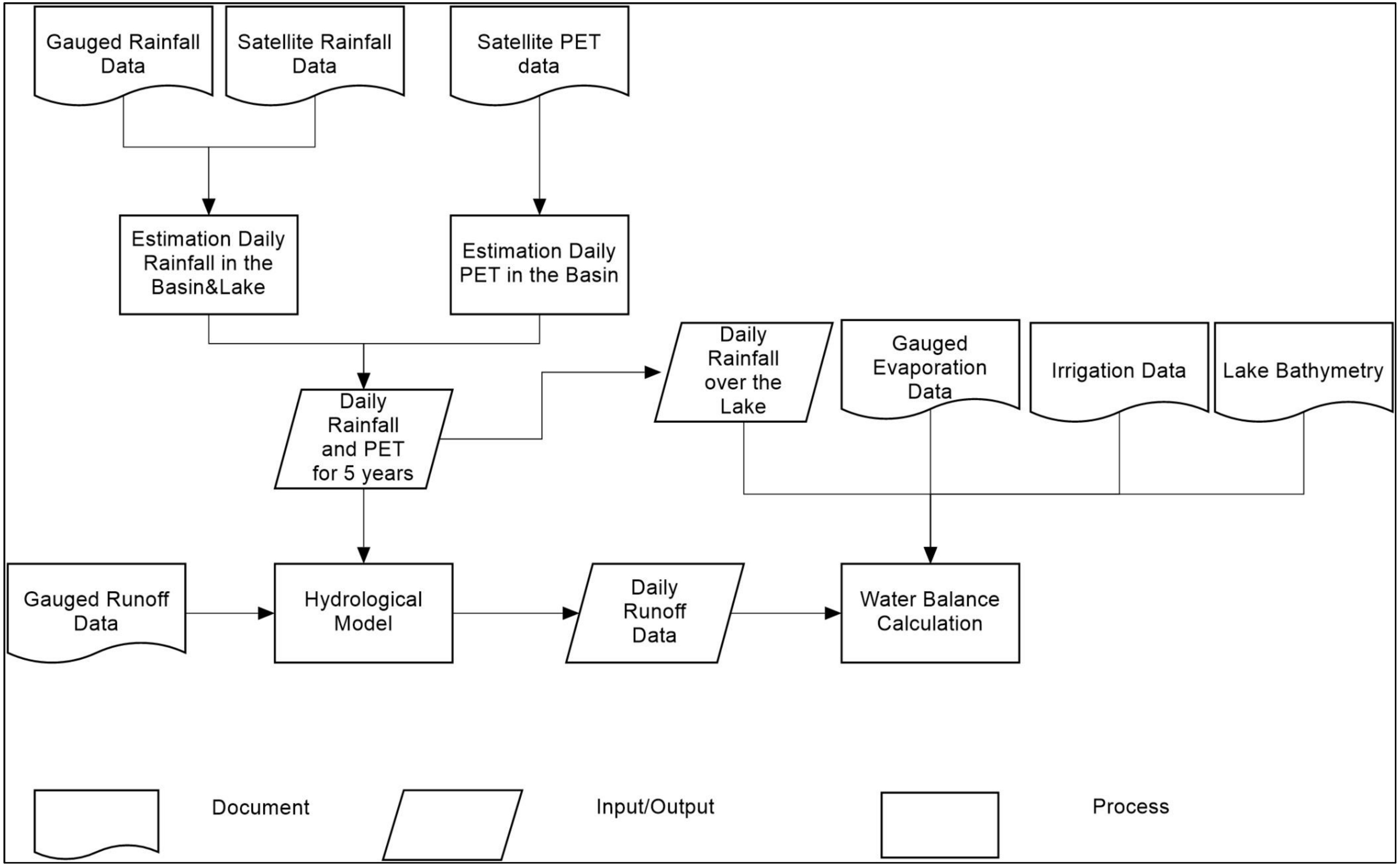

Figure 7 Flow chart

3.3. Rainfall estimation

In semi-arid and arid environments, rainfall is a critical weather component that plays a key role in water balance calculations. For lake water balance modeling, estimates of rainfall are required to simulate over-lake rainfall and for simulation of the rainfall-runoff relation from sub-catchment that drain into the lake. For water balance closure, it is essential to have reliable and accurate rainfall. In the study area, rainfall is estimated on daily basis by a small network with only nine rainfall stations. The network has low density with stations unevenly distributed in the study area. Moreover, the network of stations is not following specific design criteria. For accurate rainfall representation, networks should have sufficient density and stations should follow a specific design to observe rainfall variability in space domain. Both aspects of the network design are not respected in the study area and imply that use of rainfall time series in lake water balance modeling must be exercised with care. In addition, available time series collected during the fieldwork have different time length and constrains accurate representation of rainfall in space and time domains. Moreover, it is uncertain whether collected time series, locations and number of stations could serve an estimation over-lake rainfall given the large size of the lake.

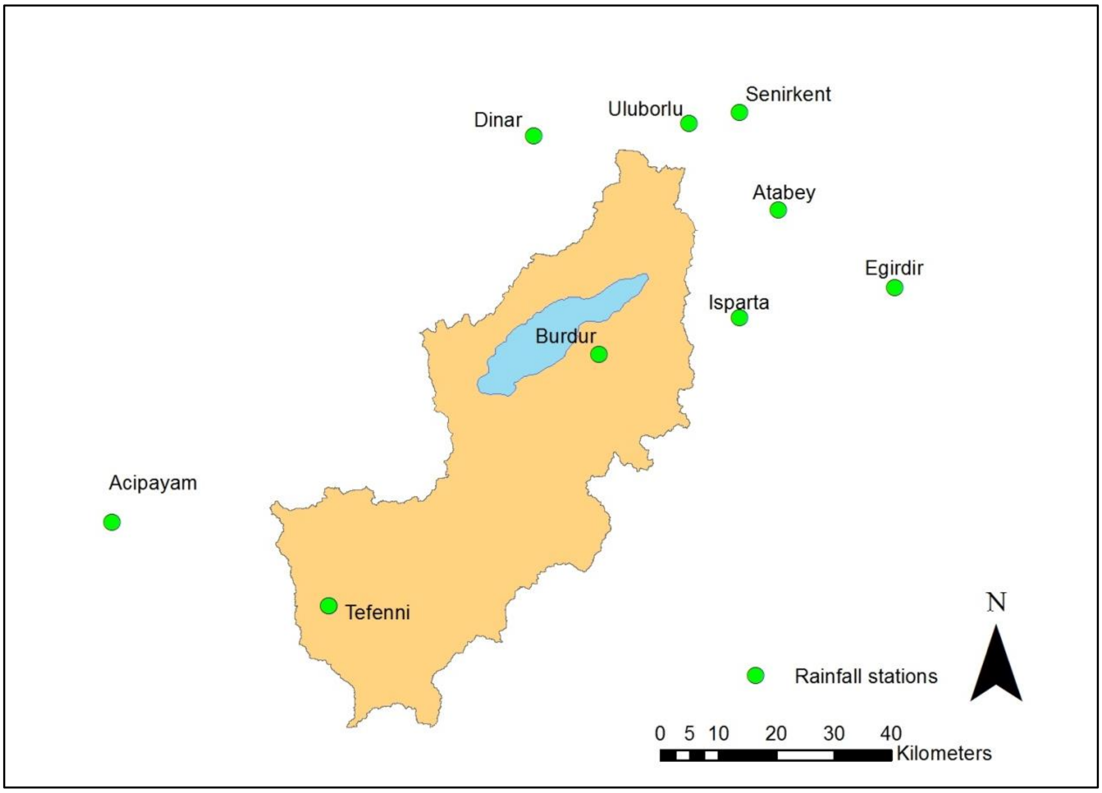

Figure 8 Rainfall stations

With respect to the specific objective of this study to analyse the closure error of the Lake Burdur water balance, it is noticed that the gauged rainfall network have limited capacity to represent rainfall variability in space and time that cause that rainfall estimation is constrained. To overcome the limitations of the gauged stations, in this study satellite-based rainfall assessments serve as an alternative rainfall source. Principle to such applications is that satellite estimates must be validated by comparison to gauged rainfall depths. In the remaining sections, the procedures to estimate rainfall consistently for a 5-year period over the study area are described. Considered aspects are screening of the gauged rainfall time series, assessments of errors, estimation bias correction factor, correction of satellite rainfall estimates and finally construction of rainfall time series at daily base for the use of rainfall-runoff modeling and lake balance assessment. Novel to the procedure is the completion of daily rainfall time series for runoff modeling, given the major data gaps in the time series made available for this study.

In the past two decades, the satellite rainfall estimate (SRE) algorithms have become of growing importance for estimating rainfall (Moazami et al., 2013). A number of SREs products exist now at time-space resolution suitable for hydrological and water resource applications such as in the present study. Globally well-known examples with wide application are the Precipitation Estimation from Remotely Sensed Information using Artificial Neural Networks(PERSIANN; Hsu et al., 2008), the National Oceanic and Atmospheric Administration (NOAA) Climate Prediction Center (CPC) Morphing technique product (CMORPH; Joyce et.al, 2004) and the Tropical Rainfall Measuring Mission (TRMM) Multi-satellite Precipitation Analysis (TMPA;Huffman et al., 2007). All the products are available at relatively high temporal (≤3 h) and spatial (≤0.25º) resolution. The high resolution not necessarily is preferred for all applications. For flash flood simulation, for instance, very high resolutions are needed to represent the highly dynamic convective, local, rainfall storms that cause flash floods. Therefore, flash floods simulation is more representative at high spatial and temporal resolution. To investigate the long-term lake water storage changes, monthly or yearly assessments have to be investigated that allow usage of satellite rainfall products of course resolution. By the objective of this study to simulate the lake water balance of Lake Burdur that is of relatively large scale, the TRMM product 3B42 was selected that is available at daily base at spatial resolution of 0.25° spatial.

SREs are provided by Geostationary satellites and by Polar-orbiting satellites. Geostationary satellites commonly use infrared (IR) channels to estimate rainfall rates using top of clouds temperature measurements while Polar-orbiting satellites use microwave channels to monitor the scattering of emitted passive microwaves (PMVs) within cloud systems. Some satellites have algorithms that combine the high temporal resolution of infrared data with the higher quality of microwave estimates, in addition to calibration of space-born data by using ground-based measurements(Kizza et al., 2012).To estimate the rainfall distribution, a combined algorithm satellite that is Tropical Rainfall Measuring Mission (TRMM) 3B42 was used in this study.

There are several reasons to select the TRMM 3B42 product for the study area. First, TRMM 3B42 algorithm provides daily base rainfall products covering the study area. This temporal resolution contributes to the use of the rainfall products for the runoff modeling to simulate Lake surface-water inflows. Moreover, the products are available for the period of study that is from 2010 to 2014.

TRMM 3B42 is a daily satellite rainfall product available at 3-hour temporal resolution and 0.25° by 0.25° spatial resolution. The product is available from 50 degrees south to 50 degrees north latitude *(http://trmm.gsfc.nasa.gov/3b42.html)*. The product combines information from IR sensors, MW sensors and in-situ measurements from ground stations. The 3B42 estimates are produced in four stages; (1) the microwave precipitation estimates are calibrated and combined, (2) infrared precipitation estimates are created using the calibrated microwave precipitation, (3) the microwave and IR estimates are combined, and (4) rescaling to monthly data is applied (Huffman et al., 2007).

In this study, the following approach was applied to estimate rainfall over the lake area and over the basin. Monthly data was obtained from nine stations that are operated by the Turkish State Meteorological Service (Table 1). First, daily satellite rainfall products were aggregated to monthly rainfalls to be compared with monthly gauged rainfall data for the period of 2010 - 2014. The aggregated rainfalls were compared with gauged monthly data. The results of comparison are available in Appendix B. Figure 8 shows the distribution of the available rainfall stations.7 stations are located outside the study area while only two stations are inside the study area. Most of the gauges are located in the northern part of the catchment, while there are only two stations in the southern part. To evenly distribute stations within the study area, new 9 stations were defined based on the central point of the pixel of TRMM product. Figure 9 shows the distribution of the redesigned stations.

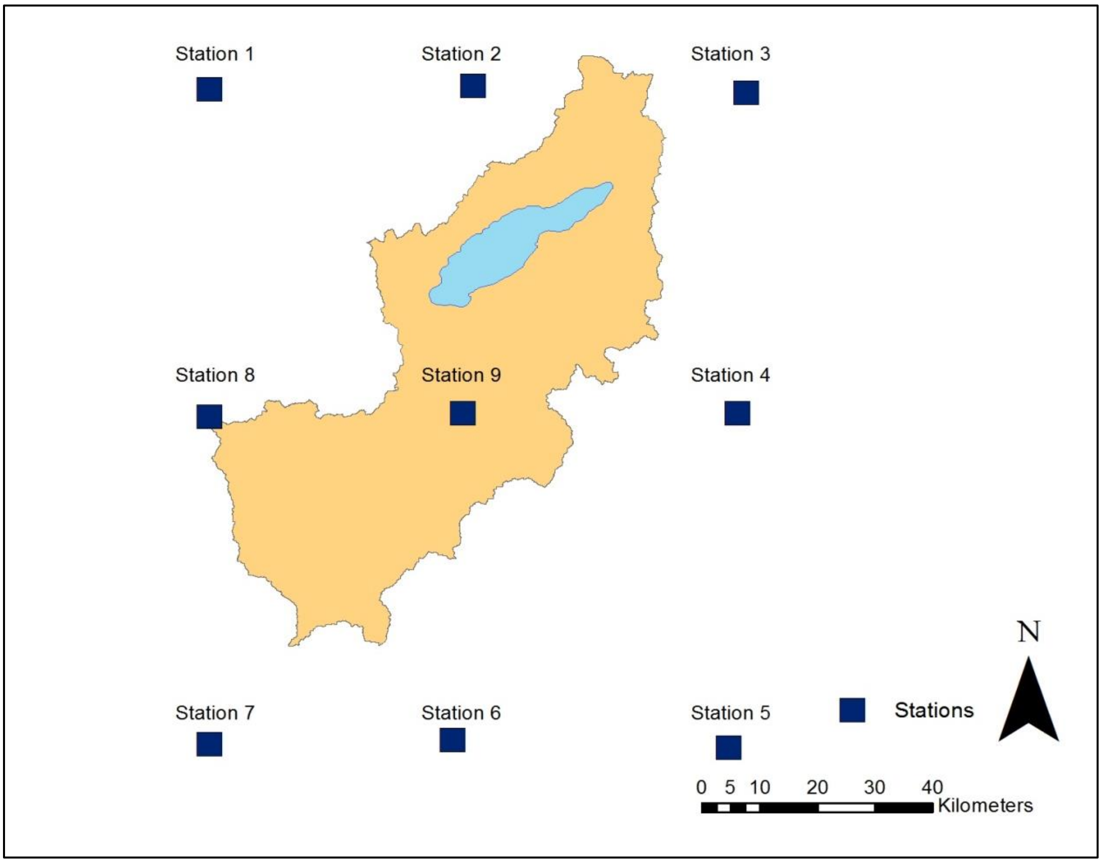

Figure 9 Location of redesigned stations

3.3.1. Bias estimation

Each satellite based rainfall product has error since SREs products and gauged products often do not match. Differences are considered errors that can be random errors or systematic errors. The precision is limited by random errors which are mostly unpredictable errors caused by precision limitations of the measurement device. By contrast, systematic errors occur systematically, either positive or negative (Aghakouchak et al., 2012). Therefore, SRE's require correction with the aim to correct for systematic errors only since random errors are difficult to identify. Systematic errors commonly is referred to as 'bias' and, therefore, correction is referred to as bias correction. Since in the study SREs are used for runoff modeling at daily base for calculation lake water inflows, the rainfall estimates have an important impact on closure of the lake water balance. To have reliable rainfall assessment, bias factors need to be calculated to correct TRMM rainfall estimates. Bias factor shows how the gauged data differs from TRMM data. If bias factor is higher than one, it means that the gauge systematically shows higher values than TRMM whereas a value lower than one implies that the gauge shows values systematically lower than TRMM. In the study, the bias factor was estimated based on certain window length, which is monthly bias factor estimation because rainfall data for nine stations were available at monthly time step.

To estimate the bias factor, an arbitrarily rainfall threshold had been set to 5mm following studies by Habib et al. (2014). Monthly rainfall (gauged and TRMM) products that have values under the defined threshold were eliminated from the bias factor calculations. Bias factor (BF) is formulated by the ratio between gauged rainfall rate and TRMM rainfall rate. For a selected month (t) and gauge (i), the monthly bias factor is calculated as follows equation:

$$BF = \sum_{t=1}^{t=12} \frac{\text{Gauged Rainfall Depth(i,t)}}{\text{TRMM Rainfall Depth(i,t)}}$$

The bias factor estimations were calculated for 5mm threshold at nine stations according to the availability of rainfall time series data for each station specified in Table 1. For some stations, bias factors were estimated between the available rainfall years of 2012 and 2014, for others the period 2010-2014 was used. First, the available gauged data were checked and ordered to match the period of the TRMM time series. Table 3 shows the rainfall depths (mm) that are estimated from TRMM product and are obtained rain gauged data.

Table 3 TRMM and gauged rainfall depths for Senirkent station

	TRMM					**Gauged**				
	2010	**2011**	**2012**	**2013**	**2014**	**2010**	**2011**	**2012**	**2013**	**2014**
January	65.3	59.3	82.3	63.1	65.6	88.8	0.0	0.0	107.8	98.4
February	109.1	61.4	85.9	65.5	34.7	157.2	0.2	0.0	129.0	18.0
March	33.0	51.7	42.7	34.3	58.4	55.2	8.8	35.4	44.0	79.6
April	74.6	64.1	53.4	66.4	41.8	0.0	56.2	7.0	60.4	43.0
May	40.6	98.5	84.8	52.7	100.7	0.0	107.4	78.4	18.4	130.2
June	80.0	66.3	17.0	22.5	66.1	0.0	70.2	1.0	12.0	57.2
July	21.5	5.0	17.8	38.2	13.1	4.8	0.0	8.6	11.6	4.0
August	18.0	10.3	25.2	11.0	14.7	0.0	0.0	20.6	16.4	2.0
September	38.5	30.9	20.7	13.2	117.8	37.6	1.6	0.8	1.2	147.4
October	92.0	78.7	30.1	73.0	63.8	77.6	0.6	14.2	101.2	35.0
November	13.8	6.3	18.6	53.9	42.0	0.0	0.8	0.0	75.2	31.4
December	88.3	48.5	95.0	20.7	92.5	0.0	0.0	93.0	11.4	131.4

After estimation of TRMM products and ordering, the values under the defined threshold eliminated and bias factors for each month were calculated according to the bias factor equation. Bias factor result for each month is shown in Table 4. The whole calculations of the bias factor for nine stations are in Appendix A.

Table 4 Result of bias factor

Threshold	Jan	Feb	Mar	Apr	May	Jun	Jul	Aug	Sep	Oct	Nov	Dec
5mm	1.52	1.31	1.06	0.74	0.91	0.82	1.15	1.15	1.11	0.81	1.07	0.98

3.3.2. Relative error estimation

Relative error (R.E.) indicates the ratio between the difference of TRMM and gauged rainfall depth to the gauged rainfall depth. In this study, gauged measurement and TRMM estimates were compared also by calculating the relative error. It is estimated as follows:

$$R.E\sum_{t=1}^{t=12}\frac{TRMM\ Rainfall\ Depth - Gauged\ Rainfall\ Depth(\mathrm{i,t})}{Gauged\ Rainfall\ Depth(\mathrm{i,t})}$$

From the values, which are in Table 3, the difference between TRMM and gauged rainfall were calculated and were divided by the gauged rainfall depth. Relative error was estimated in order to see the reliability of the estimated rainfall. Lower relative error means better estimation on the calculations. Table 5 shows the result of Senirkent station. It is noted from the table that among the year relative error has low values except on March and July. The higher R.E. values may be result of the lower number of rainy days and mismatch with satellite products. The whole calculations of the relative error estimations for nine stations are in Appendix A.

Table 5 Relative error estimates at the Senirkent station

	Jan	Feb	Mar	Apr	May	Jun	Jul	Aug	Sep	Oct	Nov	Dec
5mm	-0.34	0.04	0.84	1.71	0.41	0.32	1.68	-0.05	-0.09	0.46	0.03	0.18

3.3.3. Methods

ILWIS software was used for rainfall product correction process. The process is shown in flowchart (Figure 10). A point map with rainfall stations was created to calculate bias factor for each pixel of the area. First, the point map was generated and then the bias factor values were entered for each station. Then nearest neighbour interpolation method also called 'Thiessen method' was applied to interpolate the bias factor values for each pixel. A detailed procedure of rainfall calculation over the lake and basin by ILWIS is available in Appendix C.

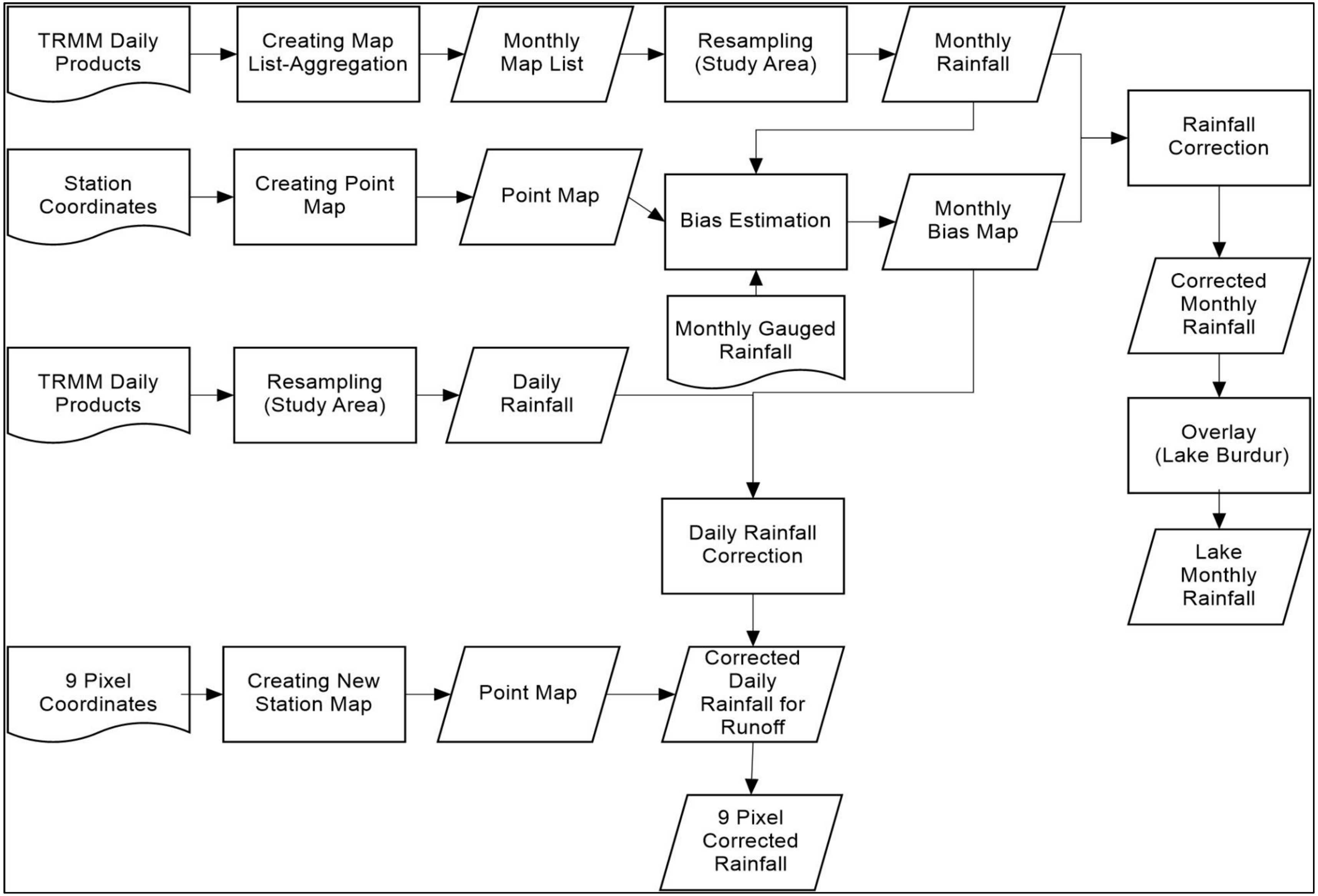

Figure 10 Flow chart of rainfall estimation

3.4. Evapotranspiration estimation

3.4.1. Introduction

Evapotranspiration (ET) is an important process for hydrological studies and its assessment is required for water resources planning, environmental studies as well as irrigation management (Gallego-Elvira et al., 2013). Evapotranspiration is the summation of evaporation and transpiration. Evaporation occurs when water move from waterbodies to the atmosphere, while transpiration is a loss of water from the plants. Since ET consists of evaporation and transpiration, it is very difficult to obtain for hydrological studies. However, there are different techniques available to obtain evapotranspiration. Ground-based and remote sensing techniques are two of available techniques to estimate evapotranspiration.

ET can be estimated by using some methods that requires ground observations. Sap flow (Allen & Grime, 1995), eddy covariance (Berbigier et al., 1996) , lysimeter are some example of the ET estimation methods. Lysimeter, for instance, measures direct ET by isolating and continuously monitoring a vegetated area (D. K. Fisher, 2012). Fisher (2012) had used two weighing lysimeters to observe ET in a specific study area. In addition to lysimeter method, Allen & Grime (1995) used 50 x 50 m area for sap flow measurements for ET estimation, and the measurements were restricted to a shrub species. Different vegetation, forest plantation, were used to estimate ET by using eddy covariance technique at a smaller spatial scale (J. B. Fisher et al., 2005). Although the methods are based on the ground measurements, which determine ET accurately, estimation of the ET for a large area is difficult by using point scale measurements. Moreover, the point scale measurements are also time-consuming for ET estimation for large areas. To estimate ET for hydrological studies, spatial distribution is essential for vast areas. For regional scale studies, spatially distributed ET maps can be obtained by using remote sensing techniques (Gallego-Elvira et al., 2013). Beside to spatial distribution, to overcome the limitations of ground measurements, satellite based ET estimation is an appropriate technique.

Evapotranspiration is derived by many techniques using remote sensing applications. Surface Energy Balance System (SEBS) is one of the remote sensing techniques to estimate evapotranspiration data at various scales with acceptable accuracy (Su, 2002). The Surface Energy Balance Algorithm for Land (SEBAL) is another remote sensing technique, which applies energy balance assessment to obtain actual evapotranspiration (Bastiaanssen et al., 1998). MOD16 (from MODIS, Moderate Resolution Imaging Spectroradiometer), and LANDSAT images (Lagomasino et al., 2015) also used for daily ET estimation.

All ground based or remote sensing methods have some limitations and strengths. The techniques that are mentioned above require intensive studies of ET, and some techniques require daily meteorological data. The best-suited technique is to select based on the data availability, time and space scale and accuracy and reliability.

3.4.2. Potential evapotranspiration estimation

Potential evapotranspiration (PET) is a representation of the amount of water that can be evaporated and transpired in case of sufficient water availability. PET requires energy for the processes and the main source of the energy is received from the sun. Humidity and wind speed are also the other important climatic factors that affect PET rates. Not only climatic factors, but also crop factors such as crop types, crop roughness etc. affect the PET rates.

Potential evapotranspiration is usually measured indirectly by using climatic factors mainly wind speed, radiation, temperature and humidity. Additionally, for PET estimation the surface type, the soil type, vegetation cover and water body type (lake or oceans) data are needed. In this study, the selected REW model requires daily potential evapotranspiration rates as input variable. Since there is no consistency in available meteorological data of the Lake Burdur basin, in this study satellite based Famine Early Warning Systems Network (FEWS NET) PET was studied for daily PET estimation.

The operational modeling of global daily potential evapotranspiration was founded by the U.S Geological Survey (USGS)/Famine Early Warning Systems Network (FEWS NET) at the Earth Resources Observation and Science (EROS) center. The main objective of model development was to monitor drought and flood conditions in data sparse region of the world (Senay et al., 2008). Senay et al. (2008) stated that the model provides daily potential evapotranspiration rate at 1.0-degree resolution by using Penman-Monteith method for its accuracy, and the meteorological data needed for Penman-Monteith is extracted from Global Data Assimilation System (GDAS), which has six-hourly meteorological data.

In this study, daily potential evapotranspiration rates between the years 2010 and 2014 were extracted by using ISOD TOOLBOX in ILWIS. A detailed procedure of PET estimation is available in Appendix D.

3.4.3. Open water evaporation

Evaporation is the conversion of the liquid water into the water vapour. The amount of evaporation depends on several factors, such as meteorological factors or water body properties. Meteorological factors that affect evaporation are net radiation, humidity and diffusion processes. Net radiation is the difference between incoming radiation and outgoing radiation. Humidity depends on the air temperature. If the temperature of the air increases, relative humidity increases that might result with high evaporation rate. The rate of evaporation might also generally influenced by diffusion processes, like turbulent air movement. Beside the meteorological factors, the properties of water body affect the evaporation rate. Water depths, size of surface are some properties of water body. If the water depth is high and surface area is large, it results in higher evaporation rate compared to small size area and lower depth of water body. The larger the water body, the greater will be the water that is evaporated(Finch & Hall, 2001).

Estimation of evaporation from open water is required for water balance studies, since it is a one of the main losses. A wide variety of methods for estimating open water evaporation is available; such as pan method, mass balance, Penman Monteith etc. Pan evaporation is an easy way to estimate evaporation in a visible way. Around the world, mostly A Pan, which is a circular galvanized iron tank, is used. It has a diameter of 1.21 m and is 255 mm deep. A hook gauge is used to measure the level of water daily (Frank ,1992).

Table 6 A-Pan data

Evaporation (mm)	Jan	Feb	Mar	Apr	May	Jun	Jul	Aug	Sep	Oct	Nov	Dec
2010	0.0	0.0	0.0	11.0	17.6	18.1	24.8	28.1	17.6	11.6	0.0	0.0
2011	0.0	0.0	0.0	9.0	12.8	20.1	29.0	19.0	19.9	7.8	0.0	0.0
2012	0.0	0.0	0.0	15.4	15.3	29.2	34.4	28.9	22.7	9.6	0.0	0.0
2013	0.0	0.0	0.0	10.7	20.3	25.1	26.4	24.6	17.3	11.9	0.0	0.0
2014	0.0	0.0	0.0	15.5	23.6	32.0	40.7	38.2	27.4	16.1	0.0	0.0

Although evaporation pan method is known to have important uncertainties both in magnitude and in timing, it is extensively used in Turkey because of its simplicity. By using A-Pan evaporation that is obtained from DSI shown in Table 6, the lake water balance assessment is studied.

Figure 11 Evaporation pans
Source : *http://www.hko.gov.hk/wxinfo/aws/evap_pan.htm*

3.5. Hydrological modeling

3.5.1. Introduction

Hydrological models are simplified systems that represent part of the real world hydrological systems, and they have become gradually important for water resources management because of several reasons. They are used for climate and land use change as well as their impacts on the water budget estimation. Moreover, they can be used to predict extreme hydrological events such as drought and flood. Prediction of the events can also be helpful to quantify the risk that may occur in the coming decades, and understand the reasons, which might also occur due to anthropologic affect.

Hydrological models are used to predict streamflow in space and time domain. A wide variety of hydrological models has been developed over the past decades. Many of the models rely on similar assumptions, while some of the models have distinctive difference. Based on spatial distribution, the hydrological models are mainly classified into three main categories: Lumped models, semi-distributed models and distributed models. Lumped conceptual models (also referred to black-box models or empirical models) have a simple structure that inputs and outputs of a hydrological system are simulated (Rientjes, 2014). In these lumped models, the weakness of the model is the catchment transfer processes and any spatial distribution of model parameters or model variables are ignored. Mostly the models are applied for large catchments. GR4J, HBV0, IHAC and TOPMO are some examples to lumped hydrological models. GR4J model (which stands for modele du Genie Rural a 4 parametres Journalier), for instance, is a daily conceptual rainfall-runoff model, which requires only four parameters to estimate stream flow (Perrin et al., 2003).

Contrary to lumped model, semi-distributed models are basic physically based model, which divides the catchment into sub-catchments. For each sub-catchment, input information is required, but demands less input data. Abu El-Nasr et al. (2005) used a semi-distributed model, SWAT (Soil and Water Assessment Tool), to compare with distributed model. Distributed models are physically based models that represent spatial heterogeneity providing detailed descriptions of hydrological processes. Physically based models rely on the physical laws, which consist of formulations based on conservation equations for mass, momentum and energy. Distributed physically based models require a large number of spatially distributed data to reflect the catchment properties in details (Li et al., 2012).

Although the models are useful to represent the hydrological process, depending on several aspects, the prediction of the model runoff results have uncertainties. The uncertainties can be because of several aspects: required data for the model might have some errors, the structure of the model can cause some uncertainties and the model parameters for each hydrological model have uncertainties in runoff estimation. Butts et al. (2004) evaluated model structure uncertainty and the performance of combinations of different model structures.

REW (Representative elementary watershed) is a semi-distributed model that was chosen in this study because of several factors. First, compared to lumped model semi distributed give better estimation on streamflow by discretizing each catchment into REWs that enable to have hydrologic relations at the REW scale (Fenicia et al., 2005). Semi distributed model, moreover, provides spatial heterogeneity that is necessary for the Lake Burdur basin since the area consists of different catchments having different rainfall and PET pattern. As REW model also enables to interpolate the input values for each discretized REWs, it is selected for this study.

3.5.2. REW model

REW approach consists of modeling the sub-catchments according to the discretization of the catchment into control volumes (Reggiani & Rientjes, 2005). Principally, the control volumes are chosen according to the different characteristics of the system. Reggiani & Rientjes (2010) pointed out "An implementation of the approach requires closing unknown REW-scale mass fluxes and forces exchanged across the REW-internal control volume boundaries and between REWs."

One of the main advantages of the REW approach is that can be applied at different spatial scales. Moreover, this approach can be applied for a square grid element and also to an irregular mesh of elements. By applying the irregular mesh of elements, model represents the natural properties of the landscape. In addition to spatial scale features of the approach, hydrological problems can be studied over a broad range of temporal scale (Reggiani & Rientjes, 2005). Although the REW approach has a lot of advantages, its application for complex geologies and multiple aquifers might not be suitable (Fenicia et al., 2005). Additionally, this approach mostly can differ from one case study to another, having different geologies (Reggiani & Rientjes, 2005).

Model consists of four main processes, which are TARDEM watershed analysis, REW analysis, pre-processor, solver and postprocessor.

3.5.2.1. The Tardem watershed analysis

TARDEM is a terrain analysis software that is used to extract the drainage network and delineate catchments to prepare for the model (Reggiani, 2012). The analysis involves drainage direction derivation, contributing area calculation and derivation of path lengths based on given Strahler order. Finally, according to the given outlet point coordinates, stream network is extracted, and sub-catchments are delineated.

The Shuttle Radar Topography Mission purpose was to obtain about 80 percent of the Earth's land surface, between 60°N and 56°S providing a global high-quality DEM at 90m resolution (Rabus et al., 2003). 90m of the DEM of the study area was used as an input for TARDEM model.

3.5.2.2. REW analysis

REW analysis is a process consists of defining REWs as 3D spatial regions, establishing inter-connectivity between REWs and calculating geometric quantities of REW (Reggiani, 2012) . This analysis is required as an input for the preprocessing step.

3.5.2.3. Preprocessor, solver and postprocessor

The main process is to assign model parameters, initial and boundary conditions to the model for each REWs , and to prepare meteorological forces for each REWs by interpolating. Meteorological forces consist of precipitation, potential evapotranspiration, temperature, relative air humidity and daily temperature excursion (Reggiani, 2012). After pre-processor, solver process performs finally hydrological simulations by solving the equations defined, and postprocessor converts the executed files into desired formats. Parameter files and meteorological forces that were used for this study is shown in Appendix E.

3.5.3. Governing equations

REW model discretize the catchment into a number of sub-catchments called REWs. According to the Strahler order, the numbers of catchments were extracted. Each REW consists of five different zones, which are saturated, unsaturated, channel reach, concentrated overland flow and saturated overland flow zones. These five different zones are simulated based on mass conservation and momentum balance equations (Zhang et al., 2005). Figure 12 illustrates 3D spatial entity of the REW model.

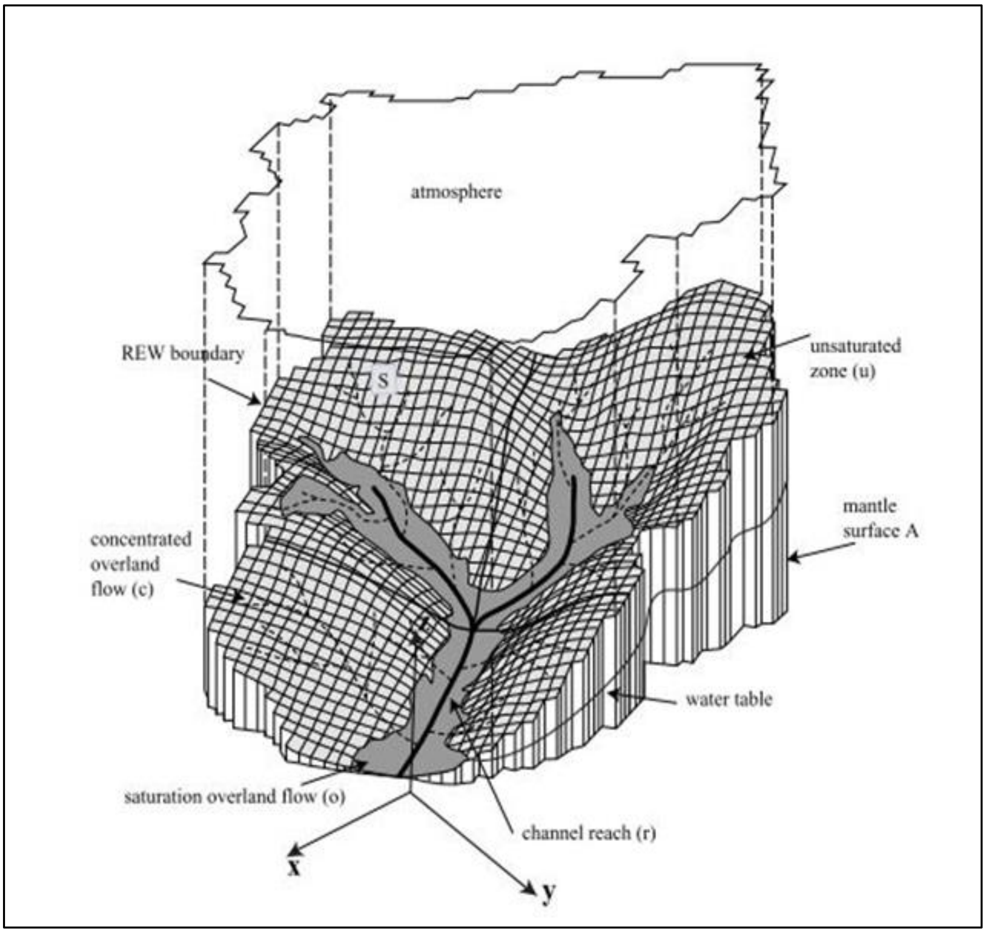

Figure 12 3-D spatial entity of a REW *Source:(Reggiani, 2012)*

Table 7 below show the mass balance equations and Table 8 shows momentum balance equations of each zone that were calculated for each REW in the study area. The superscripts u, s, o, and r refer to the unsaturated zone, saturated zone, saturated overland flow zone and river reach, respectively (Reggiani & Rientjes, 2005).

Table 7 Mass balance equation

Number	Mass balance equations	Zone
1	$\sum \epsilon \frac{\mathrm{d}}{\mathrm{d_t}}(\mathrm{s^u y^u \omega^u}) = \mathrm{e^{us}} + e^{u\,top} + e^{u}_{wg}$	Unsaturated zone
2	$\sum \epsilon \frac{\mathrm{d}}{\mathrm{d_t}}(\mathrm{y^s \omega^s}) = \sum_{i=1}^{N} \mathrm{e^{sm\,i}} + e^{su} + e^{so} + e^{sr}$	Saturated zone
3	$\mathrm{l^r} \sum \frac{\mathrm{d}}{\mathrm{d_t}}(\mathrm{m^r}) = \mathrm{e^{ro}} + e^{rs} + e^{r\,in} + e^{r\,out}$	Channel reach zone
4	$(\mathrm{s^u y^u \omega^u})\frac{\mathrm{d}}{\mathrm{d_t}}\mathrm{v^u} - \sum g\epsilon(\mathrm{s^u y^u \omega^u})\frac{\mathrm{d}}{\mathrm{d_t}}\mathrm{v^u} = \sum_{i=1}^{N} \mathrm{T^{um\,i}} + T^{us} + T^{utop} + T^{u}_{wg} + T^{u}_{wm}$	Overland Flow

Table 8 Momentum balance equation

Number	Momentum balance equations	Zone
1	$(\mathrm{s^u y^u \omega^u})\frac{\mathrm{d}}{\mathrm{d_t}}\mathrm{v^u} - \sum g\epsilon(\mathrm{s^u y^u \omega^u})\frac{\mathrm{d}}{\mathrm{d_t}}\mathrm{v^u} = \sum_{i=1}^{N} \mathrm{T^{um\,i}} + T^{us} + T^{utop} + T^{u}_{wg} + T^{u}_{wm}$	Unsaturated zone
2	$\sum \epsilon(\mathrm{y^s \omega^s})\frac{\mathrm{d}}{\mathrm{d_t}}\mathrm{v^s} - \sum g\epsilon(\mathrm{s^u y^u \omega^u})\frac{\mathrm{d}}{\mathrm{d_t}}\mathrm{v^u} = \sum_{i=1}^{N} \mathrm{T^{um\,i}} + T^{us} + T^{utop} + T^{u}_{wg} + T^{u}_{wm}$	Saturated zone
3	$\mathrm{l^r m^r}\frac{\mathrm{d}}{\mathrm{d_t}}(\mathrm{v^r}) = \mathrm{gm^r} l^r + T^{rs} + T^{r\,in}$	Channel reach zone
4	$\sum \mathrm{y^o \omega^o}\frac{\mathrm{d}}{\mathrm{d_t}}(v^o) = \sum \mathrm{g\ w^o} y^o + T^{os} + T^{or}$	Overland flow

3.5.4. Runoff estimation

3.5.4.1. Catchment delineation

Catchment delineation by TARDEM is the first process of the REW model. This process of the model requires outlet point in order to delineate catchment area. If a study area is a drainage basin or catchment, then there is only one outlet point that required to entry into the model. However, closed lake basins do not have any outlet point. Although the streams drain into the lake, any point from the lake cannot be considered as an outlet point. Because outlet point needs to be the lowest point of the catchment in order to find gradients from that point to the boundaries to delineate catchment. However, any point from the lake does not have any change in gradient among the lake area; therefore, the model cannot find any gradient to delineate the catchment boundaries. As a solution to this problem, more than one outlet points need to be defined in order to drain streams to the lake separately.

Since Lake Burdur basin is also a closed basin, identifications of different catchments outlets are required. For this purpose, DEM of the study area was separated into several DEMs by checking the streams network of the basin area that is obtained during the fieldwork. Figure 13 shows separated DEMs that were used in the model to delineate stream network of the area and catchments. Contrasting colours were used to indicate different section of them that were run separately. Each DEMs were run into the model separately and flow directions were visualized in order to define outlet points.

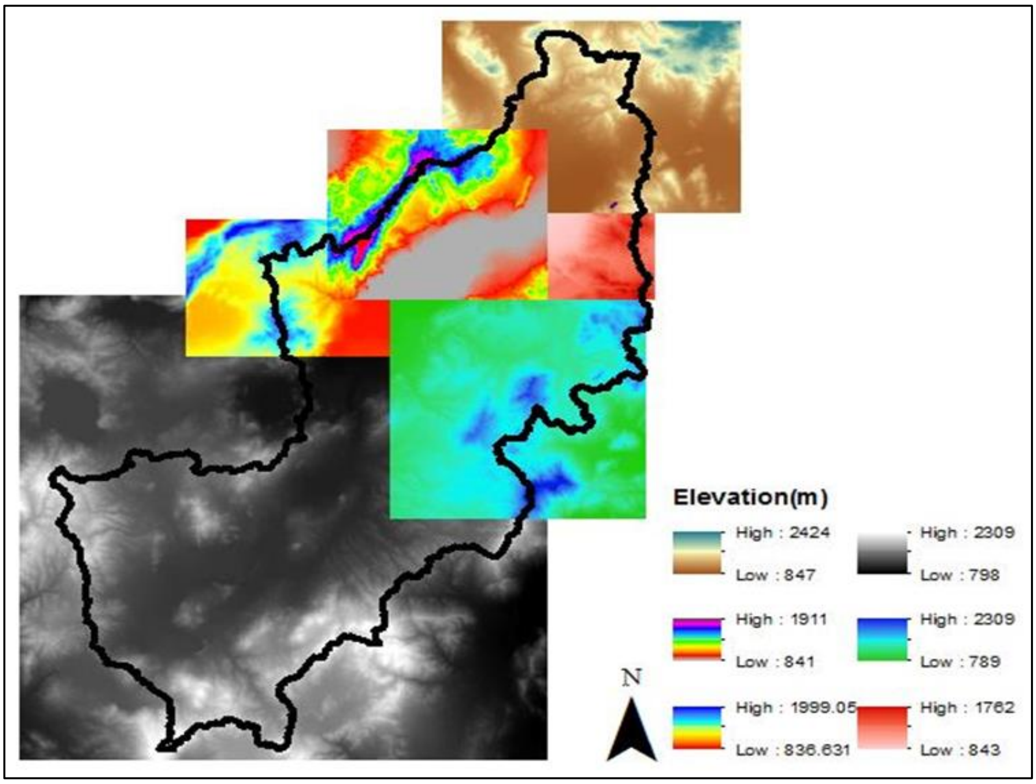

Figure 13 Separated DEM of the Lake Burdur basin area

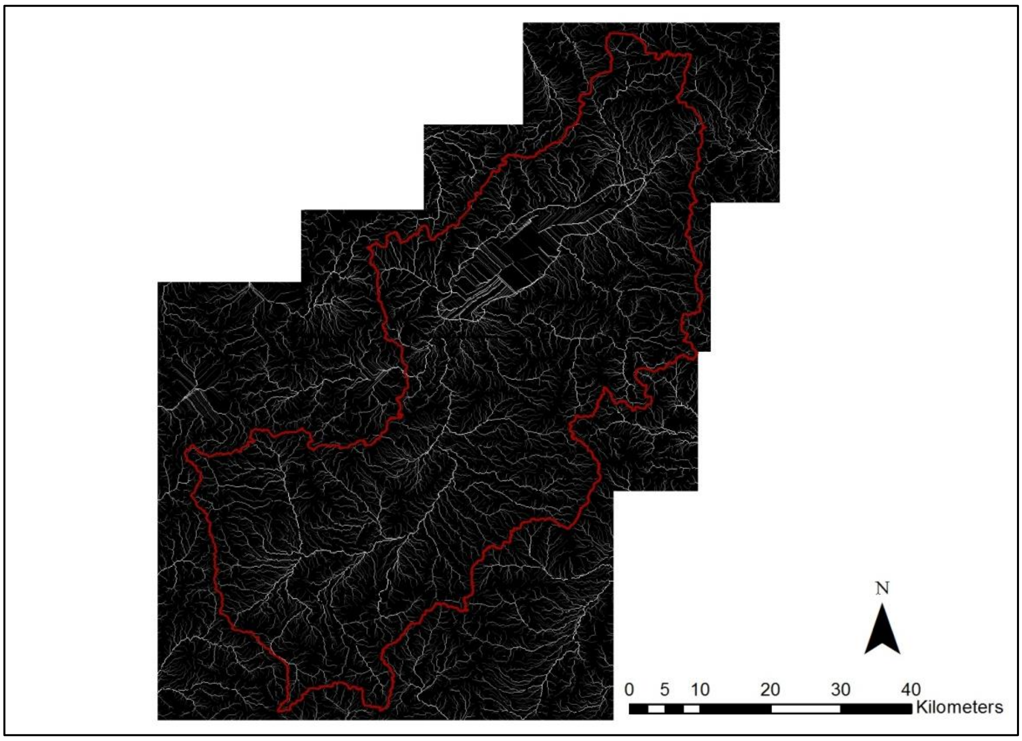

Figure 14 Extracted stream network of Lake Burdur basin area

Figure 14 illustrates the stream network of the basin, and Figure 15 shows the REWs analysis results of the entire basin. REWs are delineated by defining Strahler order as threshold (Reggiani & Rientjes, 2005). In the model Strahler order ranges from one to three. Lower Strahler order, 1, is referred to higher number of REWs while Strahler order 3 is referred to low number of REWs. Catchment 3 was analysed by choosing Strahler order 3, while for the rest of catchment Strahler order 1 was used. Table 10 shows the number of REWs according to the catchment size and Strahler order. As a result of the calculations, five catchments were extracted within the Lake Burdur basin area. However, because of the large number of small streams that cause a large number of catchments in the basin area, some areas were not extracted by using separate models but instead regionalization technique was used described in following section. 'Non-delineated' catchment is referred in this study to those catchments that were not extracted by the model. Non-delineated catchments streamflow were estimated according to the neighbour catchments streamflow and is described further in section 3.5.4.2. The non-delineated areas were named as Area A, B and C. Figure 15 shows the extracted catchment areas with REWs and non-delineated areas. Table 10 illustrates the extracted catchment areas, Strahler order and number of REWs.

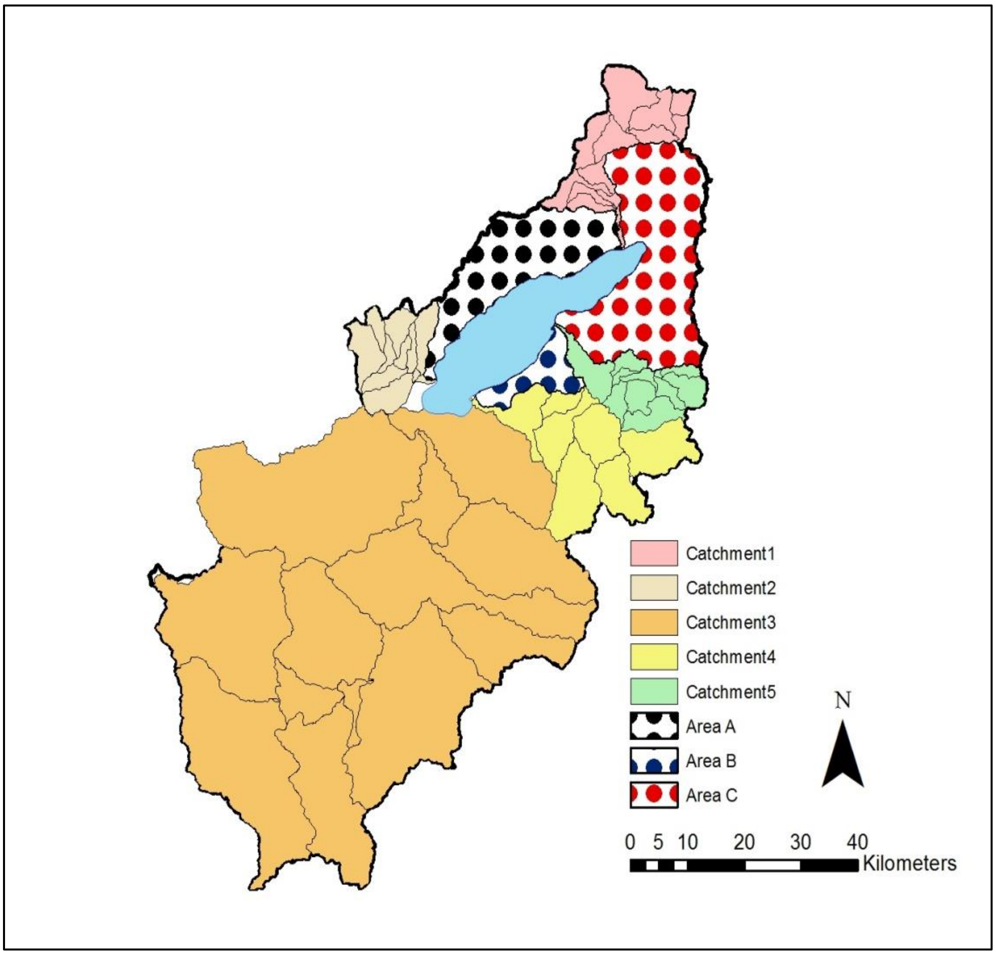

Figure 15 Catchment delineation - REWs extraction

3.5.4.2. Regionalization

Regionalisation is the method that used to transfer information from selected catchments to the catchment of interest (Blöschl et al., 1995). Although there are many different regionalization processes are available, there are two main approach based on principle of similarity by spatial proximity and on similarity of catchment characteristics (Deckers et al., 2010). Deckers et al. (2010) stated that 'the first approach based on the rationale that catchments of close proximity have a similar flow regime since climatic, topographic and physio- graphic settings are comparable'. In this study, first approach was applied by defining the neighbour catchments. The estimations of non-delineated area runoff was calculated according to the neighbour catchments streamflow. First specific streamflow where simulated streamflow is divided by respective area was calculated and then multiplied by the non-delineated area to predict streamflow. For each non-delineated area, two neighbour catchments were defined. According to two neighbour catchments, specific streamflow were calculated and finally average of the two predicted streamflow was used for non-delineated area. Table 9 shows the areas that regionalized and corresponding neighbour catchments.

Table 9 Non-delineated area and neighbour catchments

Regionalization Applied	Neighbour Area 1	Neighbour Area 2
Area A	Catchment 1	Catchment 2
Area B	Catchment 4	Catchment 5
Area C	Catchment 1	Catchment 5

Table 10 Catchment properties

	Catchment Area(km2)	Strahler order	Number of Rews
Catchment1	141.0	1	15 Rews
Catchment2	105.7	1	11 Rews
Catchment3	1955.2	3	13 Rews
Catchment4	242.6	1	7 Rews
Catchment5	86.9	1	11 Rews

3.5.5. Runoff estimation

After catchment delineation, time series of the input data were prepared from 2012 to 2013 in order to compare with gauged streamflow data. Figure 16 shows the stream network of the study area. For five catchments, stream network extraction was applied separately for each catchment. However, before to apply for the other catchments, first the model was run, warmed up and simulated streamflow was compared to gauged streamflow data. Comparison of observed and simulated streamflow is necessary to see the errors between two data sets. For this purpose, catchment 4 was selected where streamflow measurements were taken from Bozcay station. Simulated streamflow from catchment 3 was compared with gauged streamflow data. Figure 17 shows the comparison of simulated streamflow and gauged streamflow. The graph shows that the gauged streamflow have very low values, and does not show any seasonal changes, although the area has different seasons and rainfall patterns throughout the year. That can be because of several reasons. First, the instruments that is been used could have some errors. Secondly, the units might be written wrongly, since the streamflow of the big area results with very low runoff, which is not reliable. Because of these possible reasons, simulated streamflow by REW model was used for the entire basin, and lake level estimation.

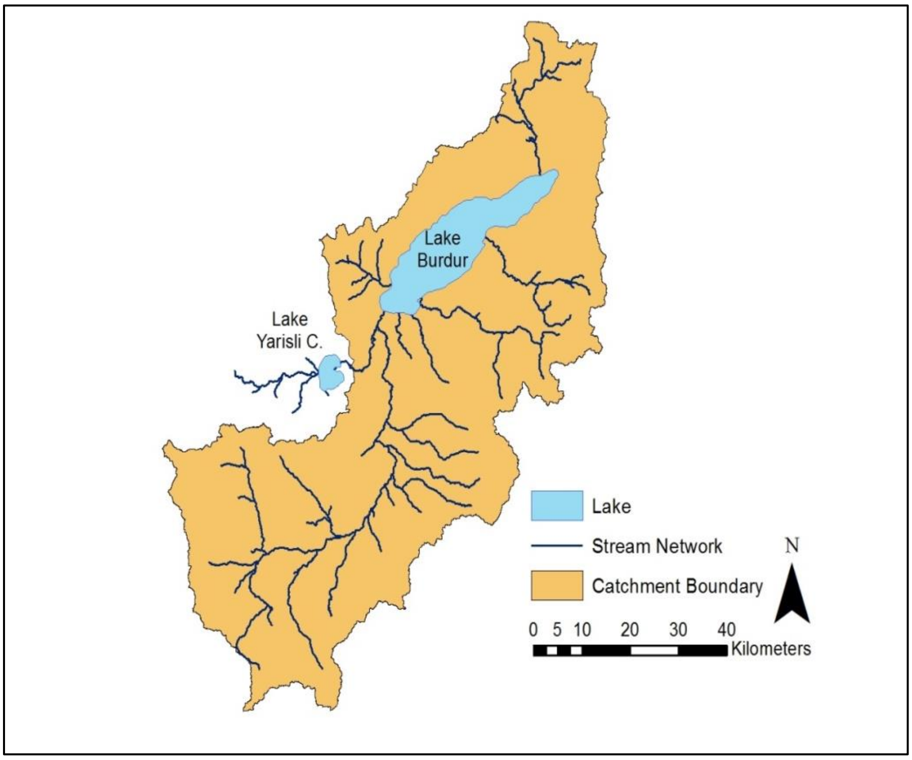

Figure 16 Streamflow network of the Lake Burdur basin

In contrast to the gauged streamflow simulation, simulated streamflows show plausible results, because simulated streamflows have seasonal changes that depend on the rainfall and PET pattern. Additionally, plausible base flow is also observed from simulated streamflow with expected small changes in the entire period. However, to have more idea about reliability of the simulated streamflow, runoff coefficient was studied explained in the result section 4.3.2. Since the calibration of the simulated streamflow is not possible due to unrealistic gauged streamflow, time series of the whole period were prepared and model was only warmed up detailed in the following section.

3.5.5.1. Warming the model

Warming the model provides reliable simulation by bringing the hydrologic processes to an equilibrium condition (Issakul et al., 2007), and it is applied in the model in order to minimize the effect of initial conditions on the model simulation results (Reed et al., 2004). Mainly, warming the model helps the model to adjust to the successive periods. In the REW model, warming the model was applied to the state variables between 2012 and 2013. State variables of the first day of the model, which is 01/01/2012, changed with the last date of the period, 31/12/2013 and then the model was run again for the catchment 3. By using ending state variables as starting state variables, the state variables of the starting day become steady. The warming the model processes were applied until the initial conditions reach steady state. In this study, after ten times of warming the model the initial conditions reached the steady condition.

Figure 18 shows the streamflow pattern for 10 warming processes. The graph shows that irregular starting base flow conditions reached to the stable condition after ten warm up processes. After obtaining steady conditions, the state variables of the tenth warming process was applied for the other catchments and streamflows were estimated for the extracted catchments.

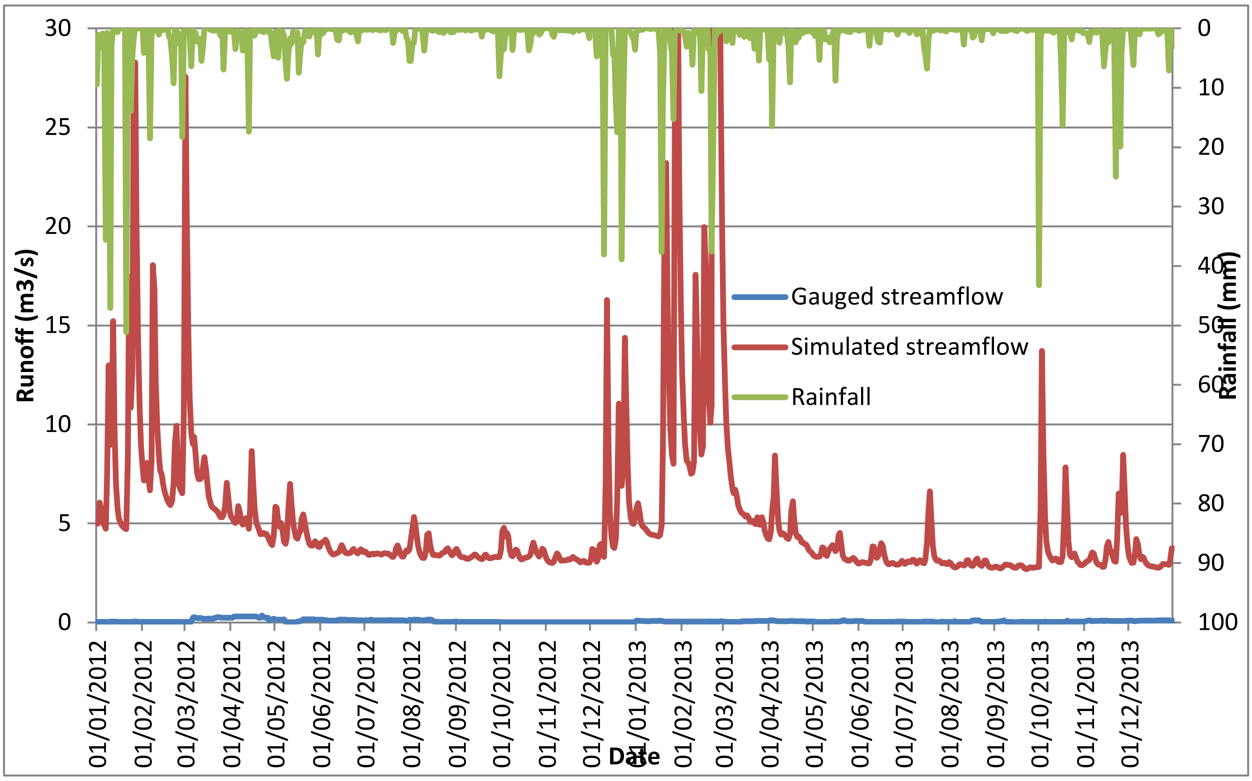

Figure 17 Comparison of simulated and gauged streamflow

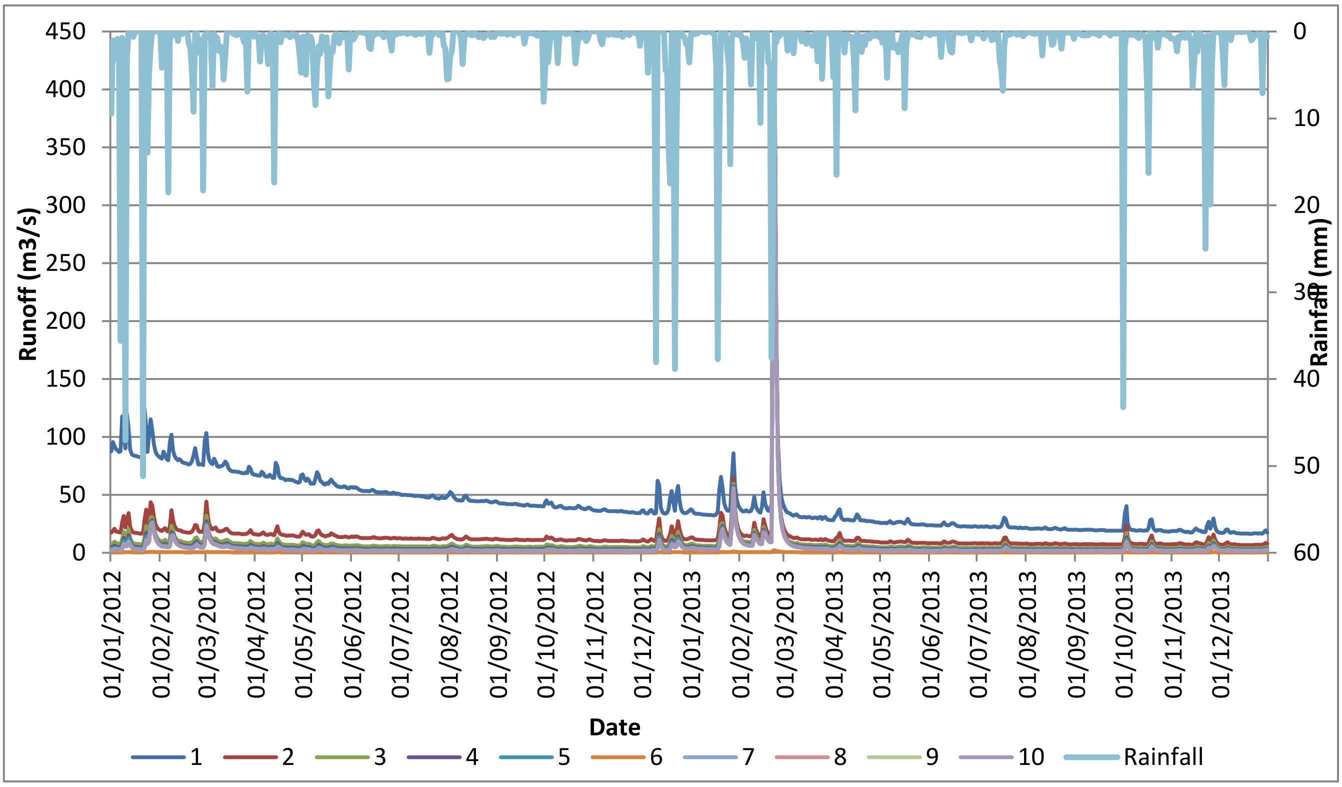

Figure 18 Streamflow results after warming processes

4. RESULTS AND DISCUSSION

4.1. Rainfall results

Over five years, daily rainfalls of Lake Burdur basin were estimated by correcting satellite products with bias factor. Figure 19 shows yearly rainfall distribution (mm) of the catchment area to give better understanding about the basin rainfall characteristics. The maps were prepared by using mean annual corrected rainfall for each year in the nine stations. Nearest neighbour method, which is an interpolation technique, was used to simulate the rainfall distribution over the basin area. Five years rainfall distribution shows variety during the years. The higher rainfall over the basin area is in the northern part of the area from 2010 to 2013 while it differs in 2013 and 2014. In 2013, higher rainfall amounts were recorded in the northern and southern part of the basin whereas in 2014, higher rainfall amounts only occurred in the northern part of the lake. The central part of the area has the lower rainfall distribution among the basin compared to the boundaries. The reason might be the lower rainfall depths in station 9 since it interpolates according to the nearest station.

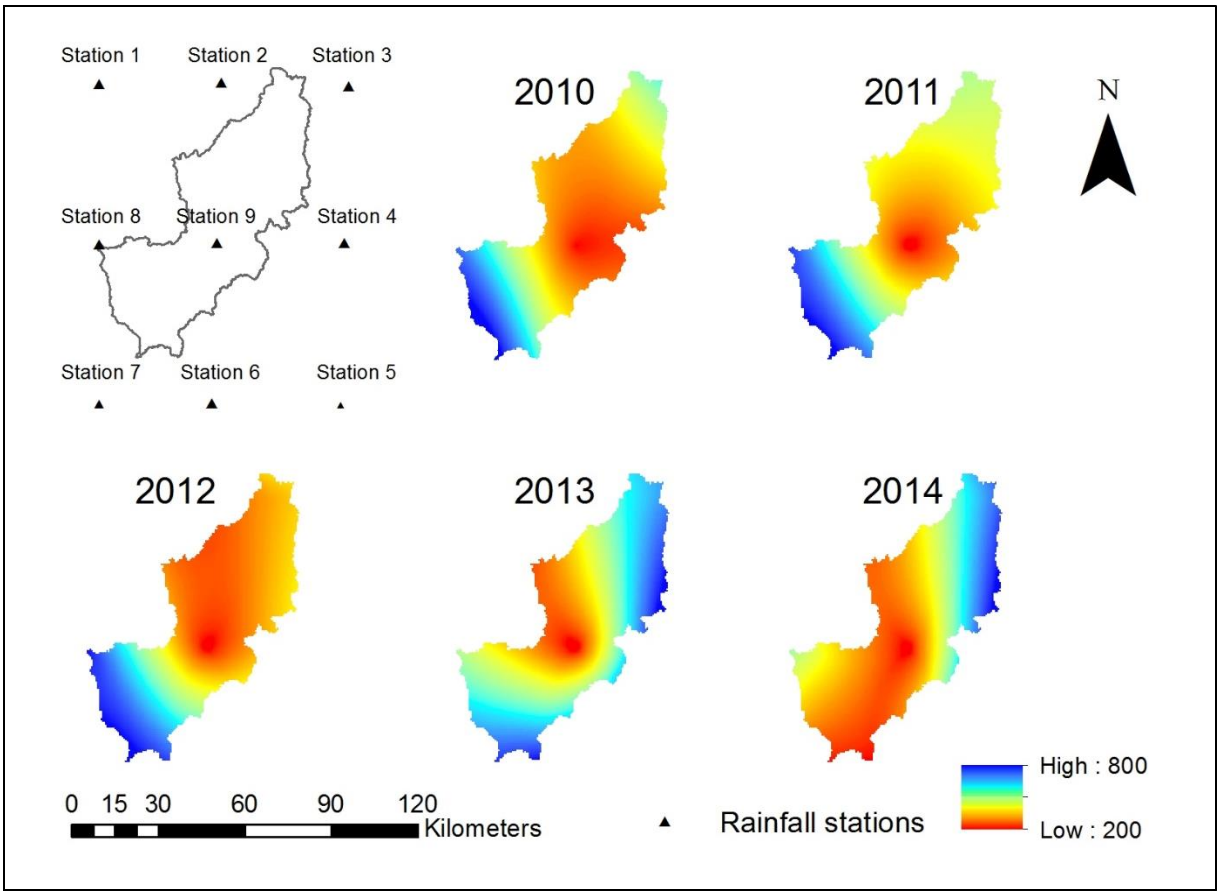

Figure 19 Annual rainfall distribution over the catchment

Rainfall is one of the main inputs for the lake water balance; therefore, it is important to see the overall rainfall pattern over the lake. Satellite based corrected rainfall were calculated over the lake areas. Figure 20 shows the areal monthly rainfall for five years to assess differences between months. Although within the years, monthly rainfall depths show variety, in general summer season has the lowest rainfall depths throughout the years. Figure 21 shows the mean monthly rainfall for nine stations over five years. It is noted that winter season (December, January, and February) has the highest rainfall depths following spring (March, April, May) and autumn (September, October, December). In this study, wet season is referred to December, January and February months whereas dry season is referred to July, August September.

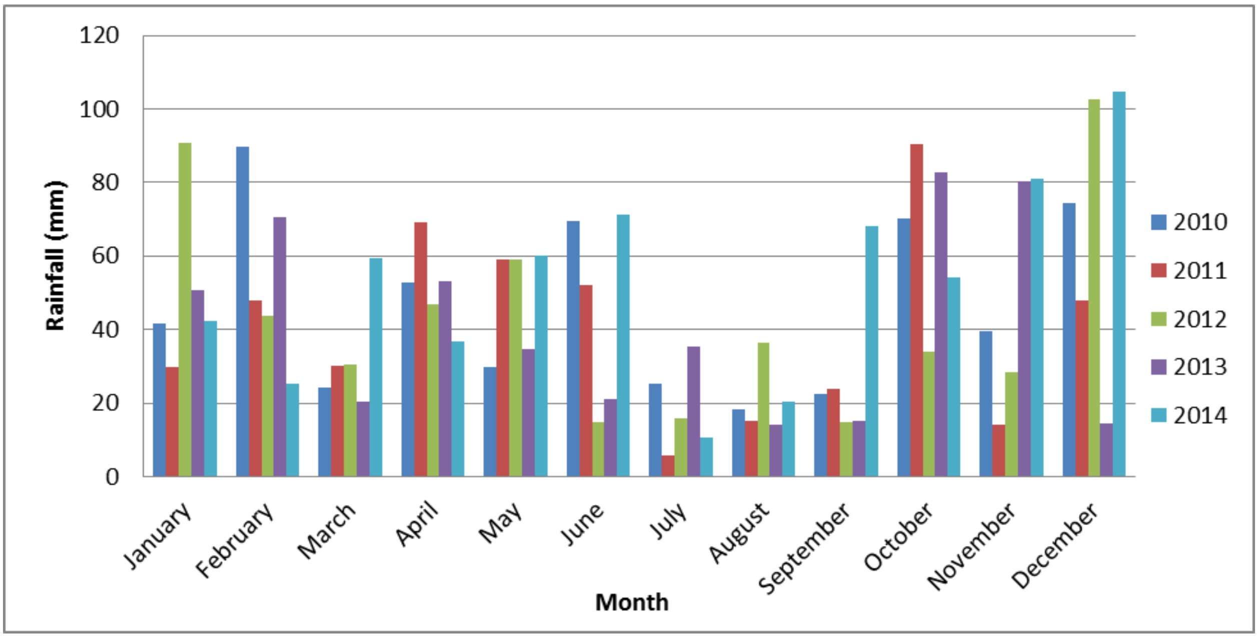

Figure 20 Lake Burdur mean monthly rainfall between 2010-2014

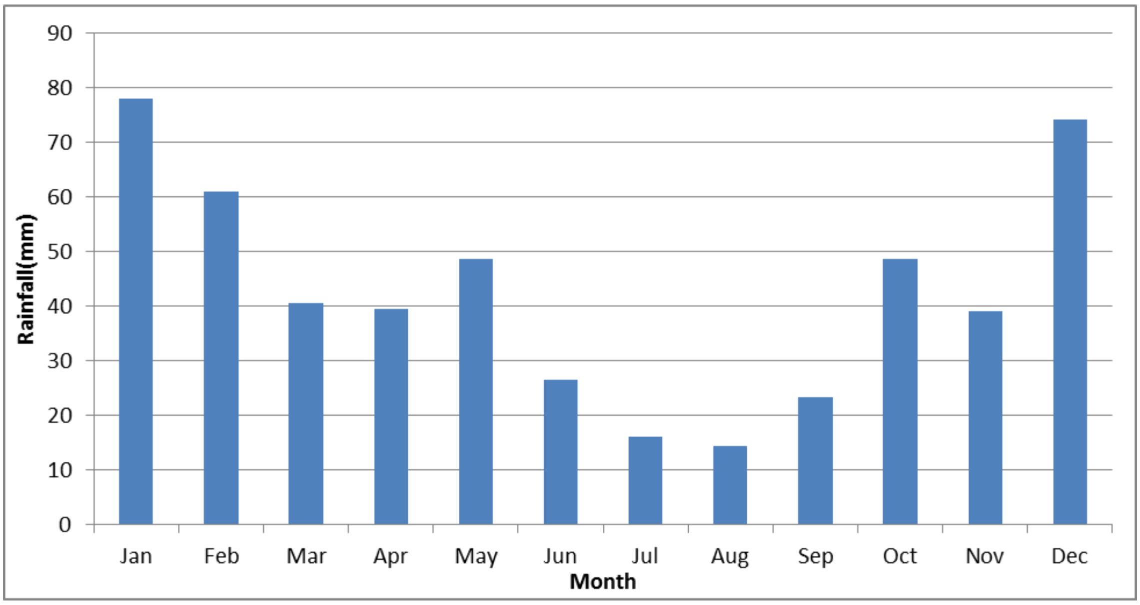

Figure 21 Mean monthly rainfall depths over the year

In order to relate the rainfall amount of the lake with lake balance study, it is important to see the pattern between the selected years for the study. Figure 22 illustrates the annual rainfall between 2010 and 2014. The period from 2010–2014 shows a positive pattern throughout the five years. From 2010 to 2014, although there are some decreases in rainfall depths in 2011 and 2013, overall pattern is upward. However, in order to have more idea about the rainfall trend, long period of the years are needed to be studied. From this study, having positive pattern gives the explanation that the reason of the decrease in lake level is not due to rainfall input of the water balance between the study period.

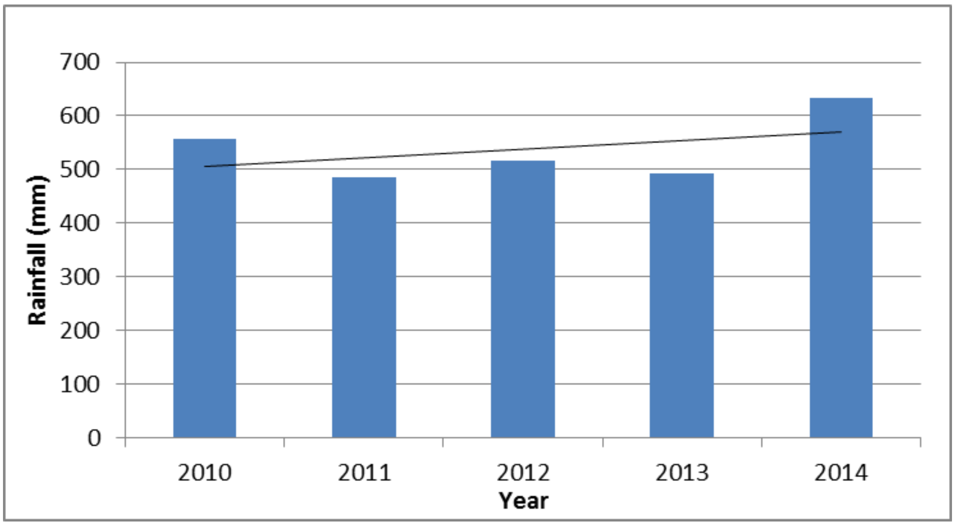

Figure 22 Annual rainfall over the Lake

Table 11 shows the result of the monthly rainfall depths (mm) over the Lake Burdur.

Table 11 Monthly estimated rainfall depths

	2010	2011	2012	2013	2014
January	41.7	29.7	90.6	50.6	42.4
February	89.6	47.8	43.7	70.4	25.3
March	24.2	30.1	30.5	20.2	59.3
April	52.7	69.2	46.7	53.1	36.9
May	29.8	59.1	59.1	34.7	60.1
June	69.5	52.0	14.6	21.2	71.1
July	25.3	5.7	15.7	35.2	10.6
August	18.3	15.0	36.5	14.0	20.3
September	22.3	24.0	14.8	15.2	68.0
October	70.2	90.4	34.0	82.6	54.2
November	39.3	14.0	28.3	80.2	80.9
December	74.5	48.0	102.5	14.6	104.8

4.2. Evapotranspiration Results

4.2.1. PET results

By the research objective of this study, required potential evapotranspiration data was estimated by using satellite products that is FEWSNET in order to use for streamflow calculations. Although validations of these products are necessary in order to reduce uncertainties, in this study, such validation was ignored, since there were no existing potential evapotranspiration data of the study area and time was limited to do extensive study. Mean annual PET maps were prepared to show PET distribution over the study area. Below Figure 23, shows estimated FEWSNET PET maps between 2010 and 2014. In general, PET values are higher in the lower part of the catchment, while in the top are lowest. In 2010,2012 and 2013, the basin have the higher range between the lowest PET value and highest PET value compared to other years. Overall, the reason of spatial variability of PET values among the basin might be a result of vegetation cover distribution.

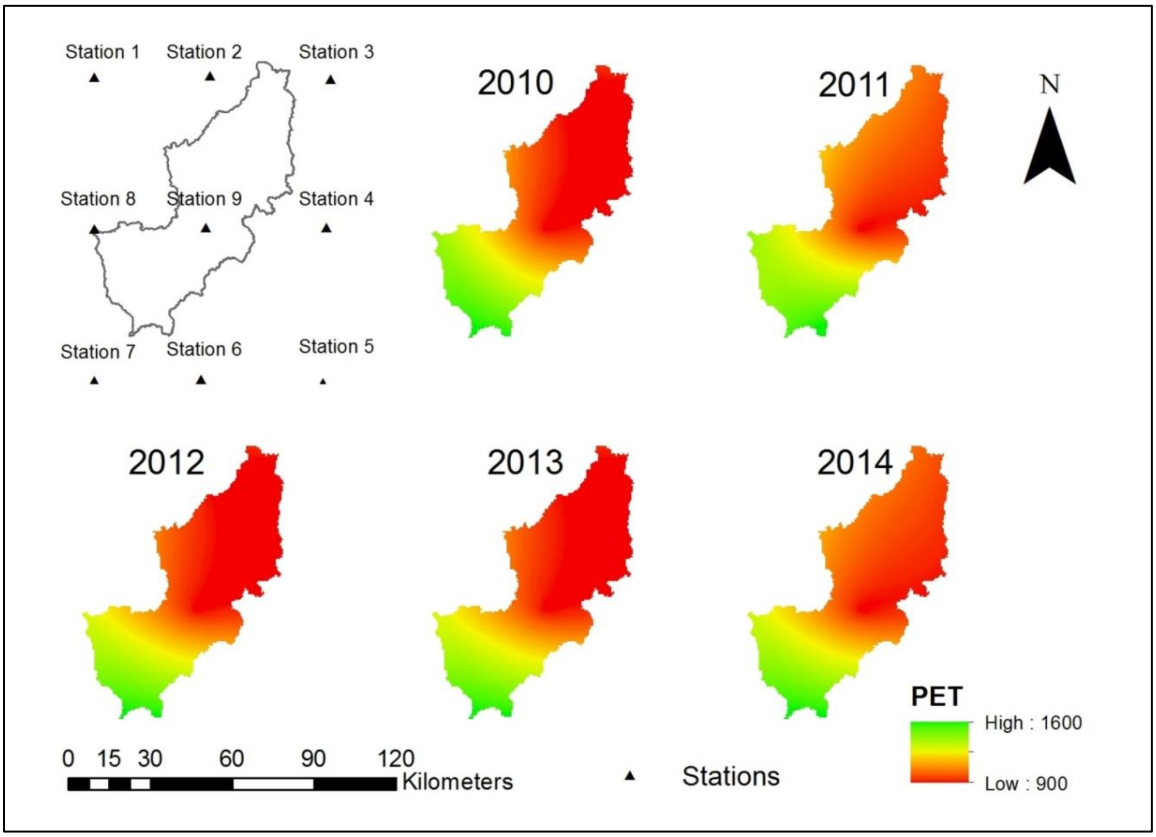

Figure 23 Mean annual PET

Figure 24 shows the mean monthly PET values which is calculated from nine stations between 2010 and 2014. The graph illustrates that PET have highest values in summer season (June, July, August) while in winter (December, January, February) have the lowest values.

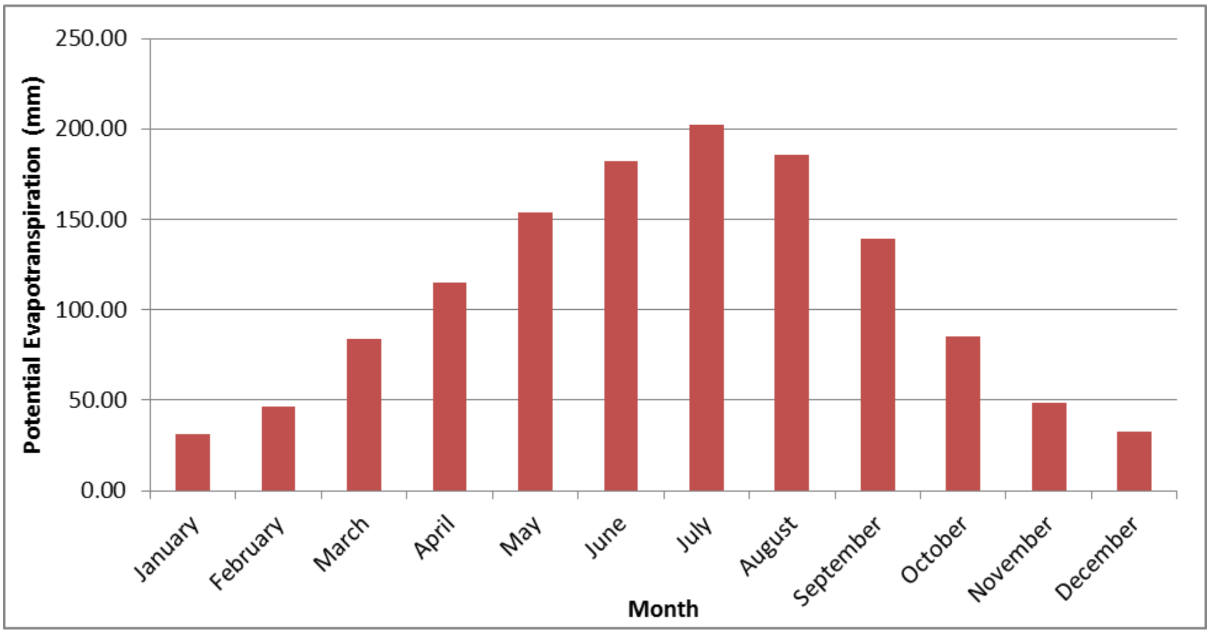

Figure 24 Mean monthly PET from 2010-2014

Table 12 Mean potential evapotranspiration

	Overall	Wet Season	Dry Season
Minimum(mm)	31.4	31.4	139.1
Maximum(mm)	202.2	46.2	202.2
Mean(mm)	108.9	36.8	175.8
Standard Deviation	60.2	6.7	26.7

To assess the differences between the wet and dry seasons, minimum, maximum and mean values were assessed. Table 12 illustrates that monthly values for the respective seasons have large difference having 139 mm difference in mean values. Standard deviations of respective seasons have expected different behavior in temporal variability. Both aspects of the differences in mean PET and standard deviations indicate that PET estimation have reasonable results since monthly and seasonal cycles match with seasonal characteristics having higher PET in dry season lower PET in wet season.

4.3. Runoff Results

4.3.1. Catchment comparison

Catchment boundary that was obtained during the fieldwork was compared with delineated basin area. The boundary map that is obtained during the fieldwork is prepared by using ArcGIS, while in this study TARDEM was used to delineate the basin area. Figure 25 shows two basins comparison to control the reliability of the extracted basin. It is noted that, except non-delineated area, extracted basin area shows similar boundary. Only one sub-catchment that is extracted was overestimated. It is because of existing lake, which is named Lake Yarisli (Figure 16); the stream cannot reach the Lake Burdur basin.

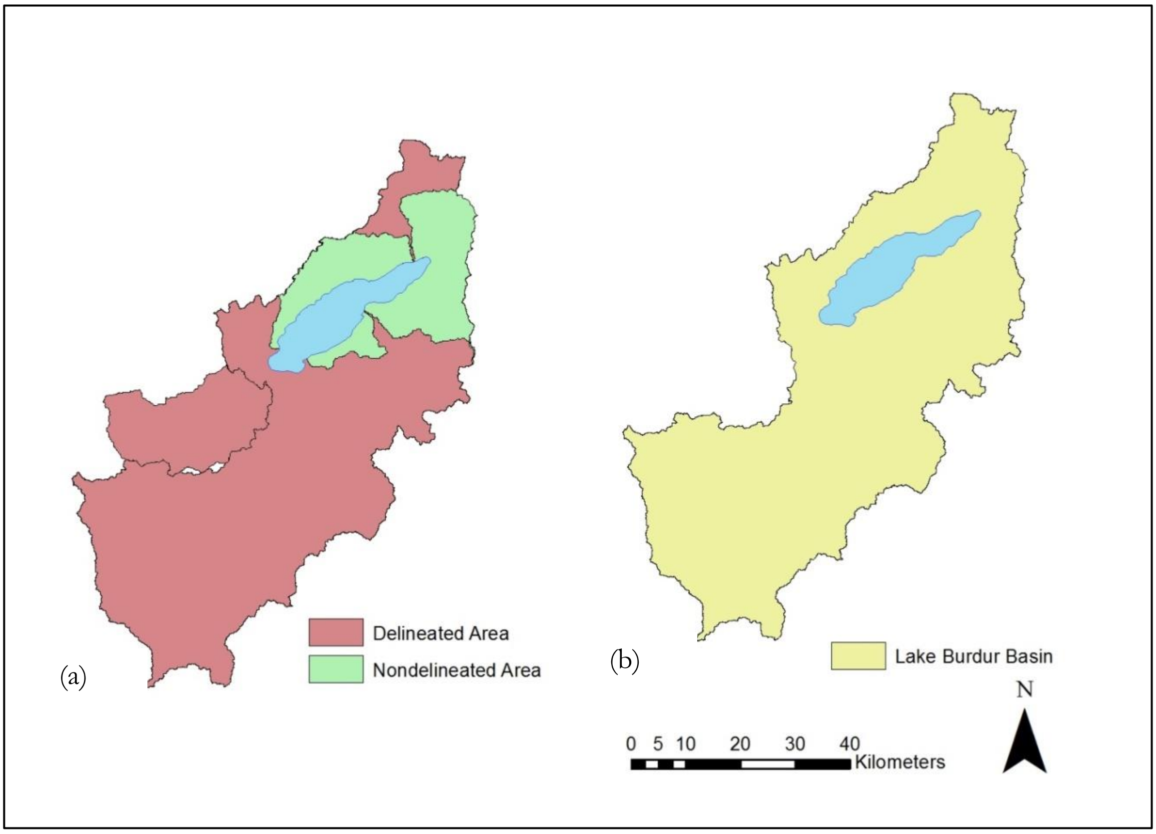

Figure 25 Comparison of the basins a)Estimated by Tardem b)Obtained from DSI

4.3.2. Runoff coefficient estimation

By means of stream flow simulation, specific runoffs where simulated streamflow is divided by the respective area as obtained for each extracted catchments. Although this study was concerned with assessing the performance of a runoff model, it was of great importance for the lake water balance that the simulated stream flow should be realistic. Due to unrealistic observed stream flow data (Figure 17), runoff coefficients of the catchments were calculated in order to have some clarification about the simulated streamflow reliability. Runoff coefficient is the ratio of runoff to the rainfall depth over the catchment. In semi-arid regions, runoff coefficient has low values compared to other regions. Martín-Vide et al. (1999), for instance, stated runoff coefficient between 0.04-0.15 in Mediterranean that has semi-arid characteristic. Moreover, Yair et al. (2002) reported that runoff coefficient differs from 0.27-0.37 at small spatial scale in semi-arid region. Runoff coefficients were calculated for wet season (December, January, February), for the rest of the year and entire year. The closest rainfall stations of the catchments were selected, and they were used for runoff coefficient estimation. Table 13 shows the runoff coefficient of the catchments. The runoff coefficients provided plausible values having low values range from 0.16 to 0.26 for entire year in semi-arid region. Wet seasons have higher values compared to the rest of the year.

Table 13 Runoff coefficient estimation

Runoff Coefficient	Wet Season	The Rest of the Year	Entire Year
Catchment 1	0.31	0.17	0.22
Catchment 2	0.29	0.20	0.23
Catchment 3	0.30	0.10	0.16
Catchment 4	0.33	0.22	0.26
Catchment 5	0.28	0.23	0.25

4.3.3. Results

Streamflow results were calculated monthly basis in order to use for lake balance assessment. Table 14 shows yearly streamflow rates for five catchment that were simulated by REW model. In this study, after comparison of catchment delineation explained 3.5.4.1, streamflow of catchment 3 was recalculated by removing the streamflow of overestimated REW (explained in 4.3.1), because the streamflow from that REW does not reach to the Lake Burdur basin area. The simulated streamflow hydrographs are in Appendix F.

The finding results indicate that catchment 3 has higher streamflow compared to other catchments while catchment 2 has the lowest. It is because the contribution area is the largest in catchment 3. From the results, it is noted that catchment 3 streamflow rates change over the years. This can be related with the existing dam within the catchment. From higher streamflow, it might be expected that some amount of water is released from the dam. That can be result of the high increase of streamflow among the years. However, for the other catchments streamflow, although there are some changes among the years, the pattern is stable.

The streamflow of the area A, B and C were estimated according to the neighbour catchments runoff explained in 3.5.4.2 section. Table 15 shows the calculated Lake level increases by streamflow contribution. Monthly basis level increases in mm by streamflow contribution are in Appendix G.

Table 14 Annual streamflow (m^3/s)

m3/s	Catchment 1	Catchment 2	Catchment 3	Catchment 4	Catchment 5
2010	148.7	131.8	1120.5	312.6	133.3
2011	136.8	121.9	1194.5	287.6	122.3
2012	132.5	119.0	2236.0	279.1	118.1
2013	131.9	119.4	2209.9	277.0	116.9
2014	135.1	120.9	2205.6	280.4	119.7

Table 15 Lake level increases in mm by streamflow contribution

	Catch.1	Catch.2	Catch.3	Catch.4	Catch.5	Area A	Area B	Area C
2010	63.5	56.3	478.6	133.5	56.9	97.2	31.6	180.9
2011	58.4	52.1	510.2	122.8	52.3	89.7	29.0	166.2
2012	56.6	50.8	955.1	119.2	50.5	87.2	28.1	160.6
2013	56.4	51.0	944.0	118.3	49.9	87.2	27.9	159.3
2014	57.7	51.6	942.1	119.8	51.1	88.8	28.4	163.2

4.4. Lake water balance assesment

Annual hydrological components of the lake balance are shown in Table 16. Amount of water that was used for irrigation purposes was obtained yearly basis from DSI regional office, Isparta. Since the lake balance was calculated monthly basis, the irrigation simply was divided into twelve months in order to have monthly quantities. Finally, by using calculated rainfall, runoff and obtained open water evaporation and irrigation, lake water balance was estimated.

Table 16 Annual components of the lake water balance for the five hydrological years

Hydrological Year	P(mm)	E(mm)	R(mm)	A(mm)
2010-2011	557.4	128.8	1051.7	569.4
2011-2012	484.9	117.6	1417.3	616.7
2012-2013	517.0	155.5	1062.4	616.7
2013-2014	491.9	136.2	1605.3	616.7
2014-2015	633.9	193.5	1022.8	777.6

During the fieldwork, it is noted that there are many illegal water abstractions for irrigation in the most of the catchments. In order to see the effect of abstraction in Lake level change, Lake water balance was estimated three different times by preparing three different abstraction assumptions. First, it is assumed that there is no illegal abstraction among the basin (Assumption A). Second, the abstraction quantity was multiplied by two assuming legal and illegal abstractions have the same number (Assumption B). Final assumption C was triple amount of abstraction of the real quantity. After calculation of Lake balance for each assumption, Lake level was simulated and was compared with observed Lake level. Figure 26 shows observed and estimated lake levels in different assumptions. The graph shows that the difference between observed lake level and lake level of assumption A is approximately seven meter while 3m with assumption B. There is almost no difference between observed Lake level and assumption C. The results show that decrease in Lake level are effected directly by abstractions in the study area.

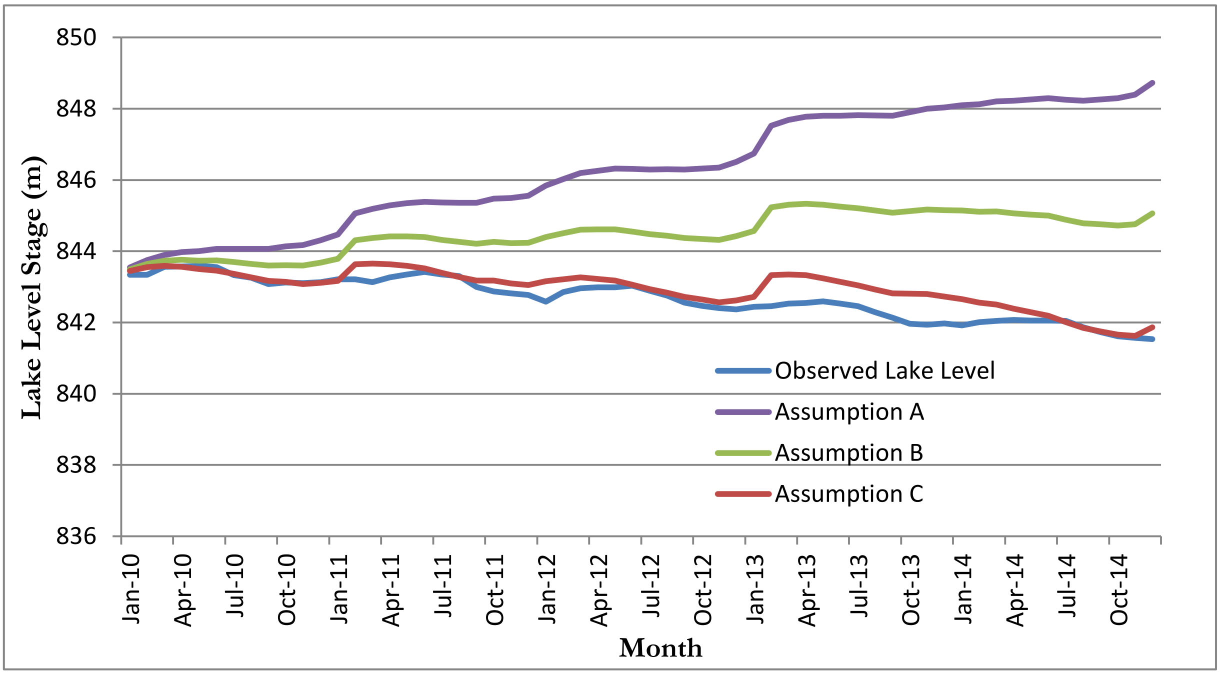

Figure 26 Lake level comparison with different amount of irrigation

According to the results, closure errors were calculated. Table 17 illustrates the changes in Lake level and closure error. Closure errors were calculated based on the observed lake level decrease that is 1.8 m. First assumption has the highest closure error while third has the lowest. It is assumed that errors are caused by some uncertainty in rainfall, potential evapotranspiration, streamflow estimation, and by uncertain lake-groundwater interaction.

Table 17 Results

	First Assumption	**Second Assumption**	**Third Assumption**
Changes in lake level(m)	+5.19	+1.57	-1.58
Closure error(m)	+7.00	+3.38	+0.23

5. CONCLUSION AND RECOMMENDATIONS

5.1. Conclusion

In this study, water balance of Lake Burdur was simulated at monthly time step to identify and assess the cause of the reduction in the lake level during five consecutive years. Satellite based estimation approach was followed due to sparse datasets of the rainfall and evapotranspiration components of the lake water balance. The satellite based estimations of the components was necessary in order to estimate ungauged catchments runoff and finally to calculate lake water balance. The time period was selected from January 2010 to January 2015 where the lake had in water level. The time period was chosen close to the present in order to have available satellite products and having rainfall time series. In the specified time period, based on conducted study the following conclusions are drawn.

- The difference between TRMM rainfall data and rain gauges data at monthly time steps was compared for water balance analysis at the Lake Burdur basin. As result of comparison, TRMM products were corrected with calculated bias factors. Daily rainfall data was required for runoff modeling whereas monthly over-lake rainfall was used for lake balance assessment. Since the available rainfall gauge network is sparse and randomly distributed over the study area, nine new gauges locations were defined. Lake and basin rainfall estimation were calculated based on the new network. However, several shortcomings occur such as the TRMM overestimates the rainfall in some years and gauges and underestimates in other years and gauges. It reduced the accuracy of stream flow simulation at daily time step and lake balance simulation.

- Potential evapotranspiration was calculated on daily basis in order to use for runoff modeling. Satellite based, FEWSNET, product was downloaded at daily time step and PET over the entire basin was calculated. The calculations show reasonable results having higher PET values in dry season compared to rainy season. 8.4% of PET occurs in dry season whereas 40.3% in wet season. Standard deviation of the dry season is 26.7 while 6.7 in wet season. Although there are plausible results, PET estimation need to be done extensively by using ground-based methods in case of data availability.

- In the Lake Burdur basin, there are 13 sub-catchments and only two of them have daily runoff. Although the aim was to calibrate the gauged streamflow with simulated streamflow, the data could not be used for calibration because it was not showing any seasonal changes and had unrealistic quantity of runoff. Therefore, the extracted catchments streamflows were simulated by REW model and were used for the lake balance assessment. Runoff coefficient was used to test the accuracy of the results although the calibration of the gauged data is the best option for better runoff simulation. The runoff coefficient calculations show that the coefficient is less than 0.26 which is plausible quantity for semi-arid regions.

- The lake water balance showed that the mean annual values of precipitation between 2010 and 2015 over the lake was 537 mm, evaporation was 146.3 mm, surface runoff water inflow was 1231.9 mm, abstractions was 639.42 and change in lake level was +942 mm. Different assumptions were applied in order to understand the decrease in lake level. Since the area has illegal abstractions problem, the abstractions were increased by multiplying two and three.

- The decline of lake level depended on anthropogenic factors, because illegal water consumption by human activities assumed for a very large part of the water depletion of the lake.

5.2. Recommendations

To further enhance the results of Lake Burdur basin simulation and satellite based estimations the following recommendations are formulated.

- It has been observed that available rainfall gauges are not well distributed to represent better rainfall estimates of the basin. In order to compare satellite data with gauged data, it is important to have more available data set having well positions in the area.

- Gauged streamflow data shows unrealistic values that might be because of several reasons. Specified units of streamflow of the observed data, or the technician mistake might be the reason of inaccurate results. Because of unrealistic flow data, the accuracy of the model results cannot be tested and calibrated. The recorded flow data will not be representative for further studies.

- In this study, an important component of groundwater interactions except base flow was ignored due to required data and extensive study. Wrong simulation of the lake can be also related with groundwater interactions; therefore, a further study has to be initiated on the lake-groundwater interactions.

- There are several constructed dams in the study area. Since the selected time period does not contain any dam construction, only abstractions were studied. To see dam constructions effects on lake level simulation, a further study has to be started based on the dam constructions years.

LIST OF REFERENCES

Abu El-Nasr, A., Arnold, J. G., Feyen, J., & Berlamont, J. (2005). Modelling the hydrology of a catchment using a distributed and a semi-distributed model. *Hydrological Processes*, *19*(3), 573–587. http://doi.org/10.1002/hyp.5610

Aghakouchak, A., Mehran, A., Norouzi, H., & Behrangi, A. (2012). Systematic and random error components in satellite precipitation data sets. *Geophysical Research Letters*, *39*(9), 3–6. http://doi.org/10.1029/2012GL051592

Allen, S. J., & Grime, V. L. (1995). Measurements of transpiration from Savannah shrubs using sap flow gauges. *Agricultural and Forest Meteorology*, *75*(94), 23–41. http://doi.org/10.1016/0168-1923(94)02201-T

Bastiaanssen, W. G. M., Menenti, M., Feddes, R. a., & Holtslag, a. a. M. (1998). A remote sensing surface energy balance algorithm for land (SEBAL). 1. Formulation. *Journal of Hydrology*, *212-213*, 198–212. http://doi.org/10.1016/S0022-1694(98)00253-4

Berbigier, P., Bonnefond, J. M., Loustau, D., Ferreira, M. I., David, J. S., & Pereira, J. S. (1996). Transpiration of a 64-year-old maritime pine stand in Portugal .2. Evapotranspiration and canopy stomatal conductance measured by an eddy covariance technique. *Oecologia*, *107*(1), 43–52. http://doi.org/10.1007/BF00582232

Bishop, C. T. (1990). Historical Variation of Water Levels in Lakes Erie and Michigan-Huron. *Journal of Great Lakes Research*, *16*(3), 406–425. http://doi.org/10.1016/S0380-1330(90)71434-7

Blöschl, G. and Sivapalan, M. (1995), Scale issues in hydrological modelling: A review. Hydrol. Process., 9: 251–290. doi: 10.1002/hyp.3360090305

Butts, M. B., Payne, J. T., Kristensen, M., & Madsen, H. (2004). An evaluation of the impact of model structure on hydrological modelling uncertainty for streamflow simulation. *Journal of Hydrology*, *298*(1-4), 242–266. http://doi.org/10.1016/j.jhydrol.2004.03.042

Cooper, M. (2010). Advanced Bash-Scripting Guide An in-depth exploration of the art of shell scripting Table of Contents. *Okt 2005 Abrufbar Uber Httpwww Tldp orgLDPabsabsguide Pdf Zugriff 1112 2005*, *2274*(November 2008), 2267–2274. http://doi.org/10.1002/hyp

Deckers, D. L. E. H., Booij, M. J., Rientjes, T. H. M., & Krol, M. S. (2010). Catchment Variability and Parameter Estimation in Multi-Objective Regionalisation of a Rainfall-Runoff Model. *Water Resources Management*, *24*(14), 3961–3985. http://doi.org/10.1007/s11269-010-9642-8

Fenicia, F., Zhang, G. P., Rientjes, T., Hoffmann, L., Pfister, L., & Savenije, H. H. G. (2005). Numerical simulations of runoff generation with surface water-groundwater interactions in the Alzette river alluvial plain (Luxembourg). *Physics and Chemistry of the Earth*, *30*(4-5 SPEC. ISS.), 277–284. http://doi.org/10.1016/j.pce.2004.11.001

Finch, J. W., & Hall, R. L. (2001). Estimation of Open Water Evaporation. *Report*, 155.

Fisher, D. K. (2012). Simple weighing lysimeters for measuring evapotranspiration and developing crop coefficients. *International Journal of Agricultural & Biological Engineering*, *5*(3), 35–43. http://doi.org/10.3965/j.ijabe.20120503.004

Fisher, J. B., DeBiase, T. a., Qi, Y., Xu, M., & Goldstein, A. H. (2005). Evapotranspiration models compared on a Sierra Nevada forest ecosystem. *Environmental Modelling & Software*, *20*(6), 783–796. http://doi.org/10.1016/j.envsoft.2004.04.009

Gallego-Elvira, B., Olioso, A., Mira, M., Castillo, S. R.-, Boulet, G., Marloie, O., … Boutron, O. (2013). EVASPA (EVapotranspiration Assessment from SPAce) Tool: An overview. *Procedia Environmental Sciences*, *19*, 303–310. http://doi.org/10.1016/j.proenv.2013.06.035

Habib, E., Haile, A., Sazib, N., Zhang, Y., & Rientjes, T. (2014). Effect of Bias Correction of Satellite-Rainfall Estimates on Runoff Simulations at the Source of the Upper Blue Nile. *Remote Sensing*, *6*(7), 6688–6708. http://doi.org/10.3390/rs6076688

Hofmann, H., Lorke, A., & Peeters, F. (2008). Temporal scales of water-level fluctuations in lakes and their ecological implications. *Hydrobiologia*, *613*(1), 85–96. http://doi.org/10.1007/s10750-008-9474-1

Hsu, K. L., & Sorooshian, S. (2008). Satellite-Based Precipitation Measurement Using PERSIANN System. *Hydrological Modelling and the Water Cycle*, 27–48. http://doi.org/10.1007/978-3-540-77843-1_2

Huffman, G. J., Bolvin, D. T., Nelkin, E. J., Wolff, D. B., Adler, R. F., Gu, G., … Stocker, E. F. (2007). The TRMM Multisatellite Precipitation Analysis (TMPA): Quasi-Global, Multiyear, Combined-Sensor Precipitation Estimates at Fine Scales. *Journal of Hydrometeorology*, *8*(1), 38–55. http://doi.org/10.1175/JHM560.1

Ito, Y., Momii, K., & Nakagawa, K. (2009). Modeling the water budget in a deep caldera lake and its hydrologic assessment: Lake Ikeda, Japan. *Agricultural Water Management*, *96*(1), 35–42. http://doi.org/10.1016/j.agwat.2008.06.009

Joyce, R. J., Janowiak, J. E., Arkin, P. a., & Xie, P. (2004). CMORPH: A Method that Produces Global Precipitation Estimates from Passive Microwave and Infrared Data at High Spatial and Temporal Resolution. *Journal of Hydrometeorology*, *5*(3), 487–503. http://doi.org/10.1175/1525-7541(2004)005<0487:CAMTPG>2.0.CO;2

Kizza, M., Westerberg, I., Rodhe, A., & Ntale, H. K. (2012). Estimating areal rainfall over Lake Victoria and its basin using ground-based and satellite data. *Journal of Hydrology*, *464-465*, 401–411. http://doi.org/10.1016/j.jhydrol.2012.07.024

Lagomasino, D., Price, R. M., Whitman, D., Melesse, A., & Oberbauer, S. F. (2015). Spatial and temporal variability in spectral-based surface energy evapotranspiration measured from Landsat 5TM across two mangrove ecotones. *Agricultural and Forest Meteorology*, *213*, 304–316. http://doi.org/10.1016/j.agrformet.2014.11.017

Li, X. H., Zhang, Q., & Xu, C. Y. (2012). Suitability of the TRMM satellite rainfalls in driving a distributed hydrological model for water balance computations in Xinjiang catchment, Poyang lake basin. *Journal of Hydrology*, *426-427*, 28–38. http://doi.org/10.1016/j.jhydrol.2012.01.013

Moazami, S., Golian, S., Kavianpour, M. R., & Hong, Y. (2013). Comparison of PERSIANN and V7 TRMM Multi-satellite Precipitation Analysis (TMPA) products with rain gauge data over Iran. *International Journal of Remote Sensing*, *34*(April 2015), 8156–8171. http://doi.org/10.1080/01431161.2013.833360

Perera, B. U. J. (2009). Ungauged Catchment Hydrology : The case of Lake Tana Basin Ungauged Catchment Hydrology : The case of Lake Tana Basin.

Perrin, C., Michel, C., & Andréassian, V. (2003). Improvement of a parsimonious model for streamflow simulation. *Journal of Hydrology*, *279*(1-4), 275–289. http://doi.org/10.1016/S0022-1694(03)00225-7

Reed, S., Koren, V., Smith, M., Zhang, Z., Moreda, F., & Seo, D. J. (2004). Overall distributed model intercomparison project results. *Journal of Hydrology*, *298*(1-4), 27–60. http://doi.org/10.1016/j.jhydrol.2004.03.031

Reggiani, P. (2012). Representative Elementary Watershed Model User Manual, 1–90.

Reggiani, P., & Rientjes, T. H. M. (2005). Flux parameterization in the representative elementary watershed approach: Application to a natural basin. *Water Resources Research*, *41*(4), 1–18. http://doi.org/10.1029/2004WR003693

Reggiani, P., & Rientjes, T. H. M. (2010). Closing horizontal groundwater fluxes with pipe network analysis: An application of the REW approach to an aquifer. *Environmental Modelling and Software*, *25*(12), 1702–1712. http://doi.org/10.1016/j.envsoft.2010.04.019

Rientjes, M. (2014). Modelling in Hydrology, (March).

Senay, G. B., Verdin, J. P., Lietzow, R., & Melesse, a. M. (2008). Global daily reference evapotranspiration modeling and evaluation. *Journal of the American Water Resources Association*, *44*(4), 969–979. http://doi.org/10.1111/j.1752-1688.2008.00195.x

Shiklomanov, I. (1993). World fresh water resources. *Water in Crisis a Guide to the World's Fresh Water Resources*.

Skop, E. (1996). Scale Issues in Hydrological Modeling. *Eos, Transactions American Geophysical Union*, *77*(20), 190. http://doi.org/10.1029/96EO00131

Su, Z. (2002). The Surface Energy Balance System (SEBS) for estimation of turbulent heat fluxes. *Hydrology and Earth System Sciences*, *6*(1), 85–100. http://doi.org/10.5194/hess-6-85-2002

Swenson, S., & Wahr, J. (2009). Monitoring the water balance of Lake Victoria, East Africa, from space. *Journal of Hydrology*, *370*(1-4), 163–176. http://doi.org/10.1016/j.jhydrol.2009.03.008

Wale, A. (2008). Hydrological Balance of Lake Tana Upper Blue Nile Basin, Ethiopia, 106. http://doi.org/10.1007/978-94-007-0689-7

Wantzen, K. M., Junk, W. J., & Rothhaupt, K. O. (2008). An extension of the floodpulse concept (FPC) for lakes. *Hydrobiologia*, *613*(1), 151–170. http://doi.org/10.1007/s10750-008-9480-3

Zhang, G. P., Fenicia, F., Rientjes, T. H. M., Reggiani, P., & Savenije, H. H. G. (2005). Modeling runoff generation in the Geer river basin with improved model parameterizations to the REW approach. *Physics and Chemistry of the Earth*, *30*(4-5 SPEC. ISS.), 285–296. http://doi.org/10.1016/j.pce.2004.11.002

APPENDIX A: BIAS FACTOR CALCULATIONS FOR EACH STATION

Tables below show bias factor and relative error calculations based on 5 mm threshold. The calculations were done for nine stations. The bias factors were applied to correct TRMM rainfall.

Bias Factor	January	February	March	April	May	June	July	August	September	October	November	December
Senirkent	1.52	1.31	1.06	0.74	0.91	0.82	1.15	1.15	1.11	0.81	1.07	0.98
Uluborlu	1.23	0.88	0.74	0.71	0.72	0.57	1.01	1.17	2.60	0.92	0.82	1.11
Dinar	0.56	0.93	0.48	0.89	0.54	1.24	1.42	1.40	0.83	0.84	0.77	0.89
Atabey	0.44	1.32	0.87	0.57	0.97	0.47	0.55	0.38	0.59	0.79	2.07	1.01
Egirdir	1.24	1.67	1.10	0.90	0.51	0.21	0.14	0.09	0.24	0.87	1.32	1.60
Isparta	0.61	0.98	0.92	0.89	0.91	1.01	1.47	1.10	0.91	0.84	1.76	1.20
Burdur	0.41	0.67	0.62	0.45	0.70	0.54	0.52	1.14	0.65	0.52	1.26	0.62
Tefenni	1.24	1.48	0.99	0.63	0.91	0.79	1.24	2.69	0.94	0.84	0.81	1.00
Acipayam	1.73	1.58	1.01	0.94	0.99	1.04	1.51	2.19	1.08	0.59	0.95	1.25

R.E	January	February	March	April	May	June	July	August	September	October	November	December
Senirkent	-0.34	0.04	0.84	1.71	0.41	0.32	1.68	-0.05	-0.09	0.46	0.03	0.18
Uluborlu	-0.10	0.24	1.34	1.62	1.85	1.48	0.39	-0.13	-0.32	0.16	0.42	-0.04
Dinar	0.95	0.08	1.36	0.13	1.64	-0.19	-0.07	-0.25	0.21	0.25	0.35	0.20
Atabey	5.77	0.26	0.20	1.46	0.03	1.38	0.95	1.78	1.01	0.32	0.10	0.05
Egirdir	-0.12	-0.32	-0.06	0.13	1.38	4.18	6.27	11.00	6.12	0.21	-0.06	-0.37
Isparta	0.81	0.69	0.34	0.19	0.24	0.41	0.68	-0.03	0.29	0.24	-0.19	0.03
Burdur	1.88	0.61	0.94	1.44	0.43	0.92	0.97	-0.12	0.55	0.92	0.13	0.98
Tefenni	-0.19	-0.30	0.24	0.70	0.17	0.58	-0.02	-0.57	0.07	0.58	0.40	0.04
Acipayam	-0.42	-0.34	0.01	0.17	0.19	0.01	-0.34	-0.37	-0.07	0.79	0.14	-0.01

APPENDIX B: COMPARISON OF GAUGED AND TRMM RAINFALL

Below graphs show the comparison of gauged and TRMM data for each station. It is seen from the graph that the results change within the years. While some years of TRMM data have good match with gauged data, the rest have not. In order to reduce this uncertainties bias factor estimation and correction were applied.

Acipayam Station

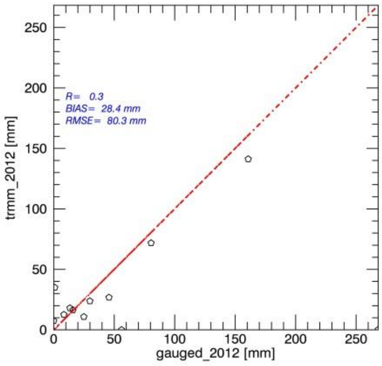

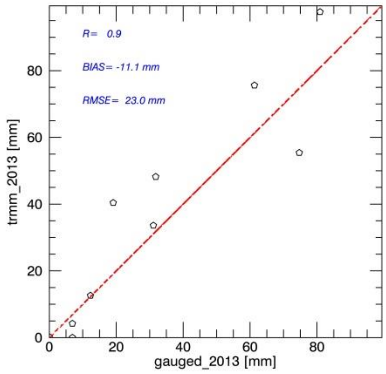

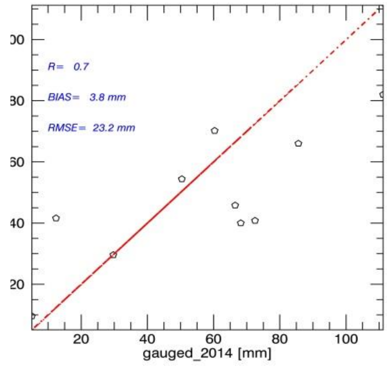

Tefenni Station

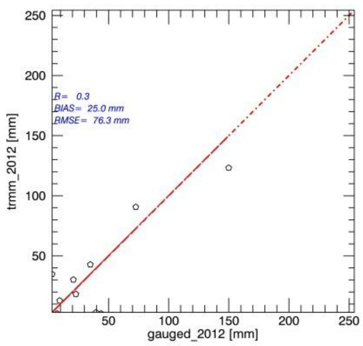

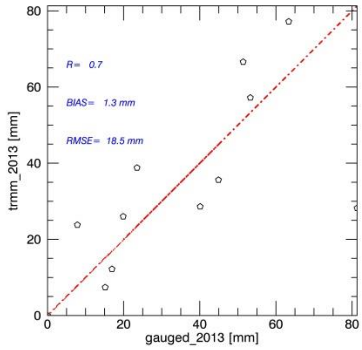

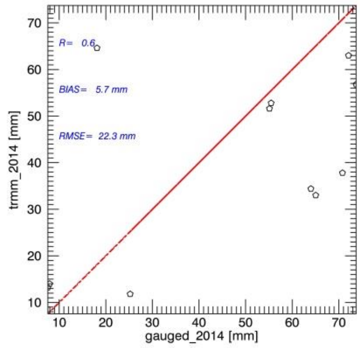

Burdur Station

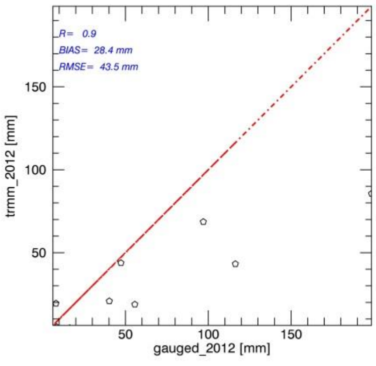

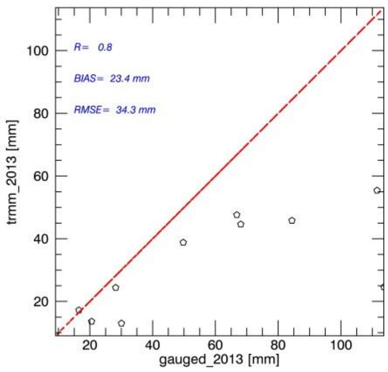

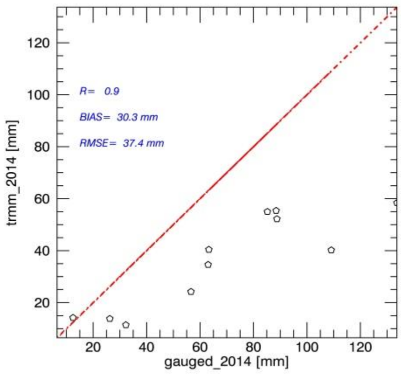

Isparta Station

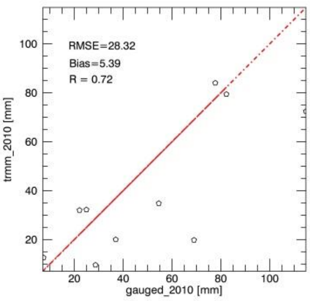

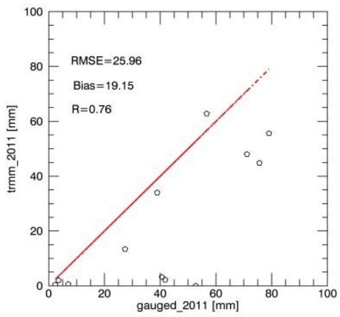

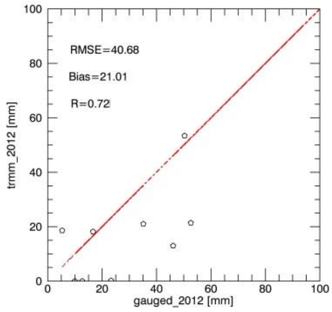

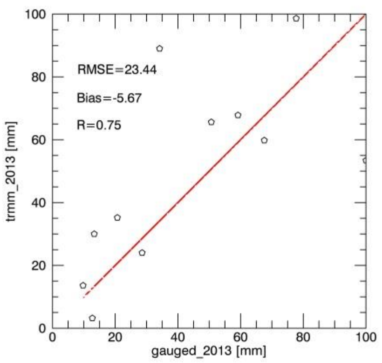

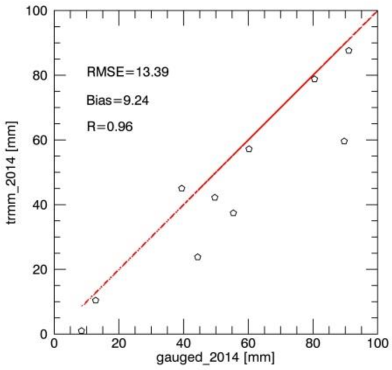

Egirdir Station

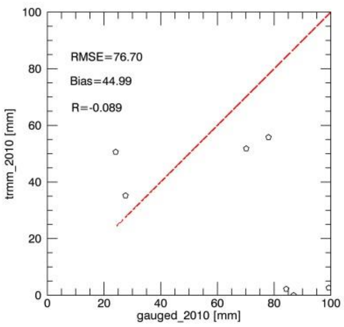

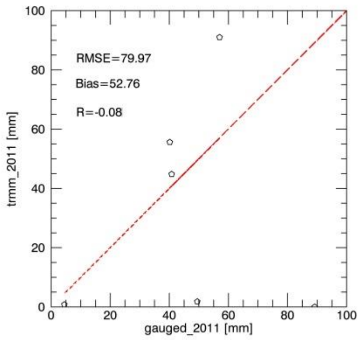

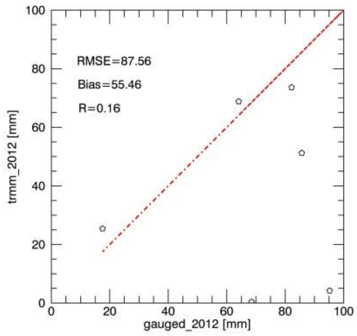

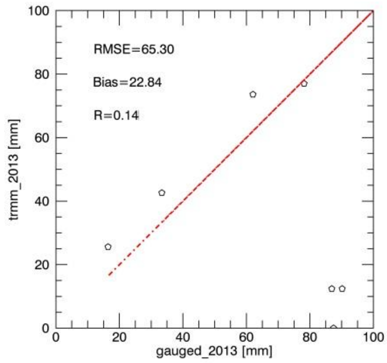

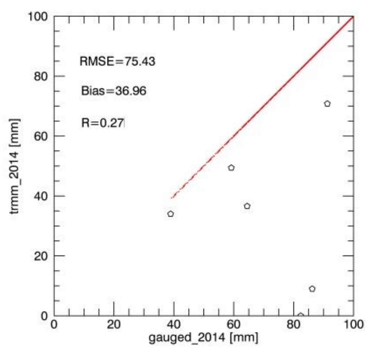

Atabey Station

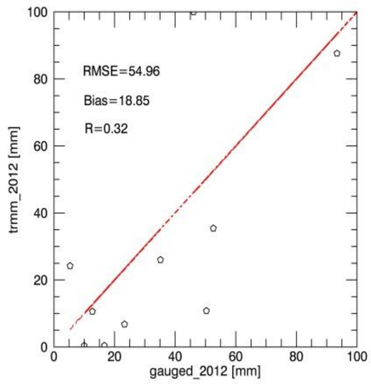

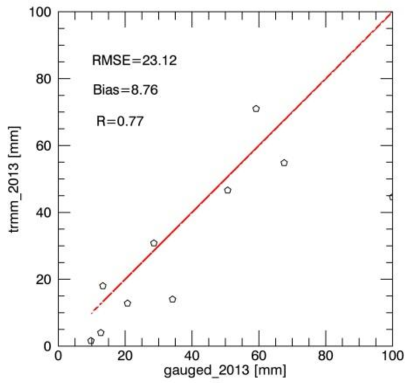

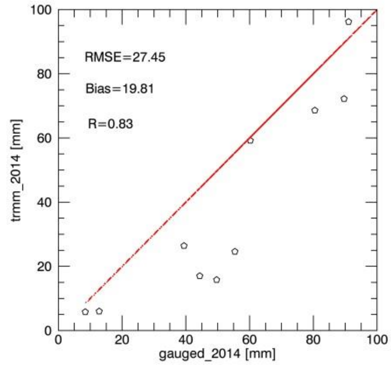

Dinar Station

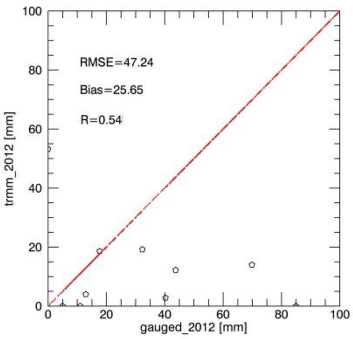

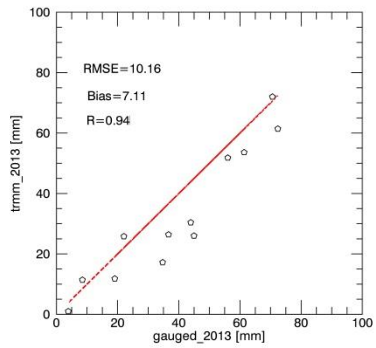

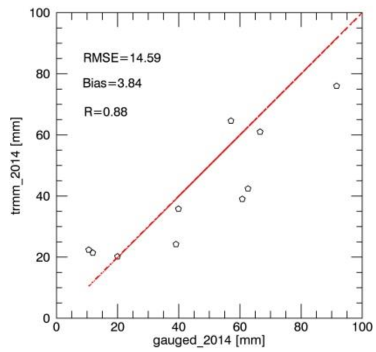

Uluborlu Station

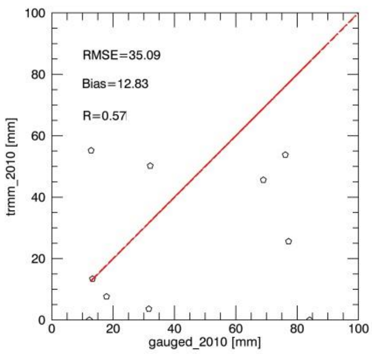

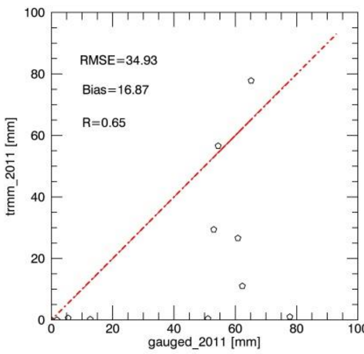

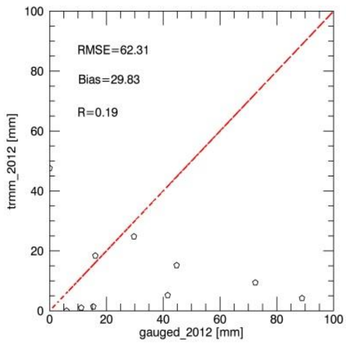

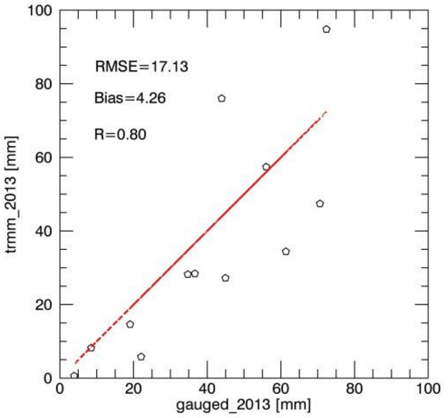

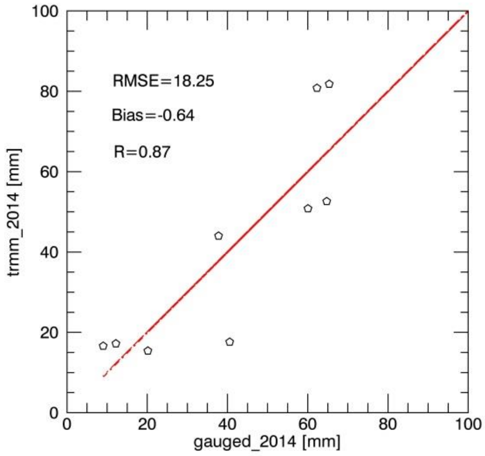

Senirkent Station

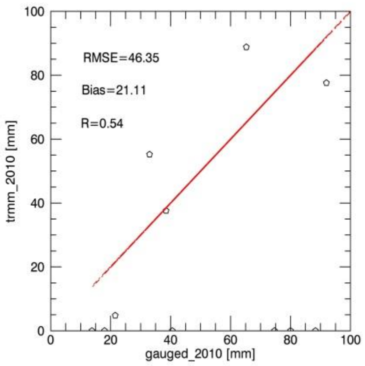

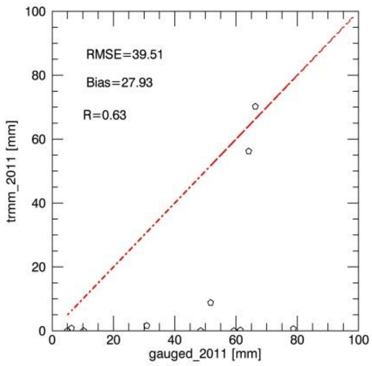

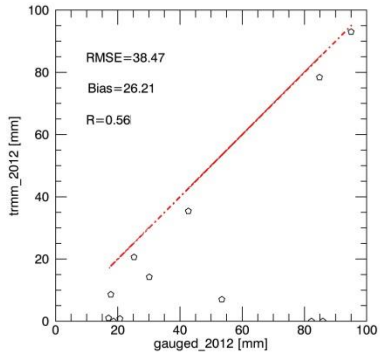

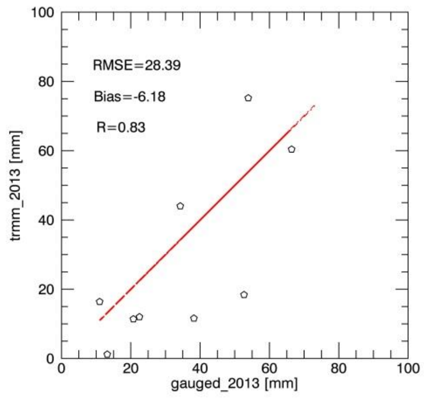

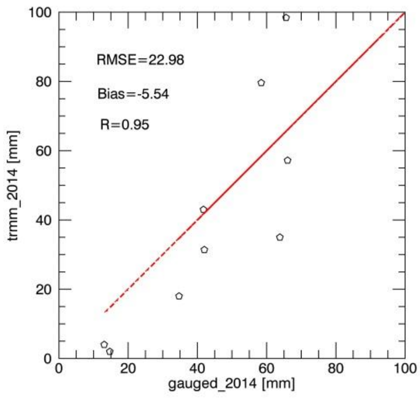

APPENDIX C: RAINFALL ESTIMATION

Nearest neighbourhood or Thiessen method was applied in order to have bias factor distribution for the study area. Nearest point method, the values are assigned according to the closest point value. Since the five stations (Senirkent,Uluborlu, Atabey,Egirdir and Isparta) are located in a same pixel, the nearest point assign only the closest station value to the pixel center point by ignoring the other values. Figure 27 shows the stations distribution within the pixel. Since in one pixel, five stations are available in the study area, the operation ignores the effect of other stations contributions. Therefore, to overcome this problem, the average bias factor of five stations is assigned to the closest station value to the pixel center, which is Atabey Station. As a result, the other 4 stations bias factor are not ignored. All the bias factor distribution estimates are done based on the georeferenced which is specified in order to cover the all stations.

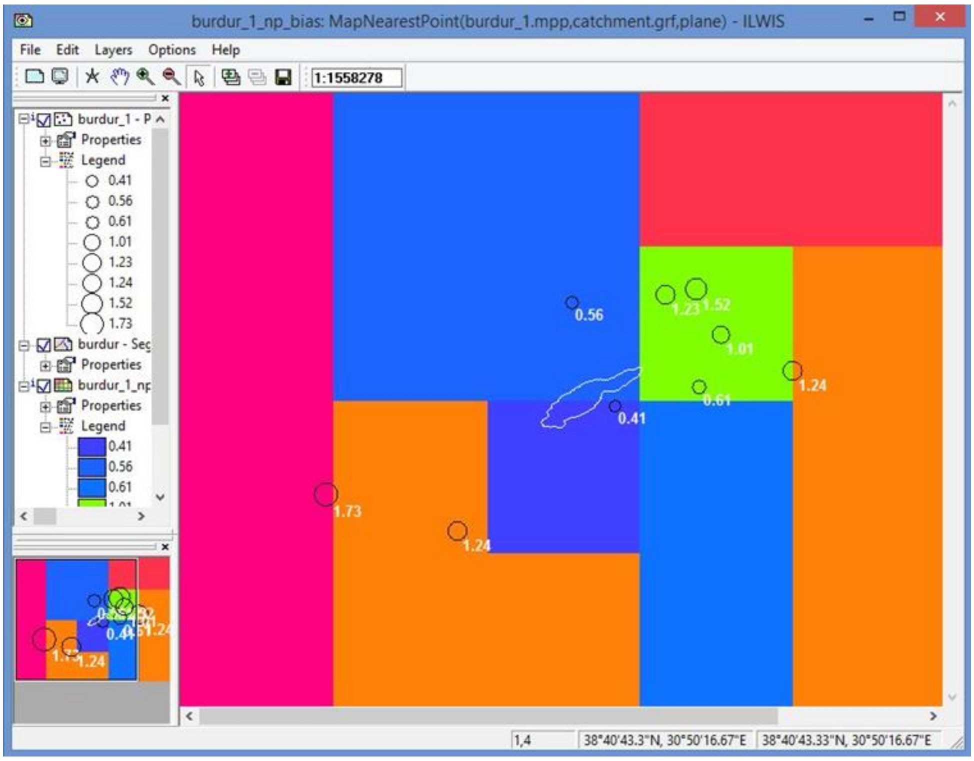

Figure 27 Result of nearest point method for the month of January

After bias factor distribution process, the daily TRMM products were stacked up in a monthly map list for 5 years (Figure 28). Second step was to get average rainfall value of total days in each month to calculate total monthly base rainfall by multiplying the days of each month (Figure 29). Finally, the total monthly rainfall map wass resampled according to the same georeferenced of point map (Figure 30).

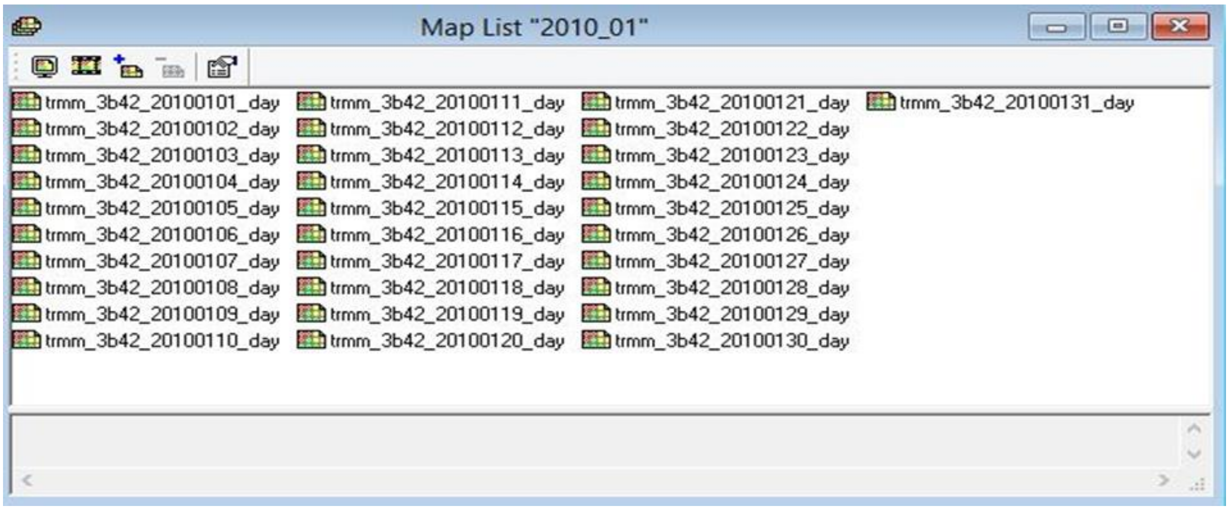

Figure 28 Map list

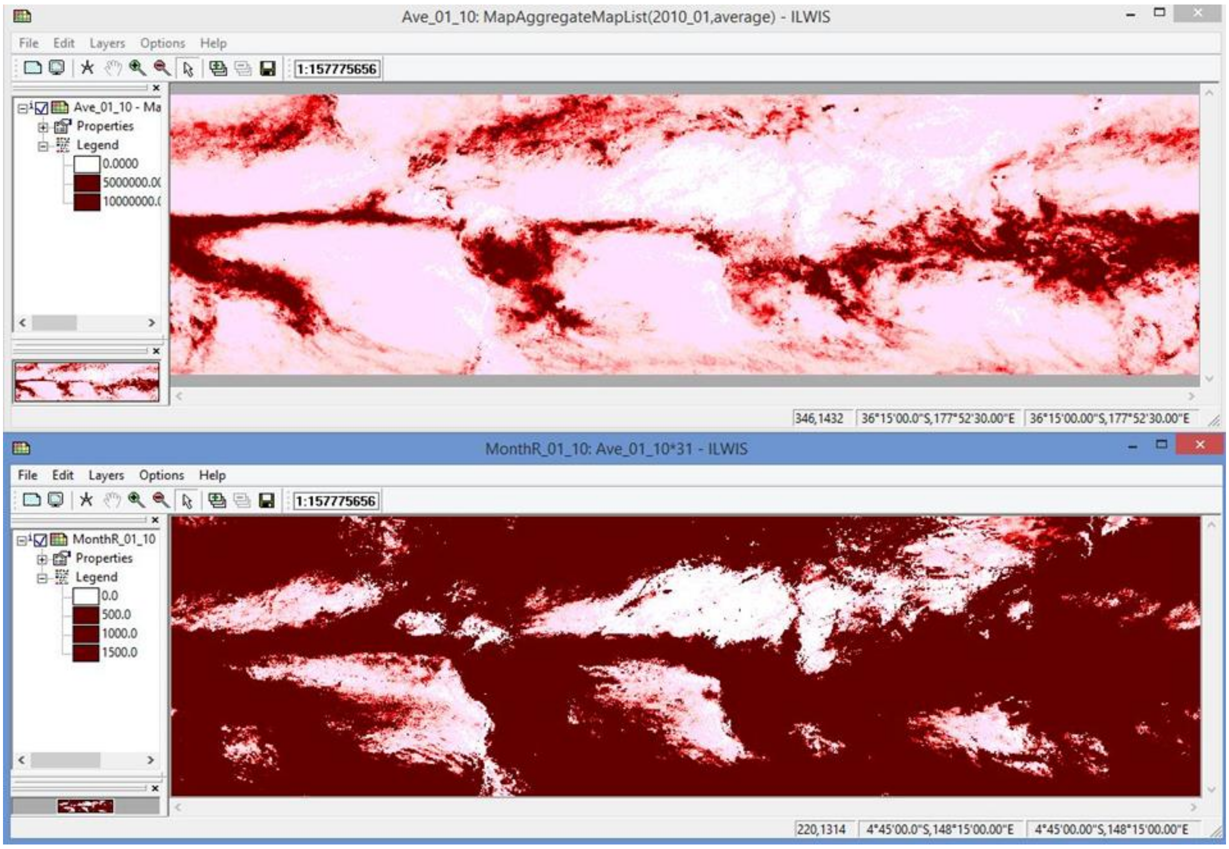

Figure 29 Above: Average rainfall map of the month January
Below: Total monthly rainfall map

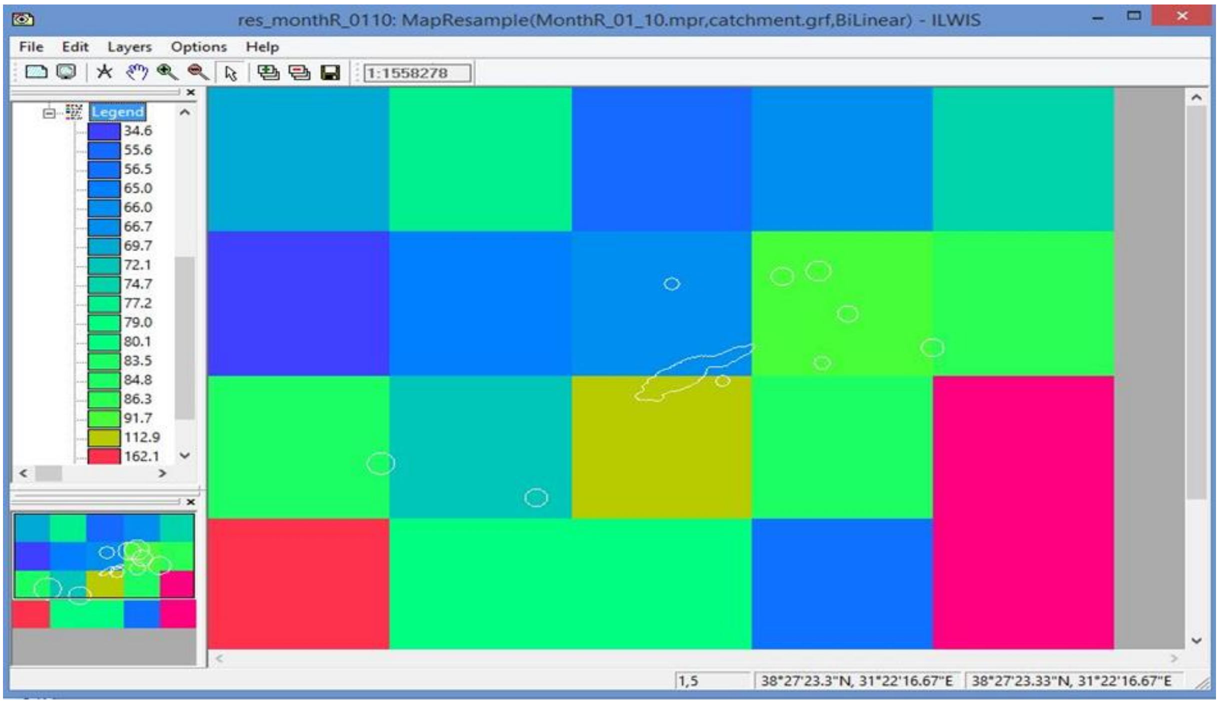

Figure 30 Resampled total monthly rainfall map

Last step was to multiply resampled monthly aggregated TRMM values and interpolate bias factor by using Map Calculation operation in ILWIS, and then it was resampled according to the Lake Burdur georeferenced (Figure 31). The resampled map calculation map was overlayed with Lake Burdur raster map in order to calculate the rainfall over the Lake Burdur area by using cross operation (Figure 32).

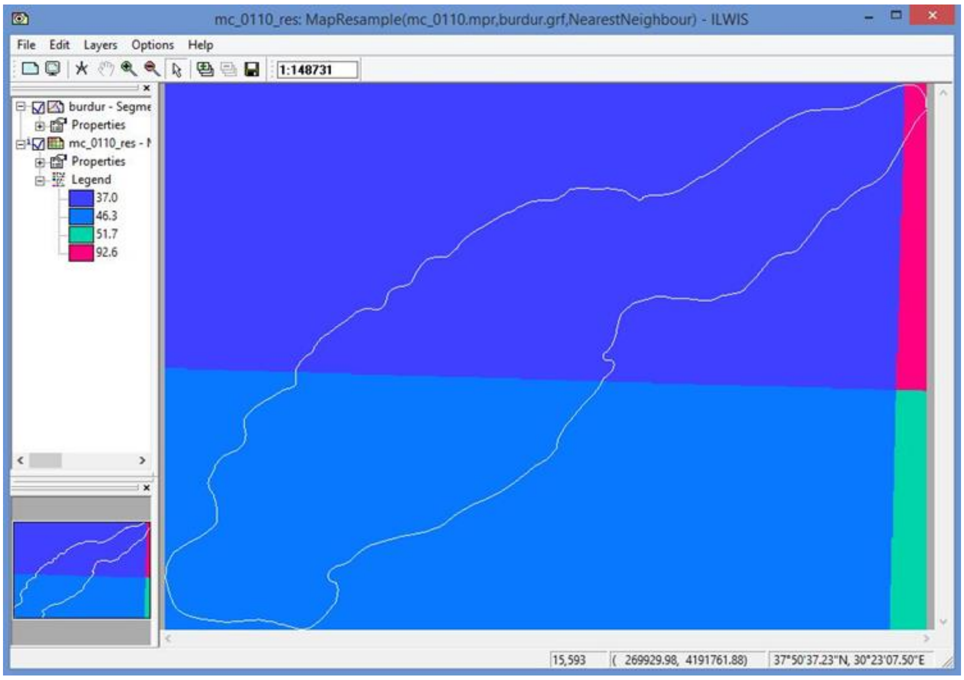

Figure 31 Resampled map calculation result

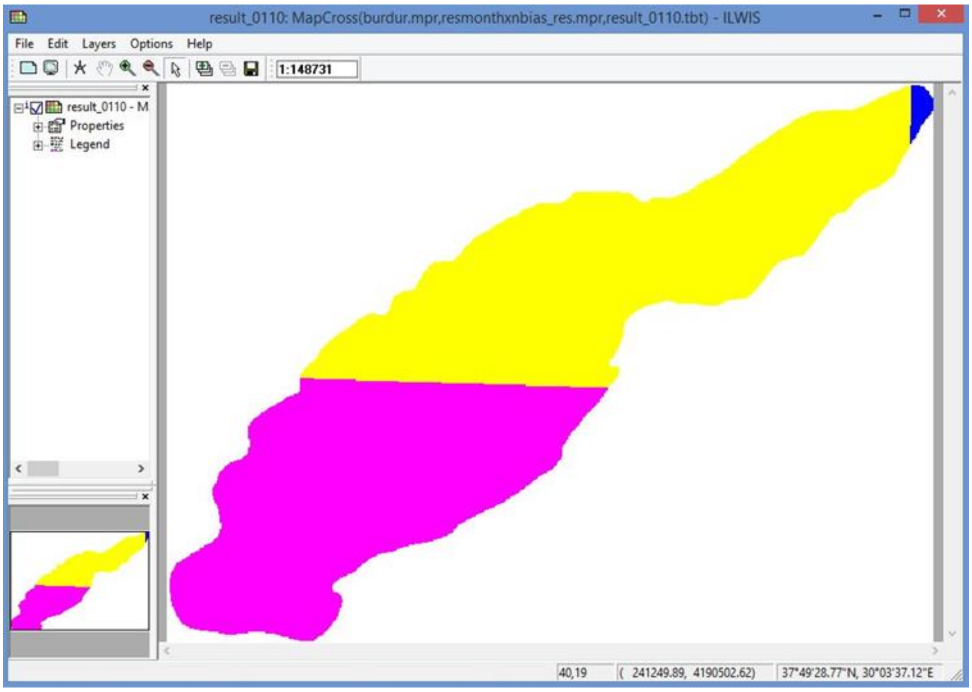

Figure 32 Monthly rainfall over the Lake Burdur

Monthly corrected rainfall rates were available after cross operation in ILWIS. Since the overall lake rainfall depth is needed, the monthly-corrected rainfall depths were multiplied with the corresponding areas. The table below shows for twelve-month rainfall rates over the lake.

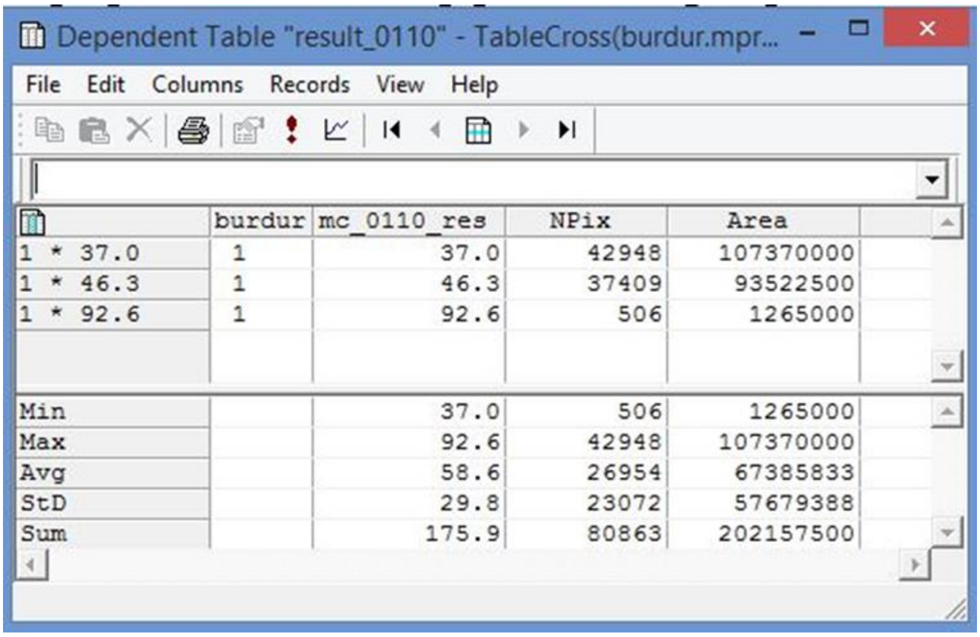
Dependent Table "result_0110" - TableCross(burdur.mpr...

File Edit Columns Records View Help

	burdur	mc_0110_res	NPix	Area
1 * 37.0	1	37.0	42948	107370000
1 * 46.3	1	46.3	37409	93522500
1 * 92.6	1	92.6	506	1265000
Min		37.0	506	1265000
Max		92.6	42948	107370000
Avg		58.6	26954	67385833
StD		29.8	23072	57679388
Sum		175.9	80863	202157500

Figure 33 Areal rainfall depths

The cross operation provides the each areal rainfall depths. By using the table, average lake rainfall depth is calculated for each month.

APPENDIX D: PET ESTIMATION

In this study, daily potential evapotranspiration rates between the years 2010 and 2014 were extracted by using ISOD TOOLBOX in ILWIS. Figure 34 shows the FEWS NET PET map on the first of January, 2010.

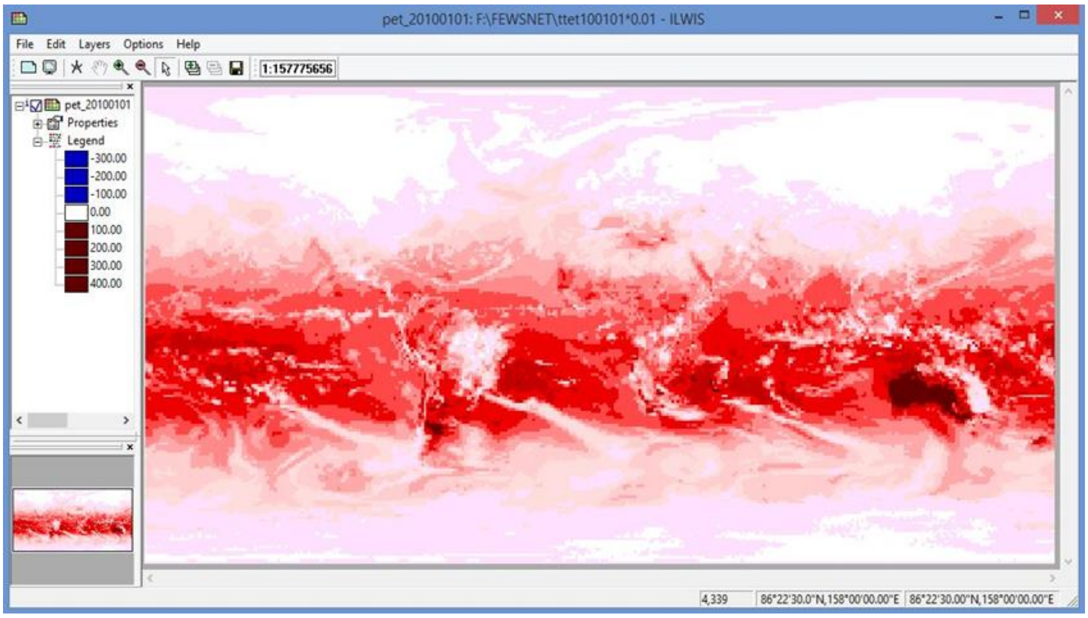

Figure 34 FEWS NET PET map

The point map, which contains the same created stations for the TRMM products, were used to extract the point-scale potential evapotranspiration. The point map was overlaid to the FEWS NET PET map to have daily PET rates input for the runoff model (Figure 35).

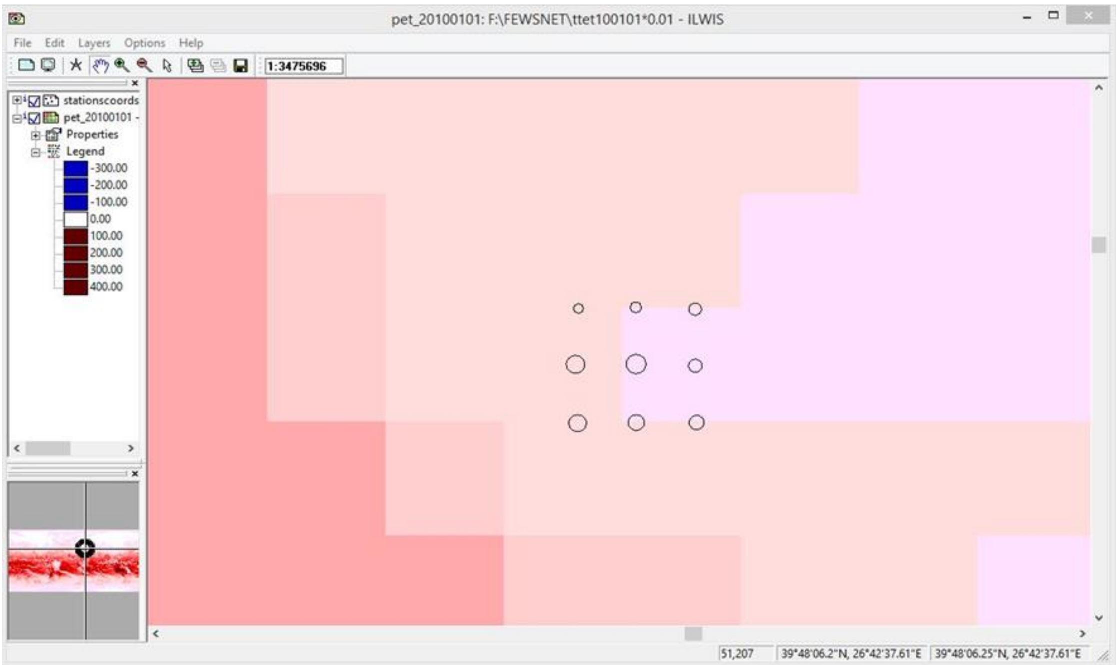

Figure 35 Point Map overlayed FEWS NET PET map

Yearly PET Map List was created in order to extract PET rates (Figure 36). Then by using Map List graph tool, PET rates were extracted in order to use in REW model (Figure 37).

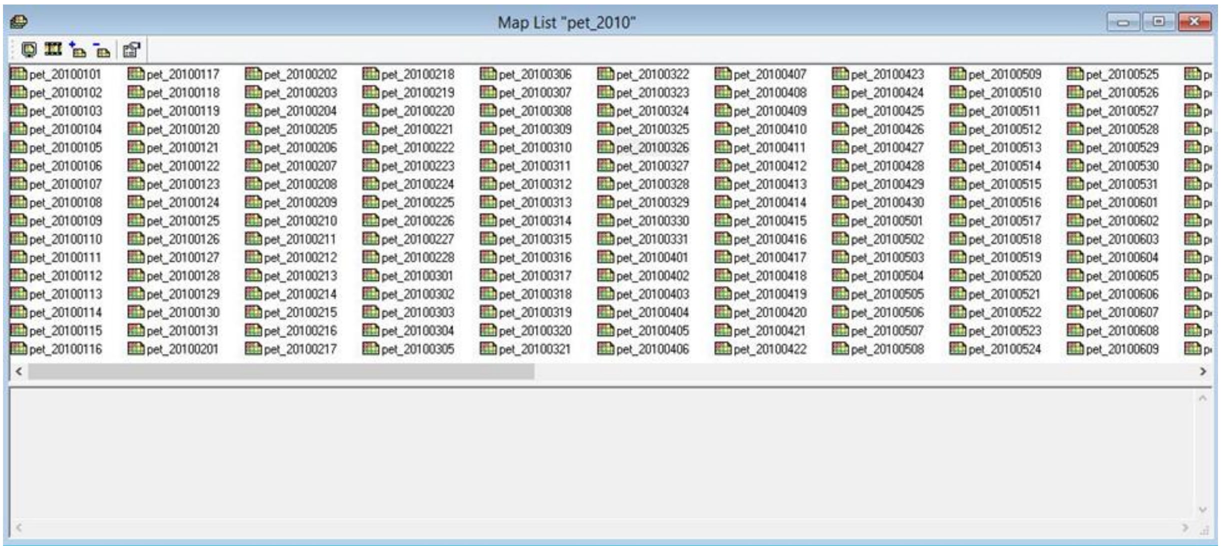

Figure 36 FEWSNET map list

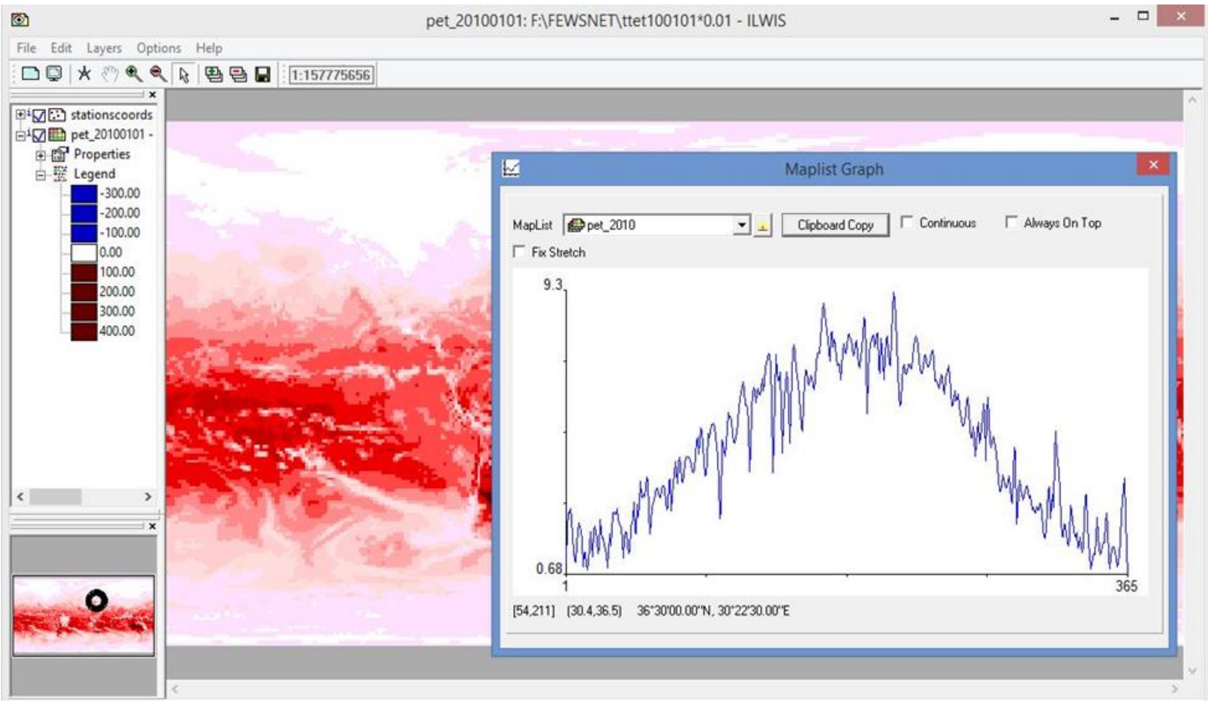

Figure 37 Daily PET rates in 2010

APPENDIX E

REW preprocessor parameter file	
steady state base flow event (mm/h):	0.01
overland flow Manning roughness parameter:	0.3
channel flow Manning roughness parameter:	0.035
min reach roughness height (mm):	200
max reach roughness height (mm):	200
at-a-station depth scaling exponent:	0.4
at-a-station width scaling exponent:	0.26
at-a-station velocity scaling exponent:	0.34
down-stream depth scaling exponent:	0.4
down-stream width scaling exponent:	0.5
down-stream velocity scaling exponent:	0.1
down-stream depth scaling coefficient:	0.23
down-stream width scaling coefficient:	7.09
down-stream velocity scaling coefficient:	0.61
discharge-area scaling coefficient:	2.00E-06
discharge-area scaling exponent:	0.8
hydraulic conductivity for channel bed (m/s):	1E-11
river bed transition zone thickness (m):	1.5
exponent in power relationship (p=1 linear):	0.55
water table depth (m):	15
bedrock depth (m):	300
soil porosity (-):	0.5
saturated hydraulic conductivity Szone (m/s):	0.0005
saturated hydraulic conductivity Uzone (m/s):	0.0005
Brooks-Corey soil parameter lambda (-):	0.8
Brooks-Corey pressure scaling parameter (m):	0.25
initial water content (-):	0.3
water content at saturation (-):	0.5
saturated hydraulic conductivity Pzone (m/s):	0.0005
exponent on transmissivity law (2<=g<=4):	2.5
depth of saturated subsurface flow layer (m):	0.5
exponent for surface precipitation partitioning:	0.15
depth of top soil layer for saturation averaging (m):	0.25
variogram (circle|exponential|gaussian|linear|polynom|spline):	circle
sweep (reduced|maximum distance|station and maximum distance):	reduced
variogram type (event|climatological):	event
calculate variance:	no
sweeping distance (m):	100000
number of trials:	1
order of derivative (first|second|third):	first

lower hard limit for rainfall data:	-60
upper hard limit for rainfall data:	1000
sill (-):	2.5
nugget (-):	1
range (m):	100000
scaling parameter alpha1:	1
scaling parameter alpha2:	1
scaling parameter alpha3:	1
scaling parameter alpha4:	1
scaling parameter beta:	1
roughness [rou>0]:	1
tension [1>=tau>=0]:	0.5
unit length:	1
unit observable:	1
over-relaxation parameter:	1.5
maximum number of iterations:	1000
# grid geometry information	
number of x mesh bins:	100
number of y mesh bins:	100
inital number of divisions along x:	30
inital number of divisions along y:	30
number of sucessive grid sub-divisions:	1
margin of mesh grid:	100
input data files:	Stations
matlab files:	Matlab
log files:	Logs
tardem files:	Tardem
ascii files:	Ascii
datools run info file:	DaTools
time series files (netcdf|xml):	xml
save forcing in XML format (daTools):	no
debug mode:	no

APPENDIX F

The figures below shows the simulated hydrographs for each catchment.

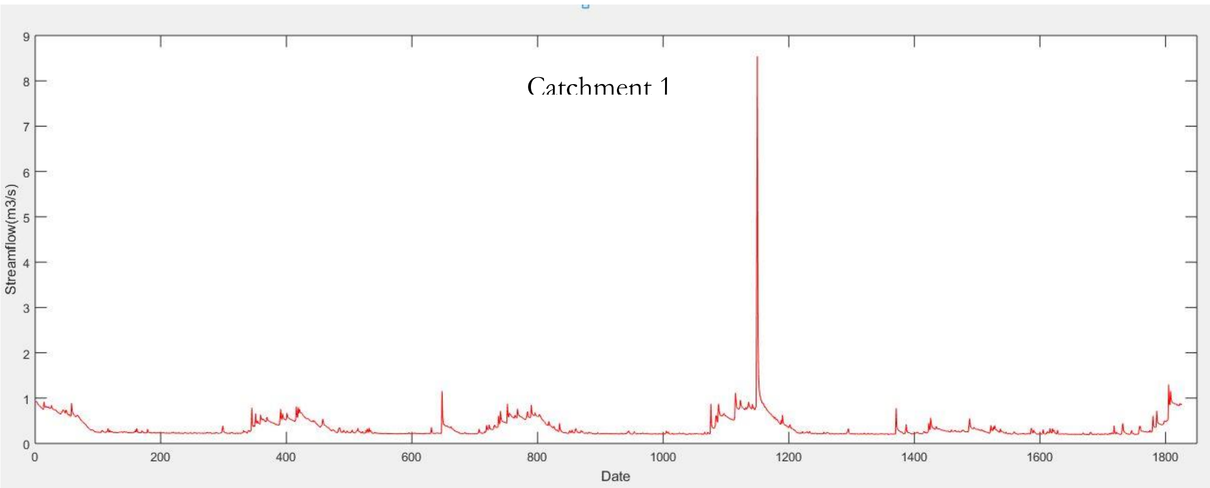

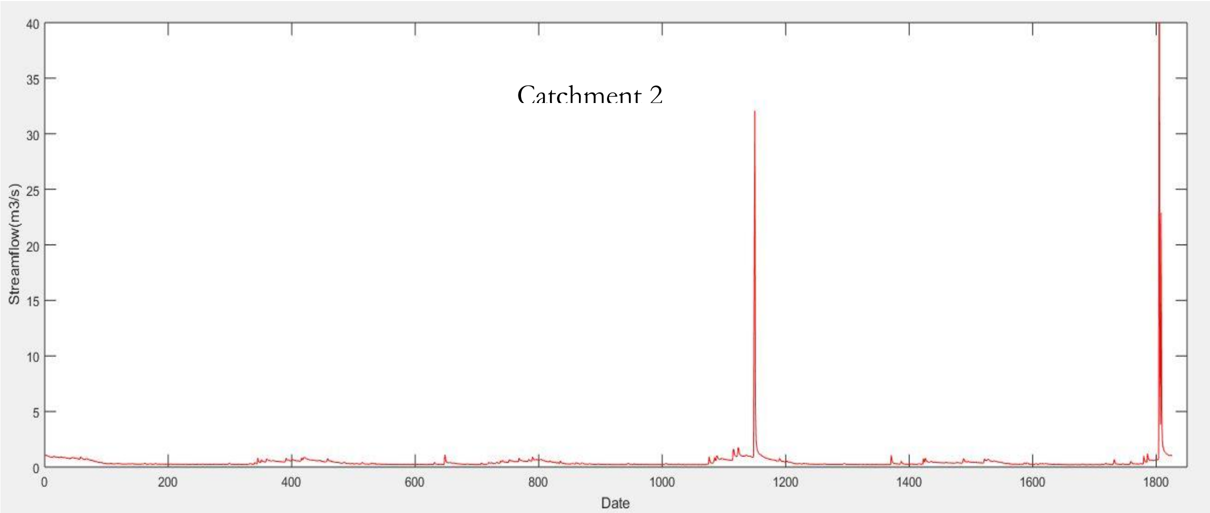

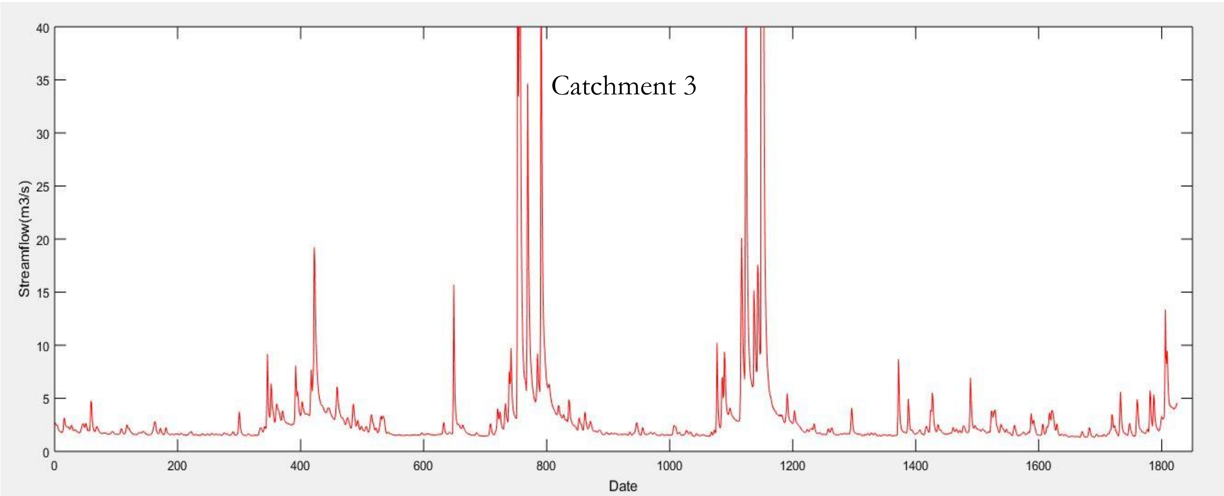

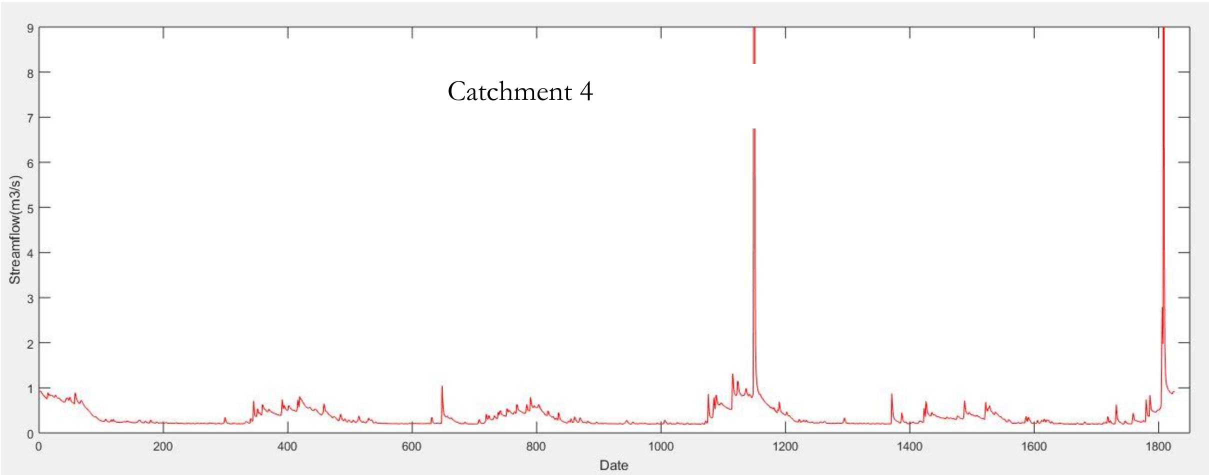
Catchment 4
Streamflow(m3/s)
Date
0
1
2
3
4
5
6
7
8
9
200
400
600
800
1000
1200
1400
1600
1800

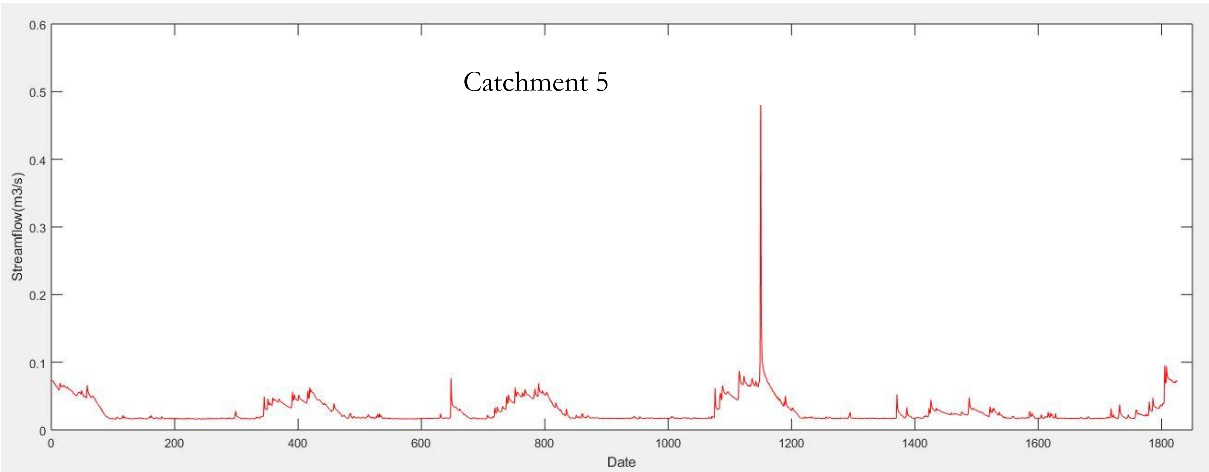
Catchment 5
Streamflow(m3/s)
Date
0
0.1
0.2
0.3
0.4
0.5
0.6
200
400
600
800
1000
1200
1400
1600
1800

APPENDIX G

Table 18 Lake level increases in mm by streamflow contribution

	Cat1	Cat2	Cat3	Cat4	Cat 5	Area A	Area B	Area C
Jan-10	12.2	10.7	87.6	26.0	11.0	18.6	6.1	34.8
Feb-10	9.5	8.2	72.4	20.7	8.8	14.4	4.9	27.5
Mar-10	8.0	6.4	82.5	17.5	7.4	11.6	4.1	23.2
Apr-10	4.6	3.7	38.2	9.8	3.9	6.6	2.2	12.6
May-10	3.6	3.3	29.2	7.2	3.2	5.6	1.7	10.3
Jun-10	3.5	3.2	20.1	7.0	3.1	5.5	1.7	9.9
Jul-10	3.3	3.1	19.5	6.8	3.0	5.2	1.6	9.4
Aug-10	3.2	3.0	22.3	6.5	2.8	5.1	1.6	9.0
Sep-10	3.0	2.9	18.4	6.3	2.7	4.9	1.5	8.6
Oct-10	3.3	3.2	22.0	7.0	3.0	5.3	1.6	9.3
Nov-10	3.1	3.0	17.8	6.3	2.7	4.9	1.5	8.7
Dec-10	6.3	5.5	48.7	12.7	5.5	9.6	3.0	17.5
Jan-11	7.1	6.5	119.2	15.3	6.3	11.1	3.6	20.1
Feb-11	7.7	7.0	517.3	17.1	7.0	11.9	3.9	22.0
Mar-11	7.7	6.6	71.3	16.5	6.9	11.6	3.9	21.9
Apr-11	5.9	4.3	36.3	11.3	5.1	8.2	2.7	16.5
May-11	4.2	3.4	23.9	8.2	3.7	6.1	2.0	11.7
Jun-11	3.6	3.2	20.6	7.5	3.2	5.5	1.8	10.2
Jul-11	3.1	2.9	23.4	6.6	2.8	4.9	1.6	8.8
Aug-11	3.0	2.9	19.6	6.5	2.7	4.9	1.5	8.7
Sep-11	3.1	2.9	18.0	6.6	2.8	4.9	1.6	8.9
Oct-11	4.9	4.6	32.5	11.0	4.5	7.8	2.5	14.1
Nov-11	3.1	2.9	28.3	6.6	2.7	4.9	1.5	8.8
Dec-11	3.9	3.6	23.6	8.4	3.5	6.1	2.0	11.1
Jan-12	6.3	6.8	185.4	16.0	5.5	10.8	3.4	17.7
Feb-12	7.1	7.4	114.3	17.8	6.2	11.9	3.8	19.9
Mar-12	7.8	7.1	116.9	18.6	6.9	12.1	4.1	22.0
Apr-12	4.6	3.7	38.2	9.8	3.9	6.6	2.2	12.6
May-12	4.0	3.3	31.9	8.1	3.5	5.9	1.9	11.2
Jun-12	3.1	2.8	22.0	6.7	2.8	4.8	1.6	8.8
Jul-12	3.0	2.8	21.5	6.7	2.7	4.7	1.5	8.6
Aug-12	3.2	3.0	24.3	6.9	2.9	5.0	1.6	9.1
Sep-12	2.8	2.7	20.0	6.4	2.6	4.5	1.5	8.2
Oct-12	3.1	2.9	24.0	6.8	2.8	4.9	1.6	9.0
Nov-12	2.8	2.7	19.3	6.2	2.5	4.5	1.4	8.0
Dec-12	6.9	5.9	52.3	14.7	6.2	10.3	3.5	19.6
Jan-13	12.0	9.0	126.1	22.9	9.9	16.9	5.5	32.5
Feb-13	35.2	15.4	520.1	52.1	26.7	39.1	13.7	91.1
Mar-13	10.7	8.9	65.4	21.4	8.7	15.8	4.9	28.9
Apr-13	6.0	4.6	37.9	12.2	5.2	8.5	2.9	16.8
May-13	3.7	3.1	25.5	7.8	3.3	5.5	1.8	10.5

Jun-13	3.1	2.8	22.2	7.0	2.9	4.8	1.6	9.1
Jul-13	3.2	2.9	25.1	7.3	3.0	5.0	1.7	9.3
Aug-13	3.0	2.8	21.0	6.8	2.8	4.7	1.6	8.7
Sep-13	2.8	2.7	19.4	6.4	2.6	4.5	1.5	8.2
Oct-13	4.4	3.6	34.6	9.1	3.9	6.5	2.2	12.5
Nov-13	4.5	3.5	30.6	8.8	3.9	6.4	2.1	12.6
Dec-13	5.5	3.9	24.9	10.3	4.8	7.5	2.6	15.4
Jan-14	5.4	3.9	31.6	10.6	4.8	7.4	2.6	15.3
Feb-14	5.0	3.4	24.2	10.0	4.5	6.7	2.4	14.2
Mar-14	7.0	3.7	33.0	11.5	5.9	8.3	3.0	19.2
Apr-14	3.7	2.8	22.0	7.1	3.1	5.1	1.7	10.0
May-14	3.7	3.1	27.2	7.8	3.3	5.5	1.9	10.5
Jun-14	3.3	3.0	30.2	7.5	3.1	5.1	1.7	9.7
Jul-14	2.9	2.7	19.4	6.6	2.7	4.5	1.5	8.4
Aug-14	2.9	2.7	19.9	6.5	2.7	4.6	1.5	8.4
Sep-14	3.5	3.0	28.0	7.9	3.3	5.3	1.8	10.1
Oct-14	3.6	3.2	28.5	7.9	3.3	5.5	1.8	10.3
Nov-14	6.2	4.6	33.7	10.5	5.0	8.6	2.7	16.6
Dec-14	53.0	10.4	63.1	26.3	23.3	46.8	9.9	105.3